Investigation of the Analytical Performance of Aerosol-Based Detectors in Liquid Chromatography

---

by

Manish Khandagale

A thesis submitted in fulfillment of the requirements for the degree of

Doctor of Philosophy

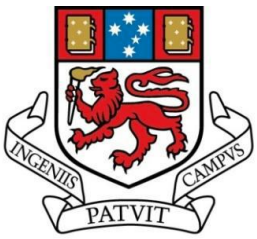

UNIVERSITY OF TASMANIA

School of Physical Sciences

University of Tasmania, Hobart

March 2015

Declaration

Declaration of Originality

"This thesis contains no material which has been accepted for a degree or diploma by the University or any other institution, except by way of background information and duly acknowledged in the thesis, and to the best of my knowledge and belief, no material previously published or written by another person except where due acknowledgement is made in the text of the thesis, nor does the thesis contain any material that infringes copyright."

Manish Khandagale

Authority of Access

This thesis may be made available for loan and limited copying and communication in accordance with the Copyright Act 1968.

A statement regarding published work contained in the thesis

"The publishers of the papers comprising Chapters 3and 4 hold the copyright for that content, and access to the material should be sought from the respective journals. The remaining non published content of the thesis may be made available for loan and limited copying and communication in accordance with the Copyright Act 1968."

Manish Khandagale
University of Tasmania
Hobart
7th March, 2015

Statement of Co-Authorship

The following people and institutions contributed to the publication of the work undertaken as part of this thesis:

Paper 1 Candidate[1] (70%), J. P. Hutchinson[2] (5%), G. W. Dicinoski[3] (5%), P. R. Haddad[4] (20%)

Paper 2 Candidate[1] (70%), R. A. Shellie[2] (5%), E. F. Hilder[3] (5%), P. R. Haddad[4] (20%)

Details of the Authors role:

Paper 1: Author 1 contributed to the design of the overall concept, experimental plan, executed all laboratory work and wrote the draft manuscript. Authors 2 & 3 contributed to the concepts and assisted in proof reading and corrections. Author 4 contributed to the concepts, publication refinement and submission.

Paper 2: Author 1 contributed to the design of the overall concept, experimental plan, executed all laboratory work and wrote the draft manuscript. Authors 2, & 3 assisted in proof reading. Author 4 contributed to the concepts, proof reading publication, publication refinement and submission.

We the undersigned agree with the above stated "proportion of work undertaken" for each of the above published (or submitted) peer-reviewed manuscripts contributing to this thesis:

Signed: _____ _____

Date: _____ _____

Prof. Paul R. Haddad	*Prof. John Dickey*
Primary Supervisor	*Head of School*
School of Physical Sciences	*Head of School of Physical Sciences*
University of Tasmania	University of Tasmania

Acknowledgements

This project was supported by a PhD scholarship from the Australian Research Council via the grant (LP0884030). The provision of a tuition fee was kindly provided by the Tasmanian government through the Department of Economic Development, Tourism and the Arts. Instrumental support was generously provided by Thermo Scientific, Australia.

The list of people I owe my sincere gratitude for their involvement in this project are:

- My primary supervisor, Prof. Paul Haddad- for his knowledge, invaluable suggestions, and constant encouragement throughout this work. Without his guidance and persistent help, this thesis would not have been possible.
- My former co-supervisors Dr. Joseph Hutchinson and Assoc. Prof. Gregory Dicinoski- for providing support and guidance to successfully settle in a new work environment and to conduct the initial part of this work.
- I also would like to acknowledge Prof. Emily Hilder and Assoc. Prof. Robert Shellie, as my co-supervisors, for their time and fruitful discussions in general.
- Australian Centre for Research on Separation Science (ACROSS) - for providing intellectually inspiring and pleasant multicultural work environment.
- Past and present members of ACROSS and the Pfizer Analytical Research Centre (PARC) for their support and friendship over the course of my PhD candidature, including Prof. Pavel Nesterenko, Prof. Brett Paull, Dr. Georg Schuster, Dr. Timothy Causon, Mr. Matthew Jacobs, Mr. Daniel Gstoettenmayr, Ms. Jennifer Nield and Mr. Murray Frith
- My friends who have helped me in many ways during past few years: Dr. Adam Gaudry, Ms. Mitra Talebi, Dr. Mohammad Talebi, Mr. Madhur Shastri, Dr. Rahul Patel, Mr. Benjamin Savareear and Mr. Vipul Gupta. We had memorable times together, that I will always cherish.
- Mr. Peter Dove, Mr. John Davis and Mr. Anthony Malone- for their expert and efficient technical assistance.

Finally, I would also like to thank my parents and two elder sisters for their endless support and love all these years.

List of abbreviations

AAS	Atomic absorption spectrometry
ACN	Acetonitrile
AES	Atomic emission spectrometry
APCI	Atmospheric pressure chemical ionisation
C-CAD	Corona-charged aerosol detector
CDHA	Canadian drug and health agency
CNLSD	Condensation nucleation light scattering detector
ELSD	Evaporative light scattering detector
ESI	Electrospray ionisation
FIA	Flow injection analysis
GC	Gas chromatography
HPLC	High performance liquid chromatography
HTLC	High temperature liquid chromatography
i.d.	Internal diameter
ICH	International conference on harmonisation of technical requirements for registration of pharmaceuticals for human use
ICP-MS	Inductively coupled plasma-mass spectrometry
LOD	Limit of detection
LOQ	Limit of quantification
MDMI	Mono-disperse dried micro-particulate injector
MS	Mass spectrometry
NSAIDs	Non-steroidal anti-inflammatory drugs
PEEK	Polyether ether ketone
PEEKSIL	Polymer (polyether ether ketone) sheathed fused silica
PGC	Porous graphitised carbon
RPLC	Reversed phase liquid chromatography
RRF	Relative response factor
RSD	Relative standard deviation

List of abbreviations – continued

SD	Standard deviation
SLM	Standard litre per minute
SMD	Sauter mean diameter
TOF-MS	Time of flight-mass spectrometry
US-FDA	United States – food and drug administration
UVD	Ultraviolet visible light detector

List of publications

Papers in refereed journals

- M. M. Khandagale, J. P. Hutchinson, G. W. Dicinoski, P. R. Haddad, Effects of eluent temperature and elution bandwidth on detection response for aerosol-based detectors, J. Chromatogr. A 1308 (2013) 96-103.
- M. M. Khandagale, E. F. Hilder, R. A. Shellie, P. R. Haddad, Assessment of the complementarity of temperature and flow-rate for response normalisation of aerosol-based detectors, J. Chromatogr. A 1356 (2014) 180-187.

Presentations at International conferences (presenting author underlined)

- M. M. Khandagale, J. P. Hutchinson, G. W. Dicinoski, P. R. Haddad. Aerosol based mass flow detectors for liquid chromatography: Potentials & challenges (poster presentation), *11th Asia-Pacific International Symposium on Microscale Separations and Analysis, (2011),* Hobart, Australia.
- M. M. Khandagale, J. P. Hutchinson, G. W. Dicinoski, P. R. Haddad. Effect of eluent temperature and elution bandwidth on detection response of aerosol-based detectors, (poster presentation), *40th International Symposium on High Performance Liquid Phase Separation and Related Techniques Conference (2013),* Hobart, Australia.
- M. M. Khandagale, E. F. Hilder, R. A. Shellie, P. R. Haddad. Utility of temperature and flow rate variation for improved response homogeneity of corona-charged aerosol detector, (poster presentation), *40th International Symposium on High Performance Liquid Phase Separation and Related Techniques Conference*, (2013), Hobart, Australia.
- P. R. Haddad, M. M. Khandagale, E. F. Hilder, R. A. Shellie. Strategies for achieving universal response and calibration for aerosol-based detectors in liquid chromatography, (oral presentation), *38th International Symposium on Capillary Chromatography*, (2014), Riva Del Garda, Italy.

- M. M. Khandagale, E. F. Hilder, R. A. Shellie, P. R. Haddad,, Eluent temperature and flow-rate programmed separation approaches to improve performance of aerosol based LC detectors, (poster presentation), *30th International Symposium on Chromatography*, (2014) Salzburg, Austria.

Abstract

A non-discriminating, robust and economical detection system, which can be easily coupled with different modes of separation, is highly desirable in the field of liquid chromatography. While the evaporative light scattering detector (ELSD) and the corona-charged aerosol detector (C-CAD) hold great promise to meet these requirements, the widespread applicability of these techniques has been hindered due to lower sensitivity and solvent dependency of the detection response. This work presents an investigation into different experimental approaches to overcome these limitations, so as to extend the field of applicability of ELSD and C-CAD.

Hyphenation of high temperature liquid chromatography (HTLC) using water-rich mobile phases with ELSD / C-CAD is an attractive solution to the solvent dependency limitations of these detectors and also offers a better detection alternative for HTLC. Therefore, experiments were conducted to investigate the effect of HTLC conditions using water-rich mobile phases on the detection response of ELSD and C-CAD. Flow-injection studies showed that eluent temperature marginally influenced the detection response. However, in chromatographic separations the response of the ELSD for the same analyte eluted at different retention times was increased up to 5-fold by increasing the separation temperature from 30°C to 180°C. Compared to the ELSD, the response of the C-CAD was found to remain relatively unaltered with variation in retention time. This increase in ELSD response was found not to result from the eluent temperature, but rather from compression of the elution band-width at elevated temperatures and hence shorter retention times. The relationship between elution band-width and the response mechanism of the ELSD was then explained using logarithmic response curves obtained by flow-injection experiments. Furthermore, it was demonstrated that a temperature gradient could be used to counteract the effects of varying bandwidths associated with isocratic-isothermal separations.

Considering the advantages of temperature gradients in attaining elutropic strength comparable to the solvent gradient, the possibility of employing isocratic separations with a combination of temperature and flow-rate variation to achieve uniform detection response of the C-CAD was investigated. Using a flow-injection

study, it was demonstrated that the response of the C-CAD remain relatively unaltered with flow-rate variation when used with water-rich eluents. Based on these findings two separation approaches were developed and their utility for C-CAD response normalisation was demonstrated using a mixture of eight analytes. In the first approach, a temperature gradient was applied under isocratic conditions, followed by response enhancement through the post-column addition of organic solvent. In the second approach, flow-rate programming was used to improve the speed of separations performed using isocratic elution coupled with a temperature gradient. The response homogeneity and applicability of these approaches were compared to the inverse solvent gradient technique for quantitative analysis. Good peak area reproducibility (RSD < 15%) and linearity (R^2 > 0.994, on a log-scale) over the sample mass range of 0.1 – 10 μg were achieved. The response deviation across an equi-mass mixture of eight analytes at seven concentration levels was 6-13% compared to 21-39% when a conventional solvent gradient was applied and this response deviation was comparable to that obtained in the inverse gradient solvent compensation approach. The applicability of these approaches for typical pharmaceutical impurity profiling was demonstrated at a concentration of 5 μg/mL (0.1% of the principal compound).

Following the above studies, the applicability of nebuliser gas flow-rate programming and inverse gradient techniques was investigated for improving the performance of the ELSD. The investigations showed that nebuliser gas flow-rate programming could be used to compensate solvent effects; however it caused significant loss in sensitivity and hence has limited applicability for the water rich eluents. Moreover, in inverse gradient experiments, elution bandwidth variability across the separation was found to contribute to response irregularity. This led to the investigation of two-dimensional liquid chromatographic (2-D LC) peak modulation approaches to improve the performance of ELSD. Experiments were conducted to assess the feasibility of elution band-width normalisation by means of post-separation flow-rate modulation using a switching valve. Furthermore, for proof of concept, utility of the switching valve as a peak sampling device to overcome solvent gradient limitations of the ELSD was demonstrated. However, some limitations of this approach were identified, especially in terms of the ability to detect peak segments of low analyte concentration.

The investigations described herein provide new insights into how unconventional LC-separation modes can be used to improve the performance of aerosol detectors and thereby contributes to extending their universal applicability.

Table of Contents

Chapter 1

Introduction and literature review

1.1 Introduction

1.1.1 Background

Over the past few decades, through continued advancements in instrumentation and theoretical understanding, liquid chromatography has evolved substantially to become the preferred analysis technique in a diverse range of fields including environmental, polymers, foods, chemicals, pharmaceuticals and forensics. In particular, a long-term interactive relationship between the pharmaceutical industry and chromatography has made a significant contribution in the mutual growth of these fields. The modern liquid chromatography era is reported to have begun in the late 1970's. During the same period, revolutionary changes in pharmaceutical industry took place through improvements in the better understanding of human biology, emergence of new approaches to drug discovery and technological advancements in the manufacturing process. These revolutionary changes in the pharmaceutical field led to the development of several new therapeutic entities, including cardiovascular drugs, non-steroidal anti-inflammatory (NSAIDs), contraceptives, antidepressants and cancer therapeutics. However, the incidence of adverse drug-reactions also rose dramatically, which initiated the development of robust separation methodologies in order to control the drug manufacturing process.

In 1984, the introduction of the drug price competition and patent restoration act (Hatch-Waxman Act) [1] brought a major strategic transformation in the pharmaceutical industry. The next two decades witnessed cutthroat competition from generic drug manufacturers. Therefore, sub-2 micron particle stationary phases and ultra-high pressure LC-systems were developed to fulfil high-throughput and resolution requirements of the pharmaceutical industry. Today, liquid chromatography has become an indispensable tool for pharmaceutical analysis via several different modes of separation, a wide range of stationary phases, and continued instrumental expansion. Nevertheless, despite the substantial progress in separation technologies, the detection aspects of LC separation have received less attention until recently. So far, the

Ultraviolet light-detector (UVD) is the most common method of LC-detection. However, considering the ever-tightening regulatory requirements and new trends in drug manufacturing, UVD has now become a problematic issue in pharmaceutical analysis because of the need to detect very small amounts of non-UV absorbing compounds.

In the global pharmaceutical sector, adherence to the guidelines provided by the International Conference on Harmonisation of Technical Requirements for Registration of Pharmaceuticals for Human Use (ICH) has now become absolutely fundamental to ensure the health and safety of the consumer. ICH-guidelines on quality topics focus mainly on the stability and impurity analysis of new drug substances and products. These guidelines are also adopted by pharmacopoeias and various regulatory bodies, such as the United States-Food and Drug administration (US-FDA), and the Canadian Drug and Health Agency (CDHA). According to ICH-guidelines any component of the drug product that is not its active ingredient or an excipient is an impurity [2], which must be reported, identified or qualified based on the daily intake of the active ingredient. For any drug substance and product the reporting threshold of impurities extends to a level of 0.05% of its active ingredient [3, 4]. ICH-guidelines mandate the inclusion of individual impurities for the validation of purity methods [5]. It is noteworthy that these impurities arise from several sources, including carryover from starting materials, intermediates, by-products, residual solvents, drug-excipient interactions and degradation. The chemical properties of these impurities can therefore differ significantly from the active ingredient, which raises questions about the reliability of the quantitative data obtained using UVD. In general the relative response factor (RRF), which is the ratio of the responses of equal amounts of the impurities and the drug substance, is used to correct the response non-uniformity. Considering the frequent lack of impurity standards, difficulty in the synthesis and characterisation of unknown impurities and validation of purity methods, impurity analysis is a major obstacle in the process of the drug development. Moreover, an increasing number of the drugs lack characteristic UV-chromophores, representing a further problematic issue in pharmaceutical analysis. Therefore, sensitive, non-discriminating detection systems that can offer reliable quantification are highly desirable to reduce the time and resources required for the establishment of RRFs and extensive validation. The use of mass spectrometry (MS) detection can potentially help to overcome these issues.

Nevertheless, the response of MS varies as a function of ionisation efficiency of the analyte, the chemical properties of the eluent modifiers and the type of ionisation (e.g. atmospheric-pressure chemical ionisation (APCI), electrospray ionisation (ESI), etc.). Moreover, due to the high cost and special operator-skill requirement, MS is not a desirable option in routine drug discovery and production applications. On the contrary, the evaporative light scattering detector (ELSD) and the corona-charged aerosol detector (C-CAD) are economical, easy to use and more importantly can potentially provide a uniform response to most of the analytes.

1.1.2 Previous reviews and scope of this literature review

Over the past two decades, through technological refinements, ELSD has emerged as a robust detection approach. On the other hand, C-CAD is a relatively new technique having a great potential to meet universal detection requirements. A number of reviews covering different aspects of ELSD and C-CAD have appeared over the years. General operating principles, major limitations, consequent instrument modifications and different applications of ELSD over the period of 20 years since its commercial introduction in 1980's have been reviewed by Megoulas and Koupparis [6]. This was followed by a review by Lucena et al. [7], which provided insight on new trends and technological improvements in ELSD. The potential use of ELSD for various vanguard/rear-guard configurations that can be used in different application areas for rapid sample screening and total indices determination was discussed in detail. Krystyna Mojsiewicz-Pienkowska [8] has presented a critical review of various response calibration approaches used by different researchers. Recently, Arndt et al. [9] compiled a review on the application of ELSD for the analysis of synthetic polymers. Effects of polymer chromatography, in particular, critical evaluation of the effects of molar mass distribution of polymers and the eluent properties on ELSD response were assessed. After the commercial introduction of C-CAD in the 2004, McCarthy and Gamache [10] described the operating principles and figures of merit of this new detection approach. A number of reviews describing general principles, instrumental advances and different applications of C-CAD appeared in the following years [11-15]. These reviews clearly show that despite continued progress in instrumentation and theoretical understanding, ELSD and C-CAD have received limited acceptance from the pharmaceutical industry. These techniques are used mainly for the analysis of non-chromophoric analytes. The problem lies in the multifaceted nature of their limitations

such as: lower sensitivity, interferences associated with changes in solvent composition and the non-linear nature of the detection response.

In this, present review, the current literature has been collated to understand the potential and challenges facing the universal adoption of ELSD and C-CAD. Although theory and operating principles of ELSD and C-CAD have been well documented in the literature, for the sake of discussion, a brief introduction on these topics has been included. The subsequent section discusses the fundamental limitations of these techniques, together with the advances made so far to overcome these limitations. Like most other aerosol based detectors, the performance of ELSD and C-CAD depend strongly on the process of sample introduction i.e. the process of nebulisation. The fundamental processes and factors that influence nebulisation and aerosol mass transport efficiency have been studied extensively in the field of atomic absorption spectrometry (AAS) and inductively coupled plasma - mass spectrometry (ICP-MS). However, the work of these research areas has been seldom cited in the literature of ELSD and C-CAD research. To explain the fundamental basis of these developments, relevant references from AAS and ICP-MS literature have been included. While mainstream adoption of aerosol-based detectors has been affected by their perceived limitations, several new trends in the usage of aerosol-based detectors have emerged in the recent years. Especially, hyphenation with high temperature liquid chromatography (HTLC) has attracted considerable attention. Therefore, in the last section of this review, studies reporting a combination of HTLC and aerosol-based detectors have been reviewed briefly. Theory, principles and applications of HTLC have already been extensively reviewed. Since the primary aim of this project is to identify potential new avenues to extend the universality of ELSD and the C-CAD, discussion in this section has been limited to a summary of the previous reviews and some critical aspects of the hyphenation of aerosol based detectors with HTLC.

1.2 Aerosol-based LC-detection techniques

The term aerosol-based detector refers to the class of detection techniques that involve the conversion of liquid sample into an aerosol to generate a response to the specific physical properties exhibited by the sample residue left after desolvation. Methods of aerosol-based detection have evolved rapidly over the years, with examples including AAS, ICP-MS, ELSD, condensation nucleation light scattering detector (CNLSD) and C-CAD. Among these, ELSD and C-CAD have attracted considerable

attention because of their compatibility with LC, their ease of use, low cost and most importantly for their ability to provide detection response for a wide range of analytes independent of their optical absorbance and chemical properties.

1.2.1 Operating principles of ELSD

The theory and operating principles of ELSD have been described thoroughly in earlier phases of developments [16-18]. The ELSD detection process can be simplified to three steps: nebulisation, evaporation and light scattering (Fig-1.1). In ELSD detectors, the chromatographic effluent is mixed with nebulizer gas and introduced into a spray chamber to form droplets containing solute particles. While passing through the spray chamber, the evaporator-tube temperature and nebuliser gas assist desolvation and consequently droplets shrink to form analyte particles. The nebulizer gas assists the solute particles and fine unevaporated droplets to travel towards the optical unit, where they are irradiated with light at an angle. Depending on the ratio of the solute particle diameter to the wavelength of the light, scattering takes place via different mechanisms. The scattered radiation is detected by a photomultiplier tube to give a signal proportional to the mass of analyte particles.

1.2.2 Operating principles of C-CAD

Fig-1.2 schematically illustrates the principle of operation of C-CAD. Similar to the ELSD detector, C-CAD involves sample introduction by a nebulisation process. However, unlike ELSD, commercial C-CAD employs a high flow-rate of the nebuliser gas (4 standard litres per minute (SLM)) to produce primary aerosols [19]. C-CAD has been covered by the patent US6544484B1 [20], which discloses a process of aerosol charging. Before entering the nebuliser, the gas flow splits into two streams: one carries aerosol into a mixing chamber at 1.5 SLM, while another stream (1.0 SLM) passes through a filter and ioniser. The second stream then passes through the ion generator. Commercial C-CAD employs a corona discharge mechanism to produce positively charged gas ions. The corona discharge unit consists of a pair of asymmetric electrodes (a curved, sharp needle-shaped electrode and a flat electrode), characterised by the non-uniform electrostatic field at the high potential difference. The curved, sharp electrode is connected to positive voltage and hence the process is commonly referred as unipolar (+) charging. A high potential difference (~ 2-5 kV) between these electrodes causes electrical breakdown of nitrogen gas (N_2) to produce an avalanche of positively charged

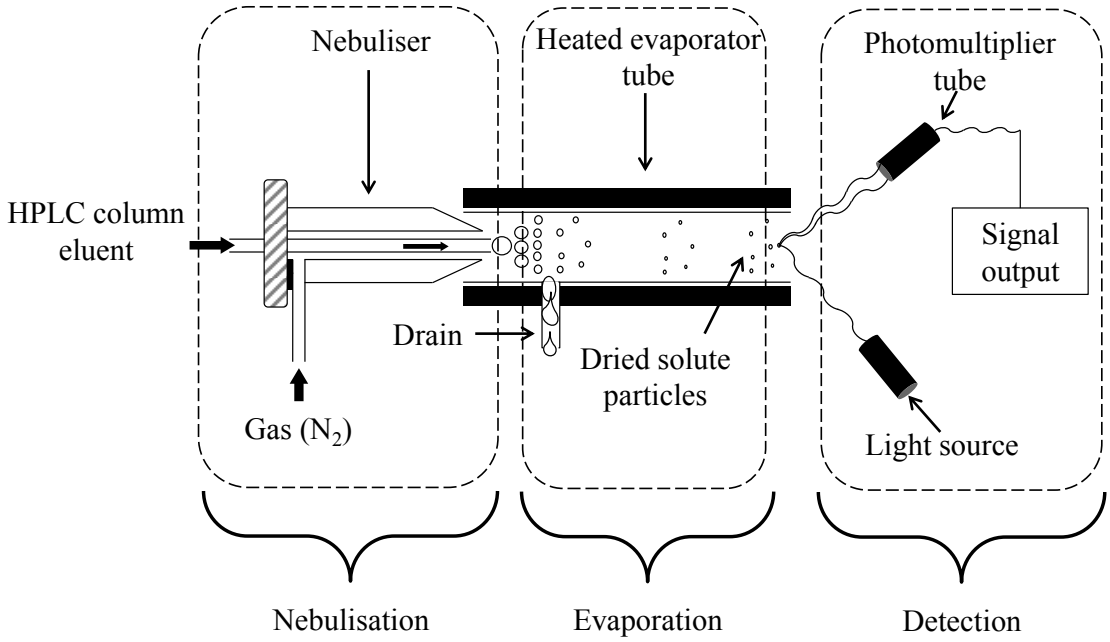

Figure-1.1: Schematic illustration of operation of the ELSD

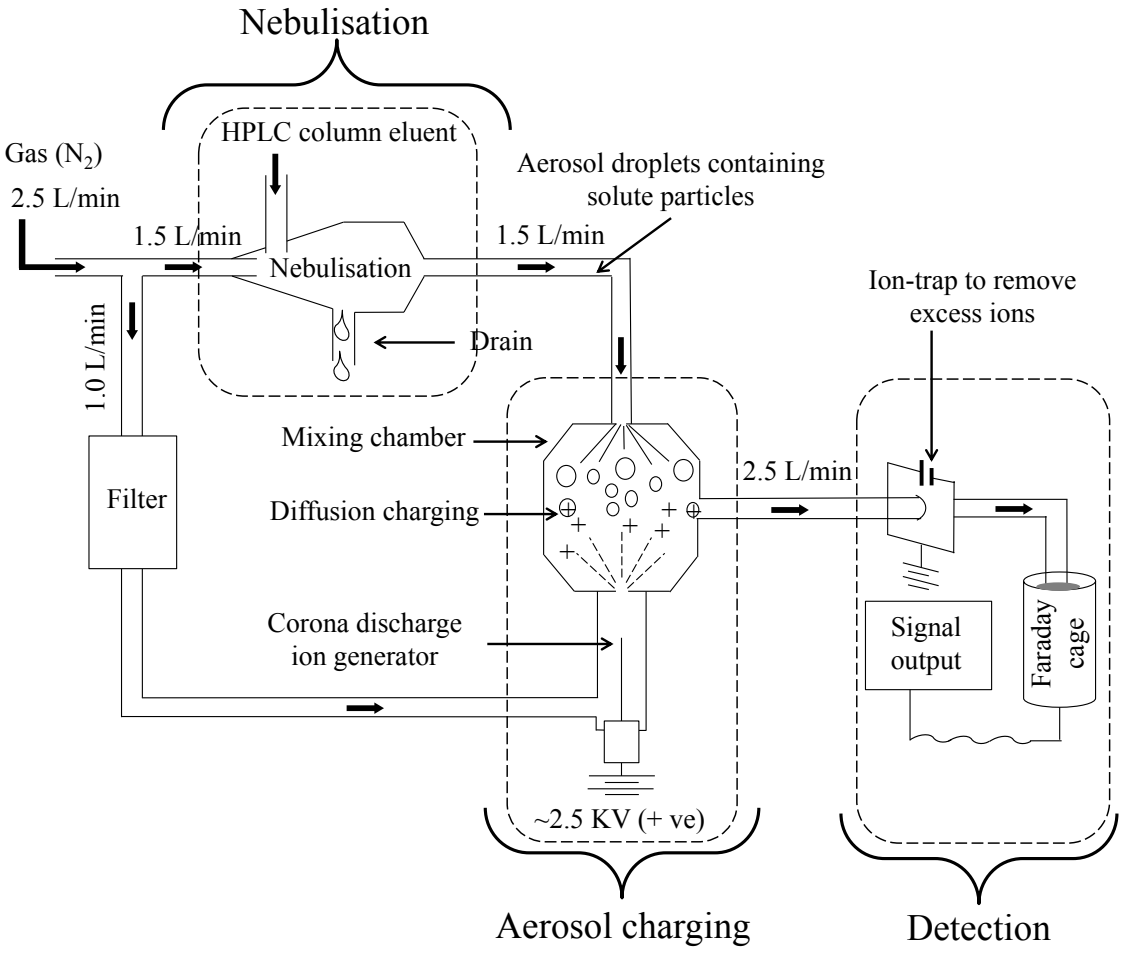

Figure-1.2: Schematic illustration of operation of the C-CAD

nitrogen ions (N^+). After ionisation, the second stream enters into a mixing chamber and imparts net positive charge to dried solute particles. Afterwards, a stream of charged particles passes through the ion-trap, towards a Faraday cage electrometer to produce a signal proportional to the of charged particles.

1.3 Limitations and new developments

1.3.1 Low sensitivity

The response characteristics of ELSD and C-CAD depend on the measurement of optical or electrical properties exhibited by the plume of dried solute particles. Therefore, these detectors are commonly regarded as mass-sensitive detectors. In quantitative analysis, sensitivity is one of the important criteria in selecting an appropriate detection technique. The sensitivity of mass-sensitive detectors is expressed in terms of signal output per unit mass of the analyte entering the detector. Since both ELSD and C-CAD respond in a non-linear manner in a given concentration range, sensitivity is normally calculated as a product of the slope and intercept obtained by log-log linearisation of the data [21]. Ramos et al. [22] compared log-normalisation and a power model to assess the performance of ELSD and C-CAD. It has been reported that the derivative of the power model can be used for accurate estimation of the sensitivity. Several publications have appeared recently documenting comparative assessment of the analytical figures of merit of ELSD and C-CAD (Table-1.1). The sensitivity of these techniques is commonly reported to be inferior to the conventional LC-detectors such as UVD and electrospray ionisation mass spectrometry (ESI-MS). Relatively low sensitivity compared to conventional LC-detectors is one of the major barriers to widespread acceptance of aerosol-based detection techniques. The mass flow and size distribution of the dried solute particle plume entering into the detection zone determine the sensitivity of ELSD and C-CAD and depend on several interrelated physical phenomena that occur at different stages of the detection process. These will be discussed in the following sections.

1.3.1.1 Nebulisation process

ELSD and C-CAD typically employ a pneumatic nebuliser to transform the liquid sample into an aerosol. Aerosol formed is then swept towards the detection zone by a secondary stream of the gas. While travelling from the nebuliser to the detection zone, the aerosol undergoes remarkable modifications through complex physical

Table-1.1: Overview of different studies involving comparative evaluation of ELSD and C-CAD

Application Details	Criteria	Key Findings
Comparison of 3 detectors: UVD, ELSD and C-CAD, for LC-separation of the anti-diabetic drugs [23]	Sensitivity	LOD of C-CAD (21-48 ng) was comparable to UVD (27-47 ng) and up to 2 fold higher than ELSD (73-77 ng).
	Linearity	Both UVD and ELSD provided linear response over the entire concentration range (1-9 µg on-column), however, for C-CAD log-transformation was required.
	Precision	%RSD (n=6) values C-CAD (1.1-9.5%) found to be higher than UVD (0.1-1.6%) but much better than ELSD (2.6-26.6%)
Comparison of ELSD, C-CAD and CNLSD with UVD for RPLC separation [24]	Sensitivity	With aqueous mobile phase LOD of C-CAD (364 ng/mL) was found to be about 2-fold lower than UVD (198 ng/mL) but was up to 6 fold higher for ELSD (2420 ng/mL). With 80% ACN, C-CAD showed 2 fold higher sensitivity compared to UVD.
	Linearity	Both C-CAD as well as ELSD exhibited a non-linear relationship with sample mass (Sample mass range – 0.0025-25 µg) and organic solvent (of 0-80% ACN)
	Precision	%RSD (n=10) values of C-CAD (~4%) found to be higher than UVD (~2%) but much better than ELSD (~11%)

Table-1.1: Overview of different studies involving comparative evaluation of ELSD and C-CAD (cont.)

Application Details	Criteria	Key Findings
Comparison of 3 detectors: ELSD, C-CAD and ESI-MS in the RPLC and hydrophilic interaction liquid chromatography (HILIC) mode [21]	Sensitivity	C-CAD and ESI-MS showed 10 times higher sensitivity in HILIC mode compared to RPLC, whereas improvements in the sensitivity of ELSD found to be less significant. Response deviation among test analytes using ESI-MS was found to be several orders of magnitude greater than that of ELSD and C-CAD.
	Linearity	C-CAD showed 2^{nd} order relationship between concentration and response, whereas ESI-MS data fit well in a 1^{st} order relationship.
	Precision	Details not reported.
Comparison of C-CAD with UVD for analysis of statins [25]	Sensitivity	C-CAD exhibited ~2-fold higher LOD (0.08 µg/mL) than UVD (0.17 µg/mL)
	Linearity	Both UVD and C-CAD yielded linear response curve with R^2>0.999 over sample mass range 0.001-0.5 µg.
	Precision	%RSD (n=6) of values C-CAD found to be < 5% and were comparable to UVD.
Comparison of LC-ELSD, LC-ESI Time of Flight (TOF) - MS and LC-UVD approaches for analysis of sesquiterpenoids in Artemisia plant species [26]	Sensitivity	LOD for 5 compounds by a) ELSD: 50, 25, 30, 100 and 75 µg/mL, b) UVD: 5, 3, 100, 100 and 7.5 µg/mL and c) LC-ESI TOF: 5, 10, 25,50 and 50 ng/mL
	Linearity	Both ELSD and UVD yielded linear response curve with R^2 > 0.999 over on-column sample mass range 0.5-10 µg, whereas for LC-MS required log-transformation to linearise response curve (sample mass: 0.0005 - 0.01 µg).
	Precision	All 3 approaches high reproducibility and low standard error.

phenomena. Based on the different stages of the transport (Fig-1.3), the aerosol is generally classified as: a) primary (aerosol that exits nebuliser) b) secondary (aerosol modified after droplet filtration) and c) tertiary aerosol (a mixture of dried solute particles and gas that enters into the detection unit). The size distribution and number concentration of the solute particles in the tertiary aerosol, relative to gas volume, determine the response characteristics of these detectors. The process of nebulisation and aerosol transport, therefore dominates the performance of aerosol-based detectors.

Analyte loss related to the nebulisation efficiency and the analyte mass transport is one of the major sources of the low sensitivity of these detectors. Nebulisation efficiency is expressed as the fraction of the total sample feed, which enters the detection unit. Typical pneumatic nebulisers transfer only 1-20% of the sample feed to the detection unit [27]. There exists a large body of research dealing with various aspects of the nebulisation process and its role in the performance of aerosol based detection techniques such as AAS, ICP-MS. Sharp [28, 29] has presented a comprehensive review on pneumatic nebulisers and spray chambers used for sample introduction in ICP-atomic emission spectrometry (ICP-AES). The mechanism of aerosol production and the effects of various factors, such as volumetric flow of gas and liquid, their relative velocity, nebuliser geometry, resultant forces which influence the aerosol characteristics at different stages of transport and overall aerosol transport efficiency have been explained in detail. Many others [30-32] have reviewed the problems associated with conventional sample introduction systems and the ways to improve the transport efficiency in the plasma spectrometry techniques

It is widely accepted that the primary aerosol characteristics such as size distribution and the average size of the droplets (D_0) profoundly influence the nature of tertiary aerosol reaching the detection zone. Primary aerosol characteristics depend chiefly on the process of nebulisation. Ideally, the nebulizer should generate primary aerosol droplets with a small size distribution, uniform velocity and of optimum surface to volume ratio to give maximum analyte transport efficiency [27]. Currently, no single nebulizer possesses all these characteristics. Typical pneumatic nebulisers operate at a liquid flow-rate in the range of 0.2–2 mL/min and produce highly polydisperse droplets. Nebuliser geometry and operating conditions, such as gas and liquid flow-rates, velocity and physical properties (viscosity and surface tension) of the liquid determine the kinetic energy available for liquid aspiration, and consequently the characteristics of the primary aerosol cone. In concentric nebulisers, the internal diameter of the liquid-

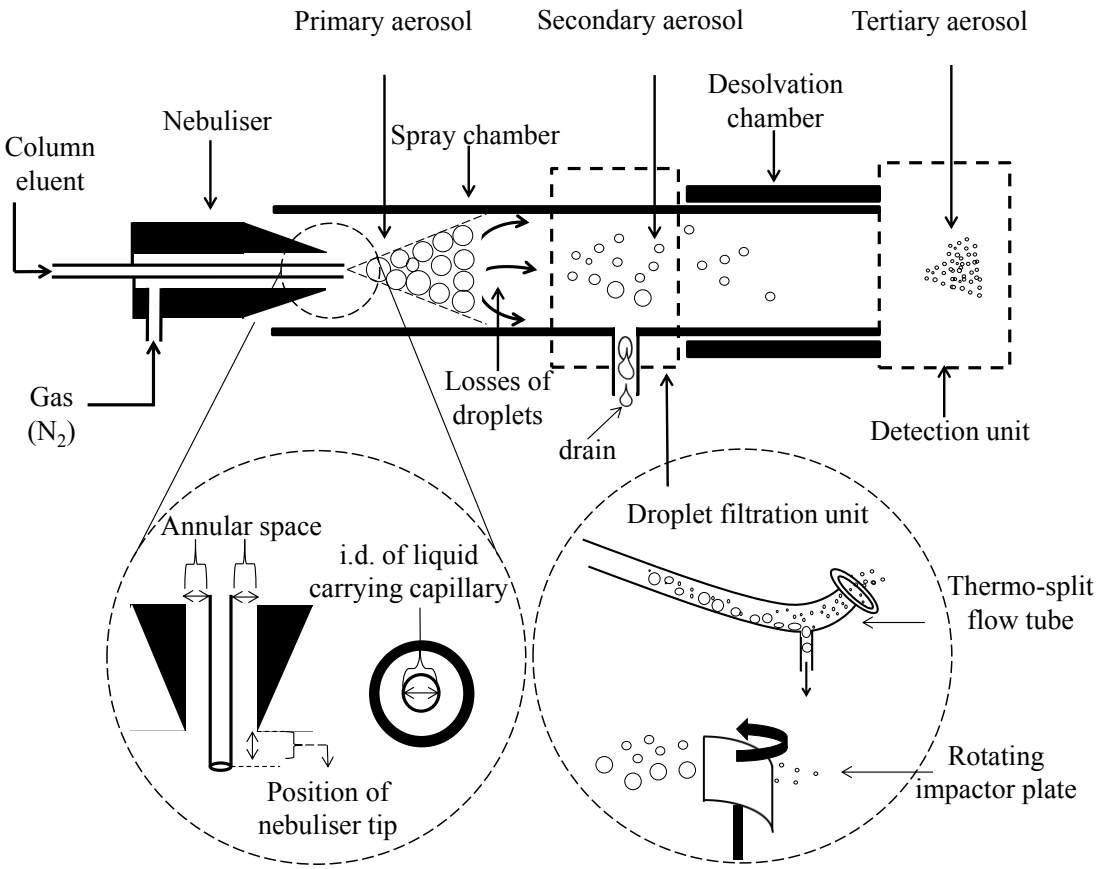

Figure-1.3: Schematic representation of the terms related to the aerosol transport process, nebuliser design and desolvation chamber, that are used to discuss the performance of aerosol-based detectors in section 1.3.

carrying capillary, the annular space between the liquid and gas carrying tube, and the position of the liquid carrying capillary with respect to the nebuliser tip also influence the average droplet size [32, 33]. The distance of the inner capillary from the gas outlet section dominates the shape of primary aerosol cone. It has been reported that the primary aerosol cone remains unaltered over approximately five times the inner diameter of the liquid carrying capillary [28]. Once the primary aerosol is formed at the nebuliser tip, losses of droplets carrying solute occur mainly by 1) impaction on spray chamber walls, 2) gravitational and centrifugal drag on large droplets and 3) coalescence. Thus, the majority of the sample passes to the drain.

To mitigate nebulisation efficiency limitation and analyte transport efficiency issues associated with the polydispersity of the aerosol, different types of nebulisation techniques such as ultrasonic, thermo-electro spray, high-efficiency direct injection and pneumatic nebulizers have been investigated in the field of ICP-MS and AAS instrument development. The ultrasonic nebulizer, which generates aerosol droplets by ultrasonic vibrations produced by a piezoelectric crystal, is reported to give 80–100% analyte transport efficiency at flow-rates in the range of 5–20 µl/min [34]. Thermo-spray techniques are commonly used for sample introduction in mass spectrometry techniques [35-37]. Use of a mono-disperse dried micro-particulate injector (MDMI); for sample introduction in ICP has been investigated for better nebulisation and analyte transport efficiency [38,39]. However, the use of these techniques in the context of ELSD and C-CAD has not been reported so far. The role of concentric and orthogonal pneumatic spraying has been investigated by different instrument manufacturers and a few research groups [40,41], and has been found to play a marginal role in detection performance. Cooling of the nebuliser by adiabatic expansion of gas results in coarser droplets, and particularly with highly volatile organic solvents nebuliser freezing can significantly influence the primary aerosol. Therefore, the majority of the commercial ELSDs offer nebuliser temperature control over a wide range. Likewise, the new generation C-CADs (Corona Ultra-RS and Veo C-CAD) allow the adjustment of nebuliser temperature over the range 20-35°C.

Besides the design of sample introduction systems, the nebulizer gas significantly influences the residence time and the extent of desolvation of droplets. It is commonly reported that nebulizer gas flow has to be in the sonic range, for stable aerosol and consequently for optimum detection. Charlesworth [16] has studied the

impact of nebulizer gas flow-rate on the process of atomization in the ELSD spray chamber. Gas pressure of 1.38 × 102 kPa (which corresponds to 2.1 × 10 $dm^3.min^{-1}$ by a plot of gas flow rate versus pressure), with a capillary tube extending at a distance of 0.5 mm with respect to the air-nozzle was found to give satisfactory atomization. Guiochon et al. [42], investigated different types of concentric nebulizers for ELSD and reported that a gas flow-rate of ~2.7 $L.min^{-1}$ give maximum response. Their results show that the response of ELSD varies in a sigmoidal manner as a function of gas flow-rate. At high gas flow-rate, detector response decreases rapidly due to a significant drop in signal as well as increased noise level, whereas at low gas flow-rate noise increases rapidly due to coarse atomization and partial desolvation [18]. In summary, poor nebulisation efficiency is still a major factor contributing to the lower sensitivity of aerosol-based detectors.

1.3.1.2 Droplet desolvation

After nebulisation, the primary aerosol flows into a desolvation chamber. At set conditions, because of the polydisperse nature of the primary aerosol produced by pneumatic nebulisers, larger droplets may traverse to the detection unit without complete desolvation and consequently produce high baseline noise. Therefore, to ensure complete desolvation of the droplets containing solute particles, in most of the commercial models of aerosol-based detectors, the larger droplets in the primary aerosol are generally removed by placing a droplet filtration unit between the nebuliser and heated desolvation chamber. There have been different approaches to remove larger droplets. In one approach, an impactor plate, which can be switched on and off in a direction perpendicular to the aerosol flow, is positioned at the entrance of the drift tube to remove larger droplets from the primary aerosol [43]. Many commercial ELSDs employ thermo-split flow technology [44]. In this approach, a curved aerosol trajectory allows small droplets to travel towards detection unit, whereas larger droplets, having low mobility, impact onto the curved surface of the drift tube and pass to the drain. In alternate designs passage of larger droplets to the detection unit is controlled by using a diffuser trap [45]. This is typically comprised of coiled, thermally conductive tubing with an internal diameter smaller than the primary aerosol cone exiting the nebuliser and positioned before the evaporator chamber. In this design, a diffuser trap prevents entry of larger droplets. Additionally, a large heated surface facilitates faster evaporation of larger droplets, which is claimed to reduce background noise and to give

improved sensitivity [45]. To address the issue related to undesirably large droplets, C-CADs normally employ an impactor-plate splitter.

The droplet filtration process results a remarkable modification in the aerosol characteristics. The resultant aerosol, which is commonly termed as a secondary aerosol, is then subjected to the desolvation process. The dependence of the solute evaporation time (t_d) upon different factors has been explained with the following equation [16]

$$t_d = \Delta H_v \, \rho_s \, r_i^2 / 2 \, M k_f \Delta T \qquad \text{(Equation – 1.1)}$$

According to this equation, the time required for complete removal of the solvent from droplets containing analyte particles vary in direct relation to the radius of secondary aerosol droplet (r_i), the latent heat of evaporation (ΔH_v), density (ρ) of the solvent and in inverse relation with molecular weight (M), thermal conductivity (k_f) of the solvent and temperature difference between air temperature and surface temperature (ΔT) of the droplet. Dependence of desolvation time (t_d) on droplet characteristics can also be given by an expression derived from Langmuir and Kelvin equations as follow [21]:

$$t_d = (D_{wet})^3 (12 D \gamma P_s) - 1 (pRT/M)^2 \qquad \text{(Equation – 1.2)}$$

Where, D_{wet} = diffusion coefficient for vapour molecules, γ = the surface tension coefficient, P_s = vapour pressure over the droplet surface, ρ = droplet solvent density, RT = product of Gas constant and temperature and M = molecular weight of vapour. Typically, evaporation is achieved by alteration of the evaporator tube temperature based on the volatility of the solvents. The extent of desolvation and hence the size of the solute particles depend mainly on the rate of evaporation of the solvents from the droplets containing analyte particles. Further, the vapour-saturated medium inside a spray chamber renders alteration in aerosol transport. The physical properties of solvents significantly influence the secondary aerosol that enters into the detection unit (optical unit in ELSD and charger unit in C-CAD) and consequently the detection performance.

1.3.1.3 Detection mechanism

The response of the ELSD is a measure of light scattered by analyte particles. In the ELSD, depending on the ratio of the diameter of the dried solute particle to the incident light wavelength, light scattering takes place through three different

mechanisms [16]. When irradiated by a light source, solute particles with a diameter (d_p) to wavelength (λ) ratio of much less than 0.1 behave like a point source and pass through the optics undetected due to Rayleigh-scattering. Particles in the size range as the incident wavelength ($0.1 \leq (d_p/\lambda) \leq 1$) lie in the Mie-scattering domain, while particles much bigger than the incident wavelength ($d_p/\lambda >> 1$) exhibit physical scattering by reflection and refraction mechanisms. Due to the polydisperse nature of the aerosol generated by conventional pneumatic nebulisers, the response of the ELSD results from a combination of different scattering mechanisms. This underlines the importance of the size of the dried solute particles in the response mechanism for the ELSD. The size of the solute particles reaching the optical unit depends on concentration (C), density of an analyte (ℓ_a) and the average size of the droplets (D_0) produced in the process of nebulisation [40].

$$d = D_0 \left(C / \ell_a \right)^{1/3} \qquad \text{(Equation – 1.3)}$$

Droplets generated in the primary aerosol undergo alterations while travelling along the length of the evaporator tube. Moreover, the number of dried particles per droplet decreases with a decrease in analyte concentration. Both of these factors result in the formation of tiny solute particles. Normally, solution with 1 ppm analyte concentration produces dry analyte particles of 0.1 μm diameter, thereby approaching the limit of detection. Because of the limitations in detecting Rayleigh scattering, the majority of analyte particles with a diameter to wavelength ratio (d_p/λ) < 0.1, pass through an optical path undetected. For instance, in the case of a commercial ELSD employing a light source of 620 nm, particles with size approximately ≤ 60 μm generally go undetected. Optimization of the nebulisation parameters to produce larger droplets could improve the detection limit of ELSD. Reducing the nebuliser gas flow-rate could be one way to increase droplet size and consequently the size of the dried solute particles [40]. Nevertheless, reducing flow-rate may result in incomplete vaporisation of the droplets and consequently increase the baseline noise. Also, for optimum performance of aerosol-based detectors, gas flow-rate has to be maintained in the sonic range [18,40]. Thus, working at a low gas flow-rate demands alteration in nebuliser design (annular space between gas and liquid carrying capillary and internal diameter of liquid capillary) to maintain optimum gas velocity.

Contrary to the ELSD, which measures light scattering intensity exhibited by dried solute particles, the C-CAD involves electrical measurement of the current produced by charged solute particles. The current generated by an electrometer is proportional to charge trapped in the Faraday cup filter, which depends on the population of dry solute particles passing through the charging region and the efficiency of charge deposition. The process of nebulisation and aerosol formation determines the mass flow of dry solute particles, whereas the efficiency of charge deposition depends on particle size, residence time of the particle in the charging zone and the mechanism of charge deposition. Thus, under controlled concentration of positively charged gas ions and electric field; the aerosol particle characteristics dominate the detector sensitivity. Liu and Pui [46] have experimentally demonstrated the strong dependence of detection sensitivity on the size of the solute particles. They observed that at fixed charger *Nt* (product of ion concentration and particle residence time) of 1×10^7, sensitivity drops from 400 pA/(10^6 particles/cm^3) to 0.056 pA/(10^6 particles/cm^3) with a decrease in particle size from 1000 nm to 7.2 nm. Furthermore, by a linear extrapolation of log-log calibration curve of sensitivity (in pA/(10^6 particles/cm^3)) versus particle size (µm), the minimum measurable current was found about 2×10^{-15}A at a particle size of 6 µm. An equation for sensitivity per particle mass concentration (S_m) was reported by Dixon et al. [19]:

$$For\ d_p < 10\ nm\ S_m = \frac{4.4 \times 10^5}{\rho_p} \cdot d_p^{\ 3.6} \qquad \text{(Equation – 1.4)}$$

$$For\ d_p > 10\ nm\ S_m = \frac{3.01 \times 10^{11}}{\rho_p} \cdot d_p^{\ -1.89} \qquad \text{(Equation – 1.5)}$$

Where, *Sm* is sensitivity per particle mass (Unit: fA m^{3}g^{-1}) and d_p is solute particle size,

The detection limit of charged aerosol detectors is related to the sensitivity of the electrometer (Faraday cup) to detect currents of less than fA, as well as the efficiency of the charger unit to deposit detectable charge on nano-scale (< 10 nm) particles. Particles with less than 10 nm diameter generate a signal of 2 mV, which is near the theoretical limit of voltage measurement [47, 48] of a typical electrometer. In commercial charged aerosol detectors designed for LC separations, the maximum signal is reported to occur in the 10–32 nm particle size range [19]. Thus, in addition to losses related nebulisation efficiency, the small size of solute particles is another major cause of the lower sensitivity of C-CAD.

1.3.1.4 Analyte properties

Besides experimental conditions, the physical properties of the analyte also influence the detection sensitivity to some extent [21, 24, 49]. The thermal stability of an analyte is a pre-requisite for optimal detection sensitivity using ELSD and C-CAD. These detectors respond to the dried solute particles that remain after desolvation of the droplets carrying solute mass. Obviously, the analyte must be less volatile than the mobile phase. Lower sensitivity of ELSD and C-CAD for semi-volatile analytes has been reported previously [24, 50, 51]. Additionally, difficult to evaporate mobile phases require a high drift tube temperature and this poses a risk of thermal decomposition of thermo-labile analytes. As described in the previous section, a new generation of ELSDs capable of sub-ambient evaporation have been introduced by instrument manufacturers [52]. Nevertheless, response variability of different models [50, 53] can limit wide adoption in the pharmaceutical industry. Sinclair et al. [54] assessed the C-CAD response accuracy using a set of 22 compounds comprised of anions, cations, zwitterions and neutrals. Their study shows how analyte-mobile phase adduct formation contributes to C-CAD response discrepancies. Based on these findings, Cohen et al. [55] have proposed an empirical approach to extend C-CAD detection of volatile organic bases. They demonstrated that C-CAD detection of volatile organic bases can be improved significantly by means of adduct formation with counter ions of mobile phase modifier. Factors such as pKa, ionisation state and steric effects of analyte and mobile phase were found to influence the formation of detectable salt. This approach demands extensive screening for selecting appropriate modifier. Also baseline noise contributed by these modifiers can adversely affect detection sensitivity. The diffusivity of an analyte and consequent varying band dispersion in the detection cell is another important factor that has been identified to cause variation in analyte response under identical conditions [51]. Snow-flake type analytes are reported to have higher response [16]. In the C-CAD, the process of charge deposition influences the response outcome. Since commercial C-CADs employ a unipolar charger, the charge state of the atmosphere surrounding the particles in the charger unit influences the charging efficiency. At higher pH electrostatic repulsion between the charged state of solute particles and positively charged analytes can adversely affect the signal.

As discussed above, there are several interrelated factors that contribute towards lower sensitivity of C-CAD and ELSD. Nevertheless, considering the

absorbance limitations of the UV-detector, the ability of these detectors to provide uniform and reproducible response for weakly chromophoric and non-chromophoric compounds can be a tremendous advantage. In comparison with ELSD, CAD is commonly reported to give much better (2 to 12% higher) sensitivity (Table-1.1).

1.3.2 Nonlinear detector response

The ability of the detector to provide linear response with respect to analyte concentration is one of the most important criteria in the selection of the detection technique for quantitative analysis. In practice, all detectors provide linear response only in a specific concentration range of analyte. A limited linearity range is one of the major limitations of the aerosol detectors. The nonlinear response characteristic of aerosol-based detectors arises from: a) modification in tertiary aerosol as a function of concentration and b) effects of solvent composition on the aerosol transport process.

1.3.2.1 Concentration non-linearity

A non-linear relationship between detector signal and the amount of analyte mass is one of the major concerns in adopting these techniques for quantitative analysis. The non-linear relationship between signal output (A) and analyte mass (m) is generally described by the equation:

$$A = a \cdot m^b \qquad \text{(Equation – 1.6)}$$

A linear calibration curve can be obtained using the logarithmic form of equation-1.6 as follows:

$$\log A = \log a + b \log m \qquad \text{(Equation – 1.7)}$$

The influence of various factors such as solvent and solute properties, nebulizer geometry and nebulisation-evaporation parameters on the response characteristics of ELSD has been investigated previously. It is commonly reported that the 'b' value of log-log correlation between detector output and sample concentration, lies in the range of 1-2, and varies in inverse relation with the coefficient 'a' [40,42,56,57]. Mojsiewicz-Pienkowska [58] has provided a detailed review of several calibration approaches that have been developed so far to take account of nonlinear characteristics of the ELSD detector. The dependence of linearity of ELSD response on concentration (C) and droplet size (D_0) has been modelled by Oppenheimer et al. [59] using light scattering

and nebulisation theories. They showed that the ELSD response curve exhibits both a linear as well as an exponential region and the linear region of a calibration curve shifts to the lower concentration as D_0 increases. At a lower concentration level, the slope of the curve was found to decrease from 2.0 to 1.87 with an increase in D_0 from 5 μm to 20 μm. The curve then approached linearity (slope = 1) with an increase in analyte concentration. However, an increase in sample concentration or modifications of the nebulizer process to generate larger D_0, has some practical implications. Larger droplets require more heat for complete desolvation, which in turn can affect the response of thermo-labile compounds. In addition, droplets containing a high concentration of analytes produce dried particles of low surface area to volume ratio, which leads to underestimation of analyte mass flow.

1.3.2.2 Solvent dependency

It is very common to use solvent gradient for HPLC separation of samples containing multiple compounds of varying physicochemical properties. In aerosol detectors the physical properties of the eluent strongly influence the aerosol characteristics, such as size distribution and average size of droplets. Therefore, for an analyte of the same concentration, the response of aerosol-based detectors varies remarkably across the solvent gradient. When used in solvent gradient separation, response correction of aerosol-based detectors requires multiple calibration curves. This poses practical difficulties in quantification because of the limited amount and / or lack of standards for impurities. Compatibility of aerosol detectors with solvent gradient liquid chromatography methods has long been an important topic of research. Many different ways to mitigate solvent gradient effects have been proposed so far. Stolyhwo et al. [18] proposed drift tube temperature programming to minimize the solvent gradient effect. According to another approach, an evaporator gas flow-rate can be varied across a solvent gradient run to compensate solvent effects [60]. The utility of this approach was demonstrated by injecting 5-fluorocytosine sample at regular intervals across the solvent gradient run. The real time modulation of the evaporator gas was claimed to control the amount of analyte particles entering the optical unit. However, application of these techniques is seldom reported. Mathews et al. [60] has proposed a generic calibration method to account for the response non-linearity of ELSD associated with sample concentration and solvent effects. In their study, a 3-D surface plot of detection response as a function of sample concentration and mobile

phase composition, constructed by multiple injections of a single non-volatile and non-retained calibrant was used to minimize the quantification errors. Similarly, a two-step response model was developed by Hutchinson et al. [61] to relate the C-CAD response with the variation in sample concentration and mobile phase composition. A set of analytes with a wide range of structures and physicochemical properties studied, using this model was found to give average absolute relative error of 12.5% between experimentally measured and calculated response values. In 2006, Gorecki et al. [62] proposed a post-separation inverse gradient approach to compensate for solvent gradient effects in C-CAD detection. Subsequently, the utility of the same approach for the response normalisation in ELSD detection was demonstrated by de Villiers et al. [63]. In this approach, a secondary stream of solvent is mixed with column effluent in a way that the mixture of aqueous-organic eluent being introduced into the detector inlet remains in equal proportions throughout the run. Lisa et al. [64] applied this approach for quantitative analysis of plant oil triacylglycerols (TGs), using non-aqueous reversed phase LC–C-CAD. A combination of C-CAD with inverse gradient solvent compensation was found to yield less than 5% response deviation and hence was claimed to be a superior approach to the atmospheric pressure chemical ionisation-mass spectrometry (APCI-MS) method.

Although several experimental and hardware modification approaches have been investigated so far, no single approach can be applied to a wide range of analytes and experimental conditions.

1.3.3 Response prediction models

As discussed earlier, there are several interrelated factors which influence the response characteristics of ELSD and C-CAD. Therefore, there has been increasing demand for reliable models to enable response optimisation. Similar to ICP-MS and AAS, primary aerosol characteristics, such as size distribution and average size of the droplets (D_0) determine the fate of the overall detection process. A few empirical studies on ICP-MS and AAS have correlated the response alterations as a function of various experimental and instrumental parameters using aerosol characterisation techniques. A correlation between various experimental factors, physical properties of solvents and consequent aerosol characteristics has traditionally been explained using the Nukiyama-Tanasawa (NT) equation, which was proposed in 1938 for simulation of fuel combustion phenomena in automotive fuel sprays [17, 40, 42].

$$D_0 = \frac{585\,\sigma^{1/2}}{(v_g - v_l)\,\rho_l^{1/2}} + 597\left(\frac{\mu_l}{(\sigma\rho_l)^{1/2}}\right)^{0.45}\left(\frac{1000Q_l}{Q_g}\right)^{1.5} \qquad \text{(Equation – 1.8)}$$

Where, D_0 = Sauter mean diameter - (μm)

v_g and v_l = velocity (m/s) of gas and liquid respectively,

σ = Surface tension - (dyne/cm)

ρ = Liquid density - (g/cm^3)

μ = Liquid viscosity - (Poise or dyne·s/cm^2)

Q_l and Q_g = Volume flow rate (cm^3/s) of liquid and gas respectively

In the context of analytical instrumentation, the Sauter mean diameter (SMD), which is a function of volume to surface area ($D_{3,2}$), is commonly used to denote the average size of the aerosol droplets. According to the NT-equation, SMD is directly proportional to the ratio of volume flow rate of liquid and nebulizer gas (Q_l/Q_g) and it varies in inverse proportion with difference in velocity of gas and liquid, *i.e*. SMD of droplets increases with an increase in the liquid flow-rate or with a decrease in nebulizer gas flow-rate. At constant gas and liquid flow-rate, droplet diameter depends on physical properties of the liquid solvent. The NT-equation is valid in the range $0.7 < \rho < 1.2$ m/ml, $19 < \sigma < 73$ dyne/cm and $0.003 < \eta < 0.5$P [17], but it is commonly criticized for overestimation of D_0 at high liquid to gas flow rate ratios. Robles et al. [65] reported that absolute size predictions by the NT-equation are larger than the experimental values by a factor of 1.8 – 8.1 for water and 3.6 to 13.3 fold for aqueous-organic solvent mixtures. The increased error for organic solvents can be attributed to the tendency of organic solvents to produce fine droplets due to lower surface tension compared to water. Browner et al. [66] experimentally evaluated the influence of parameters such as gas flow-rate, liquid flow-rate and nebulizer geometry on accuracy of the NT-predictions using water, butan-1-ol and methanol. Their results showed a decrease in SMD in the order water > butan-1-ol > methanol, which can be explained by the possibility of tiny droplet formation due to the decreasing order of surface tension for these solvents (surface tension at 20°C water- 72.58, butan-1-ol- 24.57 and methanol- 22.55; Unit: dyne cm^{-1}) and relative volatility (at 20°C water- 0.085, butan-1-ol- 0.11 & methanol- 1.00). However, predictions by the NT-equation clearly showed overestimation of SMD for all three solvents. Prediction of significantly larger SMD for butan-1-ol compared to water and methanol explains the influence of viscosity of solvents (at 20°C viscosity of water-1.002, butan-1-ol- 2.948 and methanol-0.551 Unit:

dyne S cm^{-2}) in NT predictions. According to Poiseuille's law, the effect of viscosity of a liquid is more prominent for a primary aerosol, but during transportation to the point of measurement its effect diminishes with increasing surface tension. The evaporation and coalescence phenomena, which depend on relative volatility of solvents, dominate the nature of dried particles. Thus, the second term of the NT equation, which depends on physical properties of the solvent has been claimed to be responsible for erroneous predictions. An error in determination of mean diameters by the NT-equation could also be due to the fact that the losses related to the nebulisation and impaction processes, as well as size alterations during aerosol transportation inside the spray chamber, are not considered in NT-calculation. In experimental approaches, different particle sizing techniques measure the characteristics of the aerosol, which have already undergone significant alterations between the aerosol generation and measurement steps. Gustavsson et al. [67] concluded that the NT – equation is valid for $15 < D < 10$ µm. To overcome these errors, different models predicting average droplet size ($D_{3,2}$) from properties of the gas, liquid and nebulizer geometry have been proposed [67]. In view of errors due to the first two terms in NT-predictions at high Q_l/Q_g ratio and for some solvents, Kahen et al. [68] have proposed a modification in the NT-equation to compensate for these effects. The modified NT- equation is:

$$D_{3,2} = \frac{P_1}{V}\left(\frac{\sigma}{\rho}\right)0.5 + P_2\left(\frac{\eta}{(\sigma\rho)0.5}\right)0.45\left(Exp\left(-\frac{Q_g}{106Ql}\right)\right) \qquad \text{(Equation – 1.9)}$$

The effect of the first two terms of the NT equation has been compensated by applying factors P_1 and P_2, obtained by nonlinear curve fitting of the 'plots of measured and calculated $D_{3,2}$ values versus nebulizer gas flow-rate' for different solvents. An exponential decay type NT-expression with the inclusion of new coefficients P1 = 86.4 and P2 = 105.4, is reported to give better accuracy than the original equation.

Despite these deficiencies, the NT-equation is often used to explain response characteristics of ELSD and C-CAD. The majority of work in the field of ELSD and C-CAD revolves around indirect assessment of aerosol characteristics. Seldom have aerosol characterisation techniques been used to correlate response alterations as a function of different experimental conditions. The effects of solvent and analyte properties on the detection response were investigated by Rigezza et al. [40]. Later Stolywho et al. [18] investigated the critical aspects of the detection mechanism. In the

early 1980's when ELSD was made commercially available, the focus turned towards building response prediction models. Meren et al. [69] investigated the effect of the ratio of gas/liquid flow-rates, analyte concentration, peak shape and solvent properties on aerosol characteristics. They proposed an empirical response model to simulate the ELSD response. More recently, Hutchinson et al. [61] has proposed a 3-D response model for C-CAD. Nevertheless, considering the large number of variables involved in aerosol detection, response modelling still remains a major challenge. Most of the research work has been dedicated to the determination of mean drop size at different operating conditions. In the case of non-aqueous and high temperature separations, physical properties of eluent solvents lie beyond the NT-threshold. Therefore, it would be more appropriate to use the modified NT-equation to predict possible alterations in aerosol characteristics. A correlation between SMD predictions and experimental response measurement can enable more accurate simulation of aerosol response characteristics.

1.4 Hyphenation of aerosol-based detectors with high temperature liquid chromatography

Recently there has been renewed interest in HTLC. Over the years, several reviews have appeared that cover various aspects of HTLC [70-75]. Lack of thermally stable stationary phases has been cited as one of the major obstacles to mainstream adoption of HTLC. Nevertheless, continued research in stationary phase chemistry has produced some interesting liquid chromatographic supports, such as polymer-coated zirconia and titania phases [76-78], porous graphitised carbon (PGC) based stationary phase [79-81] and polymer-based monoliths [82, 83]. A limitation in achieving elutropic strength comparable to conventional solvent gradients, due to the limited temperature range and low ramp rate of present-day column heating devices, has been identified as another major barrier to the implementation of HTLC in routine analysis. In recent years, substantial progress has been made to improve the performance of column heating modules. Critical aspects, such as radial/axial temperature gradient effects, mobile phase preheating requirements, influence of the thermal mass of a column on heat transfer and benefits of higher heating rates have been investigated extensively in conjunction with different design aspects of the column heating module [84-88]. This has resulted in a shift from high power consuming basic methods of column heating, such as an oil bath [89], hot water bath or air convection heating ovens

[86], towards more efficient resistive heating methods [90]. In 2009, Pursch et al. [91, 92] introduced a tubular resistive heating module to optimize faster and power efficient temperature programming (heating ramp up to 1800°C/min and cooling at 100-200°C/min) for capillary scale LC-separations. Using this low thermal mass (LTM) technology, a conceptual approach to selectivity optimisation by means of temperature pulsing has been reported recently [93,94]. Nevertheless, it is worth noting that LTM heating modules require packed columns with i.d. <0.5 mm. Besides these developments, compatibility of conventional LC-detectors with a high-temperature column effluent has long been a major concern in the implementation of the HTLC approach [70, 95]. Thus far, UVD has been the most common method of detection in HTLC separations. Limitations of UVD, such as the dependence of response on chromophoric properties of the analytes and baseline deviation during solvent gradient separations using UV-absorbing mobile phases are well known. Moreover, when coupled to HTLC separations, UVD require post-separation temperature conditioning of the mobile phase to avoid the baseline disturbances associated with temperature-dependent deviations in refractive index of the mobile phase in the detection cell [96]. Similarly, the detection responses of universal detectors, such as refractive index and conductivity detectors, have been reported to vary with alterations in physical properties of the mobile phase as a function of separation temperature [73].

In view of the eluent temperature limitations of the conventional LC-detectors there has been increasing interest in the hyphenation of HTLC with aerosol detectors. Both HTLC and aerosol-based detectors have their own advantages/disadvantages and therefore a combination of these two techniques demands a balance between compatibility and complementarities of these techniques. Hyphenation of aerosol-based detectors with HTLC has been reported by a number of researchers recently (Table-1.2). The majority of these studies have focused on the separation parameters and the benefits of non-aqueous HTLC, in applications involving the separation of compounds of limited water solubility, such as polymers and lipids. Interfacing aerosol-based detectors with HTLC separations employing micro and capillary scale columns is another area that has appealed to many researchers. Since the evaluation criteria of most of these studies were based on specific application needs, it is hard to draw a general conclusion about the effect of HTLC conditions on the response

Table 1.2: Experiments involving the coupling of aerosol-based detectors with HTLC separations.

Application Details	Mobile phase solvents	Column and Separation temperature	Detector
Investigations into the performance of capillary scale non-aqueous HTLC separation approach and characterisation of polymer additives [97]	Dimethylformamide, ACN and triethylamine	Capillary column (400 and 700 mm × i.d. - 0.3 mm) packed with porous Hypersil ODS (3 μm), Temperature: 30 - 175°C (isothermal and temperature gradient)	ELSD (Varex Mark III, Alltech)
Separation of oligomeric hindered amine stabilisers for comparison of their molecular weight distribution [98]	Ternary mixture of ethyl acetate, ACN, acetic acid and triethylamine	Fused silica capillary columns (350 × 0.32 mm, i.d.) packed with porous Hypersil ODS, Kromasil-100 RP18 (5 μm) and Hypersil BDS (3 μm) Temperature: 30 - 120°C (Temperature gradient)	ELSD (Varex Mark III, Alltech) with modified nebuliser
Characterisation of high molecular weight hindered amine light stabilisers [99]	Mixture of ethyl acetate, ACN, acetic acid and triethylamine	Polyimide coated fused silica capillary column (350 × 0.32 mm, i.d., 3 μm) packed with porous Hypersil ODS Temperature: 30 - 120°C (Temperature gradient)	ELSD (Varex Mark III, Alltech) and ESI-TOF-MS (MicroMass)

Table 1.2: Experiments involving the coupling of aerosol-based detectors with HTLC separations (cont.)

Application details	Mobile phase solvents	Column and Separation temperature	Detector
Evaluation of column bleeds at high temperature separation [100]	Pure water	Commercially columns packed with C18, PGC, zirconium dioxide and titanium dioxide, Temperature range: 30-200°C (temperature gradient)	C-CAD
Analysis of the reaction products resulting from the synthesis of ethylene-styrene block co-polymers [101]	1,2,4-trichlorobenzene, 1,2-dichlorobenzene, decalin and cyclohexanone	Lichrosorb-100, Perfectsil-300 and Nucleosil-500 column (250 × 4.6 mm, i.d., 5 µm), Temperature: 100-140°C (isothermal)	(ELSD) PL-ELS-1000
HTLC separation of triacylglycerols in cocoa and shea butter using PGC column [102]	Mixture of trichloromethane and propan-2-ol (80/20, v/v)	Hypercarb column (150 × 2.1 mm, i.d., 5 µm), Temperature: 30-70°C (isothermal)	ELSD (Sedex-85, Sedere)
Analysis of Sqalene, Cholesterol and Ceramide-IIIB [57]	100% propan-1-ol, butan-1-ol and ethanol	Capillary column (150 × 0.53 mm, i.d.) packed with Thermo Hypercarb (5 µm) Temperature: 100 - 150°C (isothermal)	ELSD (Eurosep DDL-31), C-CAD and Ion-trap MS with ESI and APCI source

Table 1.2: Experiments involving the coupling of aerosol-based detectors with HTLC separations (cont.)

Application details	Mobile phase solvents	Column and Separation temperature	Detector
Investigations into the effect of micro-scale non-aqueous HTLC conditions on separation kinetics in lipid analysis [103]	Mixture of ACN, ethanol, propan-1-ol, buta-1-ol and ethyl acetate	Capillary column (150 × 0.53 mm, i.d.) packed with Thermo hypercarb (5 µm), Temperature: 50 - 150°C (Isothermal)	ELSD (Eurosep DDL-31)
Analysis of Artesunate-Azithromycine combination product [104]	ACN and methanol containing formic acid	Hypercarb column (50 × 3 mm, 5µm) Temperature: 30 - 90°C (isothermal)	ELSD (CHROMACHEM Eurosep)

characteristics of aerosol-based detectors. Nevertheless, it highlights some critical factors that need to be considered for HTLC-aerosol detector interfacing; which will be discussed in the following sections.

1.4.1 Restrictor coil interface

Unlike the UVD, aerosol-based detectors do not need post-separation cooling of the column effluent. Nevertheless, at high temperatures, boiling of the column effluent causes sputtering of mobile phase at the end of the effluent transfer tubing which may interfere with the process of nebulisation and aerosol formation. Therefore, a fused-silica capillary having a small internal diameter compared to the column outlet tubing is normally used to transfer HTLC effluent into the nebuliser [57, 70, 99, 105]. It creates sufficient back-pressure to prevent phase transition of the liquid mobile phase at high temperature and, therefore, it is commonly termed a restrictor coil. The functioning of the restrictor coil can be explained on the basis of the pressure-temperature dependence of vapour pressure of eluent constituents. Fundamentally, a liquid starts boiling when its vapour pressure equals the pressure exerted by the surrounding system. Teutenberg et al. [106] investigated the temperature dependence of vapour pressures of commonly used aqueous-organic pure solvents and their binary mixtures in the range of 50°C to 250°C. Their results showed that the vapour pressure of the organic-aqueous liquid mixtures increases in a non-linear manner with an increase in temperature and organic solvent content, causing vaporisation of aqueous-organic mixtures at a lower temperature compared to that of pure aqueous constituents. At increased pressure, it requires a higher temperature for the vapour pressure of the liquid mixture to attain equilibrium with external pressure and thus the boiling point of the liquid mixture is raised. Therefore, the dimensions of the restrictor coil to be used to suppress boiling of eluent must be determined based on the separation temperature and solvent composition. In particular, solvent gradient-HTLC separation requires a restrictor coil to provide sufficiently high external pressure to cover the entire range of the vapour pressure changes that may occur during the separation. At atmospheric pressure (1.013 bar) water starts boiling at 100°C, whereas at 4.8 bar and 16 bar the boiling point of water shifts to 151°C and 200°C respectively. Due to the relatively low vapour pressure of water a restrictor coil capable of generating about 16 bar pressure would be sufficient to prevent boiling of an aqueous eluents in the normal temperature

range (< 200°C) of HTLC separations. Therefore, isocratic-temperature gradient separation employing water rich eluents appears to be a more convenient approach.

1.4.2 Effects of separation temperature on detector response

Aerosol-based detectors involve evaporation of the aerosol generated from a liquid effluent, which is why hyphenation with HTLC is generally believed to complement these detectors [41,70]. Although high temperature of an eluent can potentially assist in the process of droplet desolvation and analyte mass transport, response variation as a function of eluent temperature could be problematic when a temperature gradient is applied. Few studies have investigated the effect of eluent temperature on response of aerosol-based detectors. Hazotte et al. [57] compared the response of ELSD, C-CAD, ESI-MS and APCI-MS for micro-scale high temperature separation using non-aqueous eluents. They showed that low volume HPLC columns in combination with a high separation temperature can significantly enhance the intensity of ELSD and C-CAD responses enabling significantly lower LODs. Nevertheless, regardless of the type of the detector, peak area was found to decrease with an increase in temperature. Gieglod [107] investigated the temperature-dependent changes in the response of UVD, fluorescence and ELSD, using polycyclic aromatic hydrocarbons (PAHs) as analytes. An inverse relationship between detection response and the eluent temperature was observed for ELSD. These contradictory findings call for further investigation of the effect of eluent temperature on the response of aerosol-based detectors.

The restrictor coil connecting the column outlet to the nebuliser also serves as eluent transfer tubing. The outer diameter and the length of the restrictor coil significantly influence the rate of heat dissipation. Therefore, instead of separation temperature, the actual temperature of the column effluent entering into the nebulizer would be more relevant to detector performance investigations. Generally with conventional LC-separation conditions, a higher proportion of volatile organic solvents benefits aerosol detectors by virtue of faster desolvation. But in non-aqueous-HTLC separations, a restrictor coil may cause superheating of the eluent. Expansion of the superheated eluent stream into the relatively low-pressure atmosphere inside the evaporator tube produces a fine mist. Faster evaporation of fine droplets leaves behind very tiny particles and thus can contribute to the drop in detector response.

1.4.3 Capillary and micro-scale HTLC separations

Considering the limited range of the accessible elutropic strength and the necessity to maintain the optimum linear velocity of the mobile phase, HTLC separations are normally performed at a high flow-rate. However, the dependence of the detection response to solvent uptake rate prevents separations at higher flow-rates, when coupled to aerosol detectors. A decrease in the ELSD peak area with an increase in flow-rate under isothermal conditions (90°C) has been reported by Gaudin et al. [104]. The lower response at the higher flow-rate is reported to be related to tiny particles produced as a consequence of higher flow rates. There is also the possibility of increased loss of the majority of solute particles due to a drop in nebulisation efficiency at higher solvent uptake rates. Narrow-bore LC columns facilitate faster thermal-equilibration and allow operation at a higher linear velocity with much lower volumetric flow-rate. Combination of micro and capillary scale HTLC separations with aerosol detectors has therefore attracted considerable attention in recent years.

C-CAD and most of the commercial ELSDs contain a nebulisation cell compatible with analytical scale separations. Separation at micro-scale flow-rates produces low amounts of aerosol droplets, therefore the orifice of the nebulizer tip has to be smaller to maintain efficient atomization. Also, to avoid losses of the aerosol droplets onto the internal surfaces, a small volume evaporator tube is required. The influence of nebuliser design aspects, such as the annular space between the effluent capillary and the inside diameter of gas tube [23], the diameter of the nebuliser tip, the effect of gas/liquid volumetric flow-rate [12], and preheating of gas [24], has been investigated previously. Trones et al. [108] described the use of a modified nebuliser assembly. The feasibility of nebuliser gas preheating to overcome heat transfer limitations of the capillary nebuliser was investigated. Preheating of the nebuliser gas is reported to give a smoother baseline at relatively low drift tube temperature due to more stable and homogeneous aerosol formation. A rapid rise in baseline signal with an increase in steepness of the temperature ramp has been attributed to rapid mobile phase expansion at the high temperature ramp. Guillarme et al. [41] investigated the influence of the nebuliser cell geometry on response characteristics of ElSD, when coupled with micro-LC separations. Nebuliser cells tailored to suit low flow-rates in micro-scale separation are reported to minimise band-dispersion and improve the sensitivity of ELSD by about 20-30% compared to the conventional nebuliser cell. All these studies

underline the necessity of hardware modifications for these detectors to be used with micro and capillary scale HTLC separations.

1.5 Summary and aims

ELSD and C-CAD have emerged as powerful detection techniques for the LC separation of the non-chromophoric compounds in a wide range of application areas. With the ability to provide non-discriminating detection response, these techniques have strong potential to meet universal detection requirements. However, low sensitivity, response non-linearity and difficulty in response prediction have hindered their utility in the applications dominated by conventional detectors. Low sensitivity is attributed mainly to the poor nebulisation efficiency and complex nature of the aerosol transport and despite vigorous research from academic researchers as well as instrument manufacturers it has remained a major challenge. The dependence of the detection response on physical properties of the solvents is another important factor that contributes to the response non-linearity and sensitivity variation, thus complicating response prediction.

Because of the inherently complex nature of these limitations, in recent years the focus of the research on aerosol-based detectors has shifted towards exploiting their existing capabilities to find alternate ways to improve their analytical performance and to extend the field of applicability. Hyphenation with HTLC is among the major recent trends. Since ELSD and C-CAD involve conversion of liquid chromatography effluent into gaseous state it is believed that HTLC can complement the detection process of aerosol detectors. Likewise, by minimising the necessity of the post separation eluent cooling, aerosol detectors offer better detection alternative for HTLC and thus can assist in the regularising the HTLC approaches. HTLC separations under isocratic conditions can also potentially benefit aerosol-based detectors to overcome solvent gradient limitations. However, understanding of the effects of effluent temperature on the response characteristics of aerosol based detectors is essential for successful implementation of HTLC-aerosol-based detection approaches. Surprisingly little attention has been paid to this area.

The overall aim of this thesis is to investigate the compatibility and complementarity of the alternate separation approaches to improve analytical performance and thus extend the universal applicability of these detectors.

The specific aims were:

- To understand the effects of HTLC conditions on detection response and to investigate how HTLC can be used to improve performance of these detectors.
- To investigate the utility of temperature and flow-rate programmed separation approaches to improve the response uniformity of ELSD and C-CAD, so as to allow implementation single-point calibration for quantitative analysis.
- To seek practical means of overcoming the problems that may arise achieving these objectives.

1.6 References

[1] Drug Price Competition and Patent Term Restoration Act of 1984, Pub. L. No. 98-417, 98 Stat. 1585 (1984) (codified as amended 21 U.S.C. 355 (1994)), Drug Price Competition and Patent Term Restoration Act of 1984, Pub. L. No. 98-417, 98 Stat. 1585 (1984) (codified as amended 21 U.S.C. 355 (1994)).

[2] International conference on harmonisation of technical requirements for registration of pharmaceuticals for human use, Specifications: Test procedures and acceptance criteria for new drug substances and new drug products: Chemical substances Q6A, October, 1999.

[3] International conference on harmonisation of technical requirements for registration of pharmaceuticals for human use, Impurities in new drug substances Q3A (R2), October, 2006.

[4] International conference on harmonisation of technical requirements for registration of pharmaceuticals for human use, Impurities in new drug products Q3B (R2), June, 2006.

[5] International conference on harmonisation of technical requirements for registration of pharmaceuticals for human use, Validation of analytical procedures: Text and methodology Q2(R1), October, 1994.

[6] N. C. Megoulas, M. A. Koupparis, Twenty years of evaporative light scattering detection, Crit. Rev. Anal. Chem. 35 (2007) 301-316.

[7] R. Lucena, S. Cardenas, M. Valcarcel, Evaporative light scattering detector: trends in its uses, Anal. Bioanal. Chem. 388 (2007) 1663-1672.

[8] K. Mojsiewicz-pienkowska, On the issue of characteristic evaporative light scattering detector response, Crit. Rev. Anal. Chem. 39 (2009) 89-94.

[9] J. H. Arndt, T. Macko, R. Brull, Application of the evaporative light scattering detector to analytical problems in polymer science, J. Chromatogr. A 1310 (2013) 1-14.

[10] R. McCarthy, P. Gamache, D. D. Asa, Development and evaluation of Corona Charged Aerosol Detection (CAD): a new universal detector for HPLC, http://www.labint-online.com/uploads/tx_ttproducts/datasheet/development-and-evaluation-of-corona-charged-aerosol-detection-(cad)-a-new-universal-detector-for-hplc.pdf (2005).

[11] S. Almeling, D. Ilko, U. Holzgrabe, Charged aerosol detection in pharmaceutical analysis, J. Pharm. Biomed. Anal. 69 (2012) 50-63.

[12] T. Vehovec, A. Obreza, Review of operating principle and applications of the charged aerosol detector, J. Chromatogr. A 1217 (2010) 1549-1556.

[13] M. Ligor, S. Studzińska, A. Horna, B. Buszewski, Corona-Charged Aerosol Detection: An Analytical Approach, Crit. Rev. Anal. Chem. 43 (2013) 64-78.

[14] C. B. Fox, S. J. Sivananthan, T. J. Mikasa, S. Lin, S. C. Parker, Charged aerosol detection to characterize components of dispersed-phase formulations, Adv. Colloid Interface Sci. 199-200 (2013) 59-65.

[15] I. Sinclair, I. Charles, Applications of the charged aerosol detector in compound management, J. Biomol. Screen. 14 (2009) 531-537.

[16] J. M. Charlesworth, Evaporative analyzer as a mass detector for liquid chromatography, Anal. Chem. 50 (1978) 1414 - 1420.

[17] T. Mourey, L. Oppenheimer, Principles of operation of an evaporative light scattering detector for liquid chromatography, Anal. Chem. 56 (1984) 2427-2434.

[18] A. Stolyhwo, H. Colin, G. Guiochon, Use of Light Scattering as a detector principle in liquid chromatography, J. Chromatogr. 265 (1983) 1-18.

[19] R. W. Dixon, D. S. Peterson, Development and testing of a detection method for liquid chromatography based on aerosol charging, Anal. Chem. 74 (2002) 2930-2937.

[20] S. L. Kaufman, F. D. Dorman, Aerosol charge adjusting apparatus employing a corona discharge, US Patent 6,544,484, April 8, 2003.

[21] C. R. Mitchell, Y. Bao, N. J. Benz, S. Zhang, Comparison of the sensitivity of evaporative universal detectors and LC/MS in the HILIC and the reversed-phase HPLC modes, J. Chromatogr. B Analyt. Technol. Biomed. Life Sci. 877 (2009) 4133-4139.

[22] R. G. Ramos, D. Libong, M. Rakotomanga, K. Gaudin, P. M. Loiseau, P. Chaminade, Comparison between charged aerosol detection and light scattering detection for the analysis of Leishmania membrane phospholipids, J. Chromatogr. A 1209 (2008) 88-94.

[23] J. Shaodong, W. J. Lee, J. W. Ee, J. H. Park, S. W. Kwon, J. Lee, Comparison of ultraviolet detection, evaporative light scattering detection and charged

aerosol detection methods for liquid-chromatographic determination of anti-diabetic drugs, J. Pharm. Biomed. Anal. 51 (2010) 973-978.

[24] J. P. Hutchinson, J. Li, W. Farrell, E. Groeber, R. Szucs, G. Dicinoski, P. R. Haddad, Comparison of the response of four aerosol detectors used with ultra high pressure liquid chromatography, J. Chromatogr. A 1218 (2011) 1646-1655.

[25] L. Novakova, S. Lopez, D. Solichova, D. Satinsky, B. Kulichova, P. Solich, Comparison of UV and charged aerosol detection approach in pharmaceutical analysis of statins, Talanta 78 (2009) 834-839.

[26] B. Avula, Y.-H. Wang, T. Smillie, W. Mabusela, L. Vincent, F. Weitz, I. Khan, Comparison of LC–UV, LC–ELSD and LC–MS Methods for the Determination of Sesquiterpenoids in Various Species of Artemisia, Chromatographia 70 (2009) 797-803.

[27] J. A. Mclean, M. G. Minnich, L. A. Iacone, H. Liu, A. Montaser, Nebulizer diagnostics: fundamental parameters, challenges, and techniques on the horizon, J. Anal. At. Spectrom. 13 (1998) 829-842.

[28] B. L. Sharp, Pneumatic nebulisers and spray chambers for inductively coupled plasma spectrometry. A review. Part 1. Nebulisers, J. Anal. At. Spectrom. 3 (1988) 613-652.

[29] B. L. Sharp, Pneumatic nebulisers and spray chambers for inductively coupled plasma spectrometry. A review. Part 2. Spray chambers, J. Anal. At. Spectrom. 3 (1988) 939-963.

[30] R. F. Browner, A. W. Boorn, Sample Introduction: The Achilles' Heel of Atomic Spectroscopy?, Anal. Chem. 56 (1984) 786A-798A.

[31] J. Mora, S. Maestre, V. Hernandis, J. L. Todolí, Liquid-sample introduction in plasma spectrometry, Trends Anal. Chem. 22 (2003) 123-132.

[32] J. L. Todoli, J.-M. Mermet, 3 - Pneumatic Nebulizer Design, in Liquid Sample Introduction in ICP Spectrometry, José Luis Todoli, Jean-Michel Mermet (Editors), Elsevier, Amsterdam, 2008, p. 17-76.

[33] J. N. Alexander, Evaporative light scattering detection for microcolumn liquid chromatography, J. Microcolumn Sep. 10 (1998) 491-502.

[34] M. Tarr, G. Zhu, R. Browner, Microflow ultrasonic nebulizer for inductively coupled plasma atomic emission spectrometry, Anal. Chem. 65 (1993) 1689-1695.

[35] C. R. Blakley, M. L. Vestal, Thermospray interface for liquid chromatography/mass spectrometry, Anal. Chem. 55 (1983) 750-754.

[36] J. A. Koropchak, M. Veber, R. F. Browner, Thermospray Sample Introduction to Atomic Spectrometry, Crit. Rev. Anal. Chem. 23 (1992) 113-141.

[37] C. Yang, Z. Zhuang, Y. Tu, P. Yang, X. Wang, Thermospray nebulizer as sample introduction technique for microwave plasma torch atomic emission spectrometry, Spectrochim. Acta, Part B 53 (1998) 1427-1435.

[38] J. Olesik, S. Hobbs, Monodisperse dried microparticulate injector: A new tool for studying fundamental processes in inductively coupled plasmas, Anal. Chem. 66 (1994) 3371-3378.

[39] J. Olesik, J. Kinzer, Measurement of monodisperse droplet desolvation in an inductively coupled plasmas using droplet size dependent peaks in Mie scattering intensity, Spectrochim. Acta, Part B 61 (2006) 696-704.

[40] M. Righezza, G. Guiochon, Effects of the Nature of the Solvent and Solutes on the Response of a Light Scattering Detector, J. Liq. Chromatogr. 11 (1988) 1967 - 2004.

[41] D. Guillarme, S. Rudaz, C. Schelling, M. Dreux, J. L. Veuthey, Micro liquid chromatography coupled with evaporative light scattering detector at ambient and high temperature: Optimization of the nebulization cell geometry, J. Chromatogr. A 1192 (2008) 103-112.

[42] G. Guiochon, A. Moysan, C. Holley, Influence of Various Parameters on the Response Factors of the Evaporative Scattering Detector For a Number of Non-Volatile Compounds, J. Liq. Chromatogr. Relat. Technol. 11 (1988) 2547-2570.

[43] M. C. Benedict, Evaporative light scattering device, US Patent 6,229,605 B, May 8, 2001.

[44] J. Lu, S. F. Azlein, Aerosol splitter for ELSD, US Patent 7,290,723 B1, Nov 6, 2007.

[45] S. J. O'Donohue, F. P. Warner, P. Claes, N. Wrench, ELSD diffuser, US Patent 6122055 A, Sept 19, 2000.

[46] B. Y. H. Liu, D. Y. H. Pui, On the performance of the electrical aerosol analyzer J. Aerosol Sci. 6 (1975) 249-254.

[47] Low Level Measurements Handbook, 6th Edition - Keithley Instruments Inc.

[48] S. Dhaniyala, M. Fierz, J. Keskinen, M. Marjamäki, Instruments based on electrical detection of aerosols, in Aerosol Measurement: Principles,

Techniques, and Applications Third Edition, P. A. Baron and K. Willeke P. Kulkarni (Editor), John Wiley & Sons, Inc., Hoboken, NJ, USA, 2011.

[49] P. Sun, X. Wang, L. Alquier, C. A. Maryanoff, Determination of relative response factors of impurities in paclitaxel with high performance liquid chromatography equipped with ultraviolet and charged aerosol detectors, J. Chromatogr. A 1177 (2008) 87-91.

[50] G. K. Webster, J. S. Jensen, A. R. Diaz, An investigation into detector limitations using evaporative light-scattering detectors for pharmaceutical applications, J. Chromatogr. Sci. 42 (2004) 484-490.

[51] V. L. Cebolla, L. Membrado, J. Vela, A. C. Ferrando, Evaporative Light-Scattering Detection in the Quantitative Analysis of Semivolatile Polycyclic Aromatic Compounds by High-Performance Liquid Chromatography, J. Chromatogr. Sci. 35 (1997) 141-150.

[52] S. J. O'Donohue, N. J. Wrench, P. E. Claes, in, Google Patents, 2009.

[53] Y. Liu, S. Hou, L. Wang, S. Yang, Development and Validation of a Liquid Chromatography Method for the Analysis of Paromomycin Sulfate and its Impurities, J. Anal. Bioanal. Techniques 1 (2010).

[54] I. Sinclair, R. Gallagher, Charged Aerosol Detection: Factors for consideration in its use as a generic quantitative detector, Chromatography Today 1 (2008) 5-9.

[55] R. D. Cohen, Y. Liu, X. Gong, Analysis of volatile bases by high performance liquid chromatography with aerosol-based detection, J. Chromatogr. A 1229 (2012) 172-179.

[56] S. Heron, M. G. Maloumbi, M. Dreux, E. Verette, A. Tchapla, Experimental Proofs of a Correlation Between the Coefficients for the Slope of the Response Line and the Response Factor of an ELSD, LCGC Europe 19 (2006) 664-672.

[57] A. Hazotte, D. Libong, M. Matoga, P. Chaminade, Comparison of universal detectors for high temperature liquid chromatography, J. Chromatogr. A 1170 (2007) 52-61.

[58] K. Mojsiewicz-Pieńkowska, On the Issue of Characteristic Evaporative Light Scattering Detector Response, Crit. Rev. Anal. Chem. 39 (2009) 89-94.

[59] L. E. Oppenheimer, T. H. Mourey, Examination of the concentration response of evaporative light scattering mass detectors, J. Chromatogr. 323 (1985) 297-304.

[60] B. T. Mathews, P. D. Higginson, R. Lyons, J. C. Mitchell, N. W. Sach, M. J. Snowden, M. R. Taylor, A. G. Wright, Improving quantitative measurements for the evaporative light scattering detector, Chromatographia 60 (2004) 625 - 633.

[61] J. P. Hutchinson, J. Li, W. Farrell, E. Groeber, R. Szucs, G. Dicinoski, P. R. Haddad, Universal response model for a corona charged aerosol detector, J. Chromatogr. A 1217 (2010) 7418-7427.

[62] T. Gorecki, F. Lynen, R. Szucs, P. Sandra, Universal response in liquid chromatography using charged aerosol detection, Anal. Chem. 78 (2006) 3186-3192.

[63] A. d. Villiers, T. Gorecki, F. Lynen, R. Szucs, P. Sandra, Improving the universal response of evaporative light scattering detection by mobile phase compensation, J. Chromatogr. A 1161 (2007) 183-191.

[64] M. Lísa, F. Lynen, M. Holčapek, P. Sandra, Quantitation of triacylglycerols from plant oils using charged aerosol detection with gradient compensation, J. Chromatogr. A 1176 (2007) 135-142.

[65] C. Robles, J. Mora, A. Canals, Experimental evaluation of the Nukiyama-Tanasawa equation for pneumatically generated aerosols used in flame atomic spectrometry, Appl. Spectrosc. 46 (1992) 669 - 676.

[66] R. F. Browner, A. Boorn, D. Smith, Aerosol transport model for atomic spectrometry, Anal. Chem. 54 (1982) 1411-1419.

[67] A. Gustavsson, Prediction of Nebulizer Characteristics for Concentric Nebulizer systems with mathematical model, Anal. Chem. 56 (1984) 0815 - 0817.

[68] K. Kahen, B. Acon, A. Montaser, Modified Nukiyama-Tanasawa and Rizk-Lefebvre models to predict droplet size for microcentric nebulizers with aqueous and organic solvents, J. Anal. At. Spectrom. 20 (2005) 631-637.

[69] P. Van der Meeren, J. Vanderdeelen, L. Baert, Simulation of the mass response of the evaporative light scattering detector, Anal. Chem. 64 (1992) 1056-1062.

[70] T. Teutenberg, Potential of high temperature liquid chromatography for the improvement of separation efficiency - A review, Anal. Chim. Acta 643 (2009) 1-12.

[71] B. Wenclawiak, T. Teutenberg, High temperature liquid chromatography, Anal. Lett. 41 (2008) 1097-1105.

[72] S. Heinisch, J. L. Rocca, Sense and nonsense of high-tempearature liquid chromatography, J. Chromatogr. A 1216 (2009) 642-658.

[73] B. A. Jones, Temperature programmed liquid chromatography, J. Liq. Chromatogr. Relat. Technol. 27 (2004) 1331-1352.

[74] C. McNeff, B. Yan, D. Stoll, R. Henry, Practice and theory of high temperature liquid chromatography, J. Sep. Sci. 30 (2007) 1672-1685.

[75] C. Zhu, D. M. Goodall, S. A. C. Wren, Elevated Temperature HPLC: Principles and Applications to Small Molecules and Biomolecules, LCGC Asia Pacific 8 (2005).

[76] J. Nawrocki, P. W. Carr, Chemistry of zirconia and its use in chromatography, J. Chromatogr. A 657 (1993) 229-282.

[77] J. Nawrocki, C. Dunlap, J. Li, J. Zhao, C. McNeff, A. McCormick, P. W. Carr, Review - Part II, Chromatography using ultra-stable metal oxide-based stationary phases for HPLC, J. Chromatogr. A 1028 (2004) 31-62.

[78] J. Nawrocki, C. Dunlap, A. McCormick, P. W. Carr, Review - Part I, Chromatography using ultra-stable metal oxide-based stationary phases for HPLC, J. Chromatogr. A 1028 (2004) 1-30.

[79] L. Pereira, Porous graphitic carbon as a stationary phase in HPLC: Theory and applications, J. Liq. Chromatogr. Relat. Technol. 31 (2008) 1687-1731.

[80] S. Marin, B. Jones, W. D. Felix, J. Clark, Effect of high-temperature liquid chromatography column stability and performance under temperature-programmed conditions, J. Chromatogr. A 1030 (2004) 255-262.

[81] L. Pereira, S. Aspey, H. Ritchie, High Temperature to increase throughput in liquid chromatography and liquid chromatography - mass spectrometry with porous graphite carbon stationary phase, J. Sep. Sci. 30 (2007) 1115-1124.

[82] T. J. Causon, R. A. Shellie, E. F. Hilder, High Temperature liquid chromatography with monolithic capillary columms and pure water eluent, Analyst 134 (2009) 440-442.

[83] T. J. Causon, A. Nordborg, R. Shellie, E. Hilder, High temperature liquid chromatography of intact proteins using organic polymer monoliths and alternative solvent system, J. Chromatogr. A 1217 (2010) 3519-3524.

[84] S. Abbott, P. Achener, R. Simpson, F. Klink, Effect of radial thermal gradients in elevated temperature high performance liquid chromatography, J. Chromatogr. A 218 (1981) 123-135.

[85] H. Poppe, J. C. Kraak, Huber, Temperature Gradients in HPLC Columns Due to Viscous Heat Dissipation, Chromatographia 14 (1991) 515-523.

[86] H. Poppe, J. C. Kraak, Influence of thermal conditions on the efficiency of high performance liquid chromatographyic columns, J. Chromatogr. 282 (1983) 399-412.

[87] N. Djordjevic, P. W. J. Fowler, F. Houdiere, High Temperature and Temperature programming in high performance liquid chromatography:Instrumental considerations, J. Microcolumn Sep. 11 (1999) 403-413.

[88] R. G. Wolcott, J. W. Dolan, L. R. Snyder, S. R. Bakalyar, M. A. Arnold, Control of column temperature in reversed-phase liquid chromatography., J. Chromatogr. A 869 (2000) 211-230.

[89] J. D. Thompson, B. J. S., P. W. Carr, Dependence of thermal mismatch broadening on column diameter in high-speed liquid chromatography at elevated temperatures, Anal. Chem. 73 (2001) 3340-3347.

[90] M. O. Fogwill, K. B. Thurbide, Rapid column heating method for subcritical water chromatography, J. Chromatogr. A 1139 (2007) 199-205.

[91] B. Gu, H. Cortes, J. Luong, M. Pursch, P. Eckerle, R. Mustacich, Low thermal mass liquid chromatography, Anal. Chem. 81 (2009) 1488-1495.

[92] M. Pursch, United States patent application publication - US 2009/0173146 A1, United States patent application publication - US 2009/0173146 A1 (Jul. 9, 2009).

[93] T. J. Causon, H. J. Cortes, R. A. Shellie, E. F. Hilder, Temperature Pulsing for Controlling Chromatographic Resolution in Capillary Liquid Chromatography, Anal. Chem. 84 (2012) 3362-3368.

[94] M. Pursch, P. Eckerle, B. Gu, J. Luong, H. J. Cortes, Selectivity tuning via temperature pulsing using low thermal mass liquid chromatography and monolithic columns, J. Sep. Sci. 36 (2013) 1217-1222.

[95] D. Guillarme, S. Heinisch, Detection modes with high temperature liquid chromatography - A review Sep. Purif. Rev. 34 (2005) 181-216.

[96] K. Peck, M. D. Morris, Optical errors in a liquid chromatography absorbance cell, J. Chromatogr. 448 (1988) 193-201.

[97] P. Molander, R. Trones, K. Haugland, T. Greibrokk, Aspects and applications of non-aqueous high temperature packed capillary liquid chromatography, Analyst 124 (1999) 1137-1141.

[98] R. Trones, T. Andersen, T. Greibrokk, D. R. Hegna, Hindered amine stabilizers investigated by the use of packed capillary temperature programmed liquid chromatography J. Chromatogr. A 874 (2000) 65-71.

[99] T. Andersen, I. L. Skuland, A. Holm, R. Trones, T. Greibrokk, Temperature - programmed packed capillary liquid chromatography coupled to evaporative light scattering detection and electrospray ionization time of flight mass spectrometry for characterization of high molecular -mass hindered amine light stabilizers, J. Chromatogr. A 1029 (2004) 49-56.

[100] T. Teutenberg, J. Tuerk, M. Holzhauser, T. K. Kiffmeyer, Evaluation of column bleed by using an ultraviolet and a charged aerosol detector coupled to a high temperature liquid chromatographic system, J. Chromatogr. A 1119 (2006) 197-201.

[101] L. C. Heinz, T. Macko, H. Pasch, M.-S. Weiser, R. Mülhaupt, High-Temperature Liquid Chromatography at Critical Conditions: Separation of Polystyrene from Blends with Polyethylene and Ethylene-Styrene Block Copolymers, Int. J. Polym. Anal. Charact. 11 (2006) 47-55.

[102] B. Merelli, M. D. Person, P. Favetta, M. Lafosse, Analysis of triacylglycerols on porous carbon by high temperature liquid chromatography, J. Chromatogr. A 1157 (2007) 462-466.

[103] A. Hazotte, D. Libong, P. Chaminade, High temperature micro liquid chromatography for lipid molecular species analysis with evaporative light scattering detection, J. Chromatogr. A 1140 (2007) 131-139.

[104] K. Gaudin, P. Millet, F. Fawaz, P. Olliaro, N. J. White, C. Cassus-Coussere, U. Agbahoungha, J.-P. Dubost, Investigation of porous graphite carbon at high temperature liquid chromatography with evaporative light scattering detection for the analysis of the drug combination artesunate - Azitrhomycine for the treatment of severe malaria, J. Chromatogr. A 1217 (2010) 75-81.

[105] R. Trones, A. Iveland, T. Greibrokk, High temperature liquid chromatography on packed capillary columns with nonaqueous mobile phases, J. Microcolumn Sep. 7 (1995) 505-512.

[106] T. Teutenberg, P. Wagner, J. Gmehling, High-temperature liquid chromatography. Part I: Determination of the vapour pressure of binary mixtures-implications for liquid chromatography separations, J. Chromatogr. A 1216 (2009) 6471-6480.

[107] S. Giegold, Application of high temperature-high performance liquid chromatography (HT-HPLC): about the influence of temperature on the analysis time, selectivity and different detection systems, Fachbereich 8, Chemie, University of Siegen, Germany, Siegen, Dissertation (2008).

[108] R. Trones, T. Andersen, I. Hunnes, T. Greibrokk, Modified laser light scattering detector for use in high temperature micro liquid chromatography, J. Chromatogr. A 814 (1998) 55-61.

Chapter 2

General experimental

This section describes common instrumentation, the chemicals and general procedures used throughout the work. Specific instrumentation and procedures are described in the relevant chapters, in addition to relevant data on the analyte set.

2.1 Instrumentation

Three liquid chromatography (LC) systems were used to perform separations during this study. The work described in chapter 3 was carried out on a Dionex 3300 UHPLC system (Thermo Scientific Scoresby, Vic, Australia) equipped with a binary solvent manager, auto-sampler, column heater, photodiode array detector (PDA) and Chromeleon (version 6.8) chromatographic data processing software. An Ultimate 3300 UHPLC dual gradient system (Thermo Scientific Scoresby, Vic, Australia), equipped with auto-sampler, column heater, photodiode array detector (PDA) and Chromeleon (version 7.1) chromatographic data processing software was used for the work described in chapter 4 and 5. For the flow modulation experiments in chapter 5, a two position 10-port valve (Vici, Houston, TX, USA) was configured with a Dionex Ultimate 3300 UHPLC dual gradient system. An Agilent 1290 Infinity 2-dimensional LC system was also used for the flow modulation experiments.

Two different models of the ELSD and C-CAD were used during this study. An Alltech 3300 ELSD (Grace Davison Discovery Sciences, Deerfield, USA), a Varian 385-LC ELSD (Agilent Technologies, Santa Clara, CA, USA) and C-CAD (ESA-Biosciences Chelmsford, MA, USA) were used for work in chapter 3. The experiments described in chapter 4 were performed using a Varian 385-LC ELSD and a Corona Ultra RS charged aerosol detector (Thermo Scientific Scoresby, Vic, Australia). A Varian 385-LC ELSD was also used for the work in chapter 5. In flow modulation experiments using the Agilent 1290 Infinity 2-dimensional LC system, the ELSD signal was acquired via an Agilent 35900E dual channel interface. A refrigerated vapour trap - RVT4104 (Biolab Pty Ltd., Scoresby, Australia.) was used to collect solvent vapours emitted from the ELSD and C-CAD.

A Polaratherm oven (Selerity Technologies, Inc., Salt Lake City, UT, USA) was used for controlling the mobile phase and column temperature. The Polaratherm oven operates within the temperature range of 30–200°C and has the capability of temperature programming at a rate of up to 30°C /min.

2.2 Reagents

Unless specified otherwise, all chemicals were of analytical grade and are listed in the following table.

2.2.1 Chemicals used as test probes (alphabetical order)

Name	Chemical Formula	Supplier
Caffeine	$C_8H_{10}N_4O_2$	Sigma-Aldrich
Cytidine	$C_9H_{13}N_3O_5$	Sigma-Aldrich
DL-Tryptophan	$C_{11}H_{12}N_2O_2$	Sigma-Aldrich
Fructose	$C_6H_{12}O_6$	Sigma-Aldrich
Furosemide	$C_{12}H_{11}ClN_2O_5S$	Sigma Aldrich
Glycine	$C_2H_5NO_2$	Sigma-Aldrich
Indapamide	$C_{16}H_{16}ClN_3O_3S$	Sigma-Aldrich
Prednisolone	$C_{21}H_{28}O_5$	Sigma-Aldrich
Sucrose	$C_{12}H_{22}O_{11}$	Sigma-Aldrich
Sulfamerazine	$C_{11}H_{12}N_4O_2S$	Sigma-Aldrich
Sulfamethamine	$C_{12}H_{14}N_4O_2S$	Sigma-Aldrich
Sulfamethoxazole	$C_{10}H_{11}N_3O_3S$	Sigma-Aldrich
Sulfamethizole	$C_9H_{10}N_40_2S_2$	Sigma-Aldrich
Sulfamethoxine	$C_{11}H_{12}N_4O_3S$	Sigma-Aldrich
Thymine	$C_5H_6N_2O_2$	Sigma-Aldrich
Uracil	$C_4H_4N_2O_2$	Sigma-Aldrich
Uridine	$C_9H_{12}N_2O_6$	Sigma-Aldrich
Vit-B12	$C_{63}H_{89}CoN_{14}O_{14}P$	Sigma-Aldrich

2.2.2 Chemicals used as buffers and mobile phase modifiers (alphabetical order)

Name	Chemical Formula	Supplier
Acetic acid, glacial	CH_3COOH	Sigma-Aldrich
Acetonitrile	CH_3CN	Scharlau Chemie
Ammonium hydroxide	NH_4OH	Sigma-Aldrich
Formic acid	HCOOH	Sigma-Aldrich
Methanol	CH_3OH	Scharlau Chemie

2.3 General procedures

2.3.1 Preparation of eluents and sample solutions

High purity water (18.2 MΩ.cm at 25°C) produced by a Millipore Milli-Q water purification system (Millipore, Molshiem, France) was used to prepare all samples and buffer solutions. All buffers were degassed under vacuum sonication and were filtered through a 0.45 μm nylon filter paper (Whatman brand, purchased from Thermo Scientific Scoresby, Vic, Australia).

Chapter 3

Effects of eluent temperature and elution bandwidth on detection response for aerosol-based detectors

3.1 Introduction

HTLC separations and the quasi-universality of aerosol-based detectors are two current frontiers of research in separation science. Benefits such as high-throughput analysis, altered separation selectivity and the prospect of green chromatography have been the driving forces for continued research in HTLC over the past few decades [1-3]. In particular, recent advances in the development of thermally stable stationary phases [4-8], low thermal mass column hardware [9-11] and efficient heating modules [12-14] have rejuvenated interest in the HTLC mode of separation. Early research in HTLC was focused chiefly on different aspects of separation and challenges related to thermal equilibration, so the possibility of using different detection methodologies has been relatively less explored.

Aerosol-based LC detectors, such as the ELSD [17, 18] and the C-CAD [19] provide responses which are independent of optical absorbance properties and do not require mobile phase cooling. While passing through the nebulizer, a liquid stream undergoes rapid cooling due to the coaxial flow of a high velocity nebuliser gas. Moreover, expansion of gas at the nebulizer tip and a process of evaporation further contribute to the cooling of aerosol droplets. Thus, aerosol-based detectors present an attractive detection option for HTLC separations. Moreover, since aerosol-based detectors require evaporation of the mobile phase to leave dried analyte particles [17, 20], high temperature mobile phases are believed to complement, rather than hinder, these detection techniques [1, 21]. At the same time, isocratic separations using a temperature gradient can help to overcome the solvent gradient limitations (response variation as a function of solvent composition) [20, 22] observed with aerosol detectors.

Hyphenation of aerosol detectors with HTLC has been demonstrated by many researchers in recent years [13, 21, 23-28]. At high temperature, reduced solvent viscosity leads to lower column backpressure and simultaneously increases the analyte diffusion co-efficient, which in turn allows operation at a higher linear velocity without

increasing theoretical plate height ('H' term in Van Deemter equation). Therefore, HTLC separations employing UV-Vis detection are usually carried out at higher flow-rates. However, with aerosol-based detectors, the higher input rate of mobile phase directly influences the process of nebulisation and evaporation. Aqueous mobile phases possess higher viscosity and lower vapour pressure compared to organic solvents [29, 30]. Therefore, aqueous mobile phases, when introduced at a higher input rate into aerosol detectors, put an extra burden on the process of evaporation, causing a wide distribution in analyte particle size and only partial desolvation of the droplets [18], which adversely affects the detection performance. Moreover, slow thermal equilibration as a result of the high thermal mass of analytical scale columns is known to affect the separation performance [9-11]. Flow-rate limitations [18] of the aerosol detectors can be overcome partially by using micro- and capillary-scale columns [23, 25] and this has led researchers to investigate the effects of nebuliser cell geometry on the response characteristics at micro- and capillary-scale flow-rates. Modifications to the LC-detector interface for commercially available ELSDs to enable use with micro-scale separations have been proposed [21, 26, 31]. The majority of the published studies in the context of HTLC-ELSD hyphenation have been carried out in the non-aqueous HTLC mode [25, 32-34]. For instance, Hazotte et al. [35] have investigated the effect of non-aqueous micro-HTLC separation conditions on the response characteristics of commercially available aerosol based LC detectors (ELSD, C-CAD and APCI-MS). Their study showed that peak area of both ELSD and C-CAD decreased with an increase in temperature and the intensity of the ELSD signal was reported to drop by two fold at 150°C compared to that at 50°C. Conversely, response enhancement of aerosol-based detectors, such as ELSD and ESI-MS, has also been reported [1]. The alteration of ELSD response due to band dispersion induced in the nebuliser cell has been reported by Guillarme et al. [21], however the effect of on-column dispersion on ELSD response has received less attention.

Contributions to the literature concerning HTLC-aerosol detection are predominantly discrete experiments focused either on specific application needs or to a lesser extent on hardware modifications of the commercially available aerosol detectors, where the major aim has been to improve detector response. Since there are several operational parameters that can be manipulated on these detectors to affect response, it becomes difficult to draw a generalised approach for method optimisation. However, one common thread among these various studies is the way different

experimental changes, such as the use of micro-capillary scale separations, nebuliser cell modifications and physical properties of the mobile phases influence the characteristics of the plume of solute particle passing through the flight tube. Unlike concentration-based detectors, aerosol-based detectors respond to analyte mass transport per unit time. Therefore, the scattered light intensity pattern in ELSD or the efficiency of charge deposition in C-CAD depends on compactness, uniformity and migration rate of the plume of dried solute particles.

The purpose of the present study was to examine some practical aspects of aqueous HTLC with aerosol-based detection and the effect of these parameters on detector response. In particular, this study focuses on how mobile phase temperature and the bandwidth of the eluted analyte affect the detector response. A better understanding of these effects on detector response should contribute to the wider adoption of HTLC using aerosol-based detectors.

3.2 Experimental

The general experimental details (instrumentation and chemicals) are given in Chapter 2. The test analytes (see Table 3.1) used in this study were of analytical grade and purchased from Sigma-Aldrich. Stock solutions of individual analytes were prepared at a concentration of 1 mg/mL in water and stored in a refrigerator at 4°C. Nitrogen gas obtained from an in-house nitrogen generator was used as the nebuliser gas for the ELSD and C-CAD detectors. Throughout this study, the ELSD parameters employed were: nebulisation and evaporation temperatures, 60°C, gas flow-rate 1.6 Standard litres per minute (SLM), and a gain factor of 4. C-CAD was used with the manufacturer-recommended setting of 35 psi for the gas flow at ambient temperature. A Polaratherm oven (Selerity Technologies, Inc., Salt Lake City, UT, USA) was used for controlling the mobile phase and column temperature.

3.2.1 Flow-injection analysis (FIA)

The possible role of mobile phase temperature in detection response of the ELSD and C-CAD detectors was evaluated using FIA of a set of analytes at six different temperatures. In order to obtain peak-widths ($W_{5\%\ height}$) comparable to a chromatographic separation, the injector outlet was connected to 180 µm x 3.0 m, 1/32" (od) stainless steel tubing. Further, it was connected to the detector inlet using 50 µm x 50 cm polymer-sheathed fused silica (PEEKSIL) tubing to provide back-pressure, so as to, prevent the mobile phase from boiling at high temperature. Considering the low

thermal conductivity of PEEK as well as fused silica, the temperature drop caused by heat dissipation from the transfer tubing (PEEKSIL tubing) was expected to be insignificant. To ensure that there was no major temperature loss from the transfer tubing, the temperature of the effluent at the outlet of the PEEKSIL tubing was measured using a RTD (resistance temperature detector)-probe. The temperature of the liquid at the end of the PEEKSIL tubing was found to be within ±5°C of the oven temperature. Sample concentrations of 0.2 mg/mL in mobile phase were prepared from stock solutions. Each sample was analysed in triplicate over a temperature range from 30°C to 180°C, using 30°C intervals. Four mobile phases were investigated, namely water, 0.5% (v/v) aqueous formic acid in water, methanol/water 4:6 (v/v) and ACN/water 2:8 (v/v). The mobile phase flow-rate was maintained at 0.5 mL/min throughout the study.

The effect of elution bandwidth on the response of the ELSD was examined by FIA of a set of sucrose solutions within the concentration range of 0.05–0.3 mg/mL. Each solution was injected in triplicate, keeping the injection volume constant at 25µL to obtain actual mass load in the range 1.25-12.5 µg. The FIA manifold for this study was equipped with a series of tube-fittings of different id and length to obtain peak widths ($W_{5\%\ height}$) of the injected analyte band in the range of 0.1-1.0 min. To examine the effect of sample bandwidth only, the temperature of FIA manifold was maintained at 30°C throughout this study.

3.2.2 Chromatographic separations

Separations were carried out using a Thermo Hypercarb*HT column (100 x 2.1 mm, 3 µm particle size), purchased from Thermo Fisher Scientific, Scoresby, Vic., Australia. This column was connected to an auto-sampler and injector using the Polaratherm mobile phase preheating coil. The ELSD or C-CAD inlet was connected to the column outlet using 50 µm x 50 cm of 1/16’ (od) of pressure restrictor tubing. When the UV detector was used, a pressure restrictor coil was connected to the column effluent outlet.

The effect of separation temperature on detector response was evaluated using triplicate injections of a uracil solution (0.2 mg/mL) under isocratic conditions within a temperature range of 30-180°C. This study was performed using two different models of ELSD (Alltech-3300 and Varian-385 ELSD), C-CAD and a UV-Vis detector

Table 3.1: A summary of the physico-chemical properties of the test probes used in FIA investigations)

Compound	Molecular Formula	Molecular weight (g/mol)	Exp. 'W' sol at 25°C (mg/mL)	Exp. MP (°C)	Vapour pressure (mm Hg)
Glycine	$C_2H_5NO_2$	75.07	2.49E05	262.0	2.65E-08
Uracil	$C_4H_4N_2O_2$	112.09	3.60E01	338.0	4.67E-05
Uridine	$C_9H_{12}N_2O_6$	244.21	1.00E06	165.0	2.08E-18
Caffeine	$C_8H_{10}N_4O_2$	194.19	2.16E04	238.0	8.12E-10
Sucrose	$C_{12}H_{22}O_{11}$	342.30	2.12E06	185.5	6.58E-18
DL-Tryptophan	$C_{11}H_{12}N_2O_2$	204.23	1.34E04	282.0	2.08E-10
Vit-B12	$C_{63}H_{89}CoN_{14}O_{14}P$	1356.40	1.25E04	>300	2.06E-13

Experimental values of water solubility (Exp.'W' sol) and melting point (Exp. MP), and calculated vapour pressure values (Antoine method) were obtained by Estimation program interface (EPI Suit v4.10) developed by US Environmental Protection Agency (EPA) [36]

operated at 254 nm used for comparative purposes. Temperature-induced alterations in detector response were assessed separately for each detector. Finally, separations of a mixture of analytes (glycine, uracil, sucrose, thymine, and cytidine) were performed using isocratic-isothermal and isocratic-temperature gradient conditions.

3.3 Results and Discussion

3.3.1 Effect of mobile phase temperature on aerosol detector response

The NT-equation [37] has been commonly used to explain the dependence of aerosol detection response on the nebulisation conditions used [17-18, 37]. According to this equation, the SMD of aerosol droplets depends on viscosity, surface tension and density of the carrier solvent used, as well as on nebulisation parameters, such as the flow-rate of nebuliser gas and liquid effluent and the difference between the linear velocity of liquid and nebuliser gas. Since water undergoes dramatic changes in viscosity and vapour pressure as a function of temperature [29, 30], the temperature would be expected to have a considerable effect on SMD when aqueous mobile phases are used. Therefore, it has been hypothesised that heated aqueous mobile phases can facilitate the nebulisation-evaporation process and thereby improve the performance of aerosol detectors [21]. An initial evaluation of the effect of separation temperature on the detection response of the ELSD and C-CAD detectors was performed under isocratic conditions by injecting uracil onto the HyperCarb*HT column using the temperature range from 70-180°C. Fig. 3.1 shows the responses of the ELSD, C-CAD and UV detectors as a function of separation temperature. Even though the nebulizer cell geometry and the aerosol trajectory of the two ELSD models used for this study were different, both detectors exhibited approximately a five-fold increase in peak area when performing isocratic separations at increasing separation temperatures from 30-180°C. In contrast, whilst the C-CAD detector also showed a somewhat enhanced response with increased temperature of the mobile phase, this enhancement was much less significant. A decrease in C-CAD response at 180°C was confirmed by repeated analysis. In UV-detection, the response was constant over the entire temperature range. These observations were contrary to those reported by Hazotte et al. [35] who observed a two-fold decrease in ELSD response with increase in separation temperature from 50-150°C.

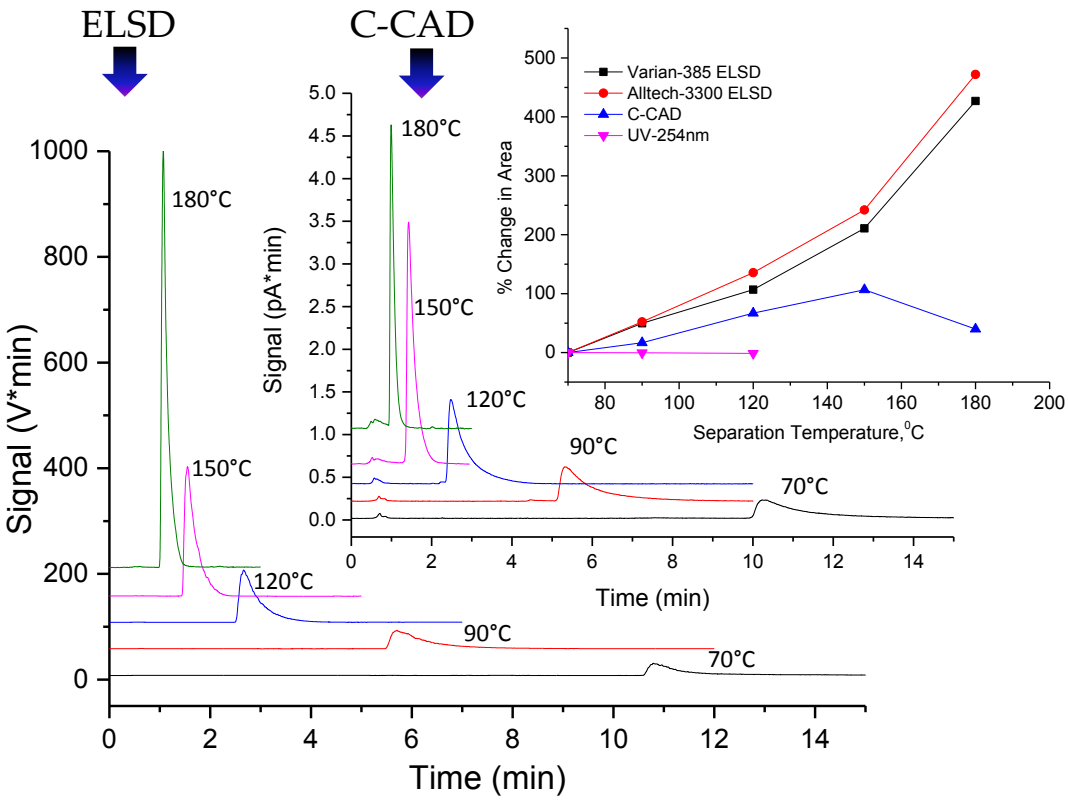

Figure 3.1: Comparison of ELSD, C-CAD and UVD for percent change in peak area as a function of column temperature in isocratic elution. Sample- Uracil (0.2 mg/mL in water); chromatographic conditions: column: Thermo Hypercarb*HT, mobile phase - water (100%); flow-rate - 0.5 mL/min; injection volume - 25 µL; instrumental conditions as in experimental section 3.2

In order to evaluate the effect of mobile phase temperature on the detector response of the ELSD and C-CAD detectors, a set of analytes was analysed using FIA at six different temperatures. This study was performed without a separation column to avoid on-column contributions towards the band broadening caused by the mass-transfer and thermal mismatch effects. This approach allowed the effect of mobile phase temperature on the detector response to be investigated independently. In general, the peak shape achieved using the FIA configuration differed from the peak profile produced in a chromatographic separation. Because of the very short residence time, in conventional FIA, analytes eluted much faster, giving narrower (taller) peaks. It is commonly known that the response of the aerosol detectors depends strongly on eluent composition. Moreover, these detectors suffer from limited dynamic range. Taking into account these factors, trials were carried out to optimize the FIA fitting that can provide optimum signal intensity for different eluents within the temperature range 30-150°C. A FIA set-up giving a peak width of approximately 0.5 min was used to investigate the effect of eluent temperature. The relevant properties of the test analytes used in the FIA study are shown in Table 3.1. These analytes were selected based on their compatibility with the selected mobile phase systems and the need to be non-volatile, so that the entire sample was detected. Detector response was measured using peak area and peak height at the respective temperature points for each analyte. The percentage change in detection response (peak area and peak height) as a function of mobile phase temperature was calculated with respect to the initial response (average of three replicate injections). Fig. 3.2 shows results for the ELSD using the four different mobile phase compositions, while Fig. 3.3 shows the corresponding data for the C-CAD. For most analytes in the test mixture, both detectors showed a small increase (<10%) in peak area with an increase in mobile phase temperature. Comparison of the results obtained from on-column (Fig. 3.1) and FIA studies (Figs. 3.2 and 3.3) showed that the enhancement of detector response as a function of mobile phase temperature was much more pronounced in the chromatographic separations. These results show that the increased responses observed in Fig. 3.1 were not attributable to increases in the mobile phase temperature.

It is known that the viscosity of a mobile phase decreases with an increase in separation temperature, causing an increase in diffusion coefficient of the solutes,

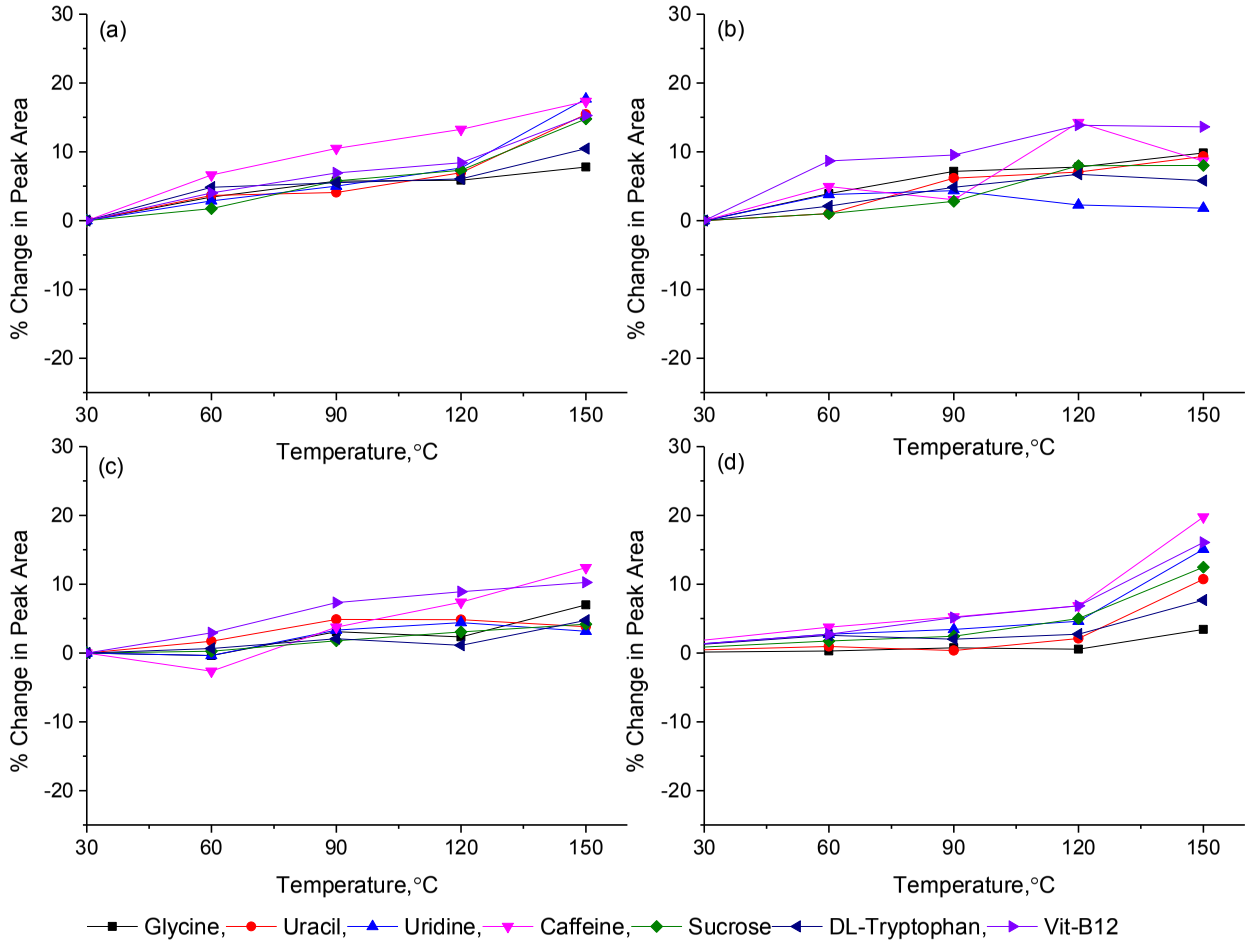

Figure 3.2: Evaluation of the effect of inlet solvent temperature on response of ELSD using different eluent systems (a) pure water, (b) 0.5% formic acid in water (v/v), (c) 40% methanol in water (v/v) and (d) 20% ACN in water (v/v). Flow-injection conditions and instrumental parameters are detailed in experimental section 3.2

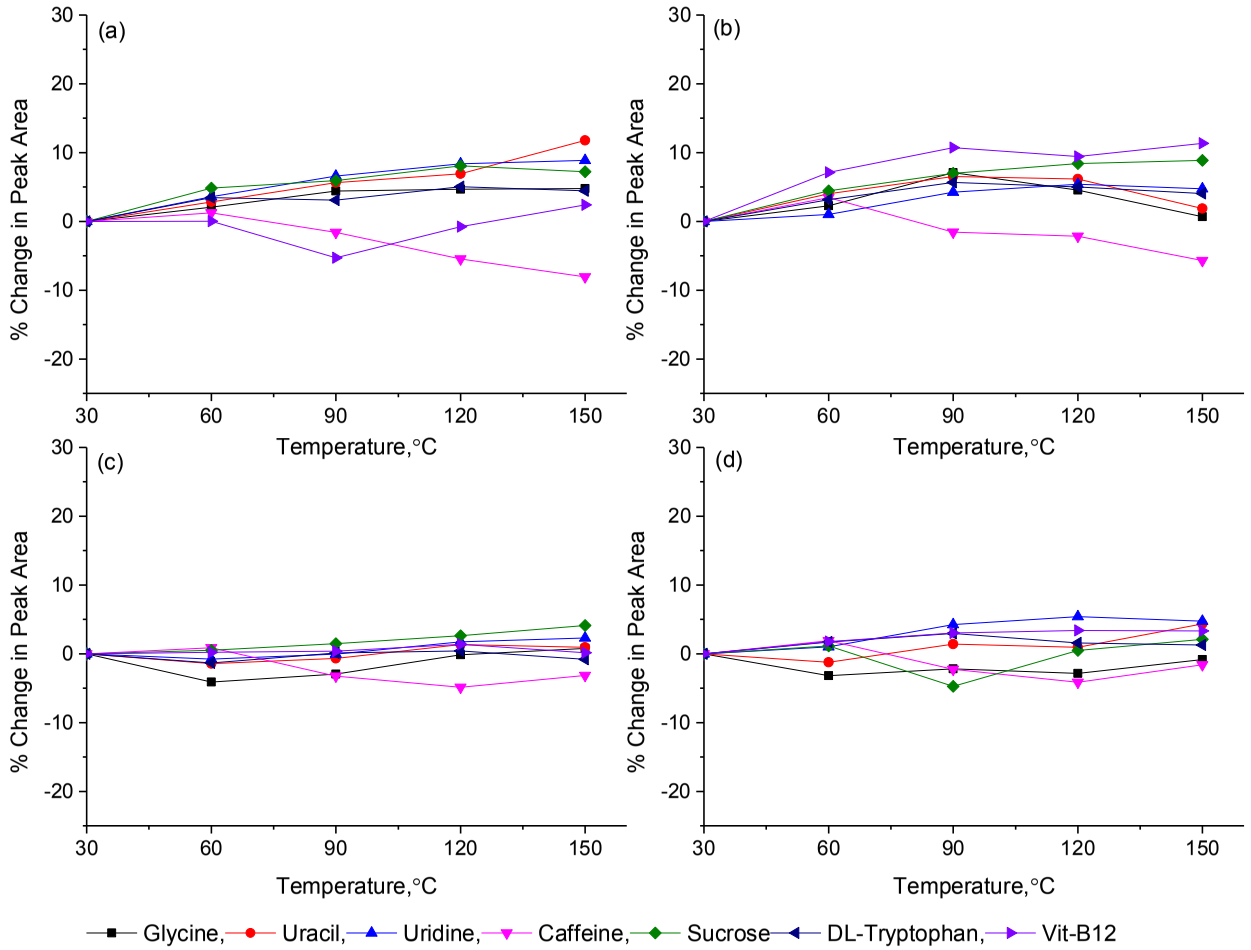

Figure 3.3: Evaluation of the effect of inlet solvent temperature on response of C-CAD using different eluent systems (a) pure water, (b) 0.5% formic acid in water (v/v), (c) 40% methanol in water (v/v) and (d) 20% ACN in water (v/v). Flow-injection conditions and instrumental parameters are detailed in experimental section 3.2

which in turn increases the rate of mass transfer between the solid stationary phase and liquid mobile phase. This results in shorter elution times, less peak dispersion leading to sharper peaks, and an increase in peak heights. In chromatographic separations using C-CAD, the peak width ($W_{5\%height}$) of uracil decreased from 3.7 to 0.3 min with the increase in column temperature from 70°C to 180°C. Under similar conditions, with ELSD detection, the peak width ($W_{5\%height}$) decreased from 2.1 to 0.3 min. The peak compression as a function of increase in separation temperature was more noticeable in C-CAD (about 12-fold change) compared to ELSD (about 7-fold change). Despite this, Fig. 3.1 shows that the response enhancement was more pronounced in ELSD. This indicated that the response enhancement observed in the chromatographic separations was related to the temperature-induced alterations in elution bandwidth rather than to the temperature of the mobile phase itself. Further, the magnitude of this effect appeared to be dependent to some extent on the mechanism of aerosol detection.

3.3.2 Relationship between elution bandwidth and ELSD response

Experiments were performed to evaluate the possible effect of analyte bandwidth on the ELSD response. In order to study the effect of peak width only, chromatographic dispersion was mimicked using FIA sample introduction through the tubing of varying length and internal diameter. In this way, peak widths were varied over the approximate range 0.1-1.3 min, but with the absolute amount of injected analyte remaining constant at a specified value (Fig. 3.4). Fig. 3.5(a) shows there was an inverse relationship between elution bandwidth and ELSD response. The results of this study have been summarised in Table-3.2. The lower concentration levels were found to be more sensitive to the bandwidth variation. A plot of log (peak area) versus log (sample mass) for different elution bandwidths is given in Fig. 3.5(c) and shows that the spread of the log A values corresponding to different bandwidths was relatively greater at lower concentration. This is due mainly to the nonlinear concentration response of ELSD. Moreover, it can be seen that the slope of the response curve moved from 1.45 to 1.80 with an increase in peak width from ~0.1 to ~1.3min. This can be interpreted as a gradual shift of scattering mechanism towards the Rayleigh region with an increase in peak width. In the ELSD, depending on the ratio of the diameter of the dried solute to the incident light wavelength, light scattering takes place through three different mechanisms [17]. When irradiated by a light source, solute particles with a diameter (dp) to wavelength (λ) ratio of much less than 0.1 behave like a point source

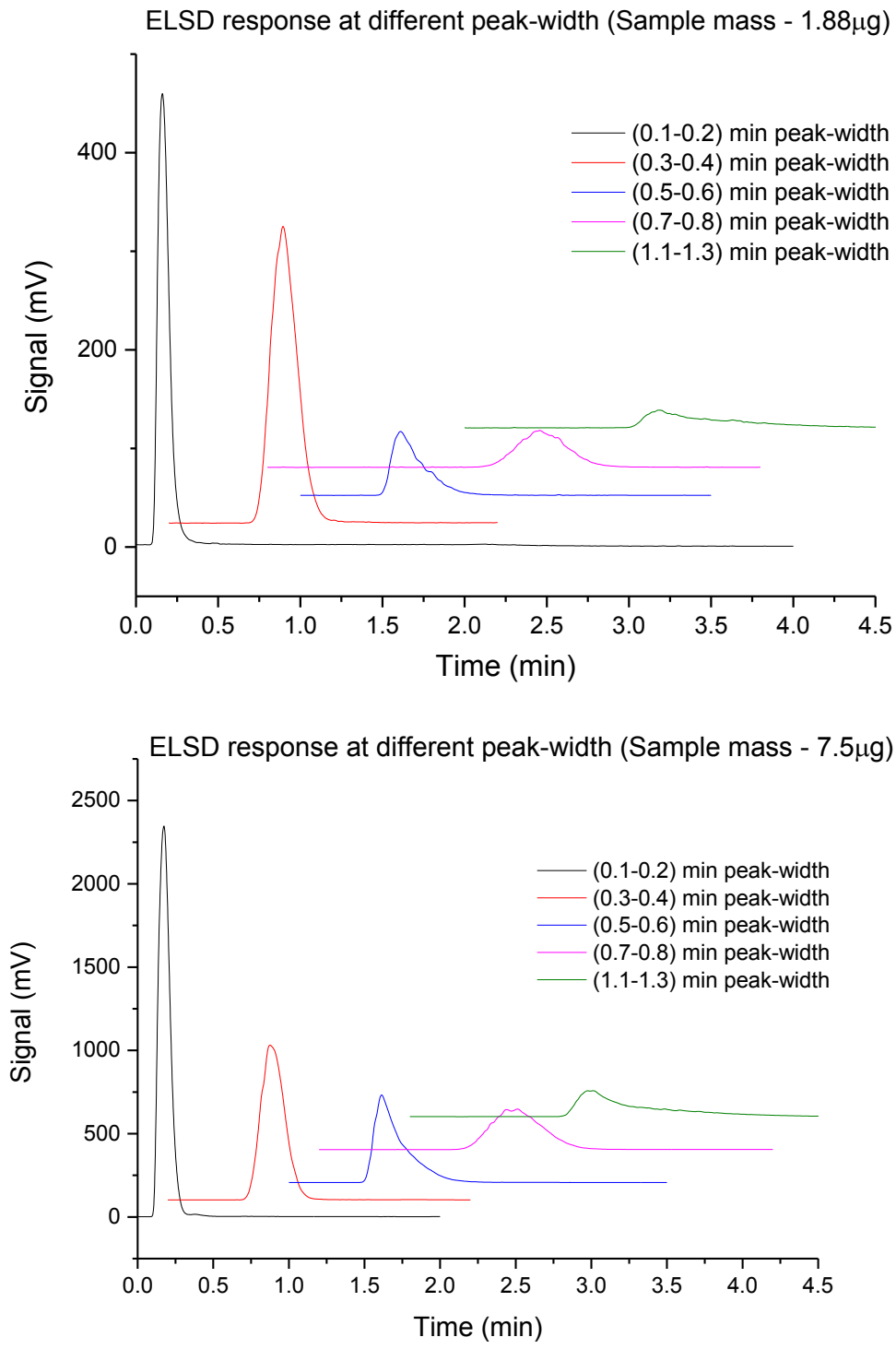

Figure 3.4: Representative FIA chromatograms illustrating inverse relationship between elution bandwidth and ELSD response

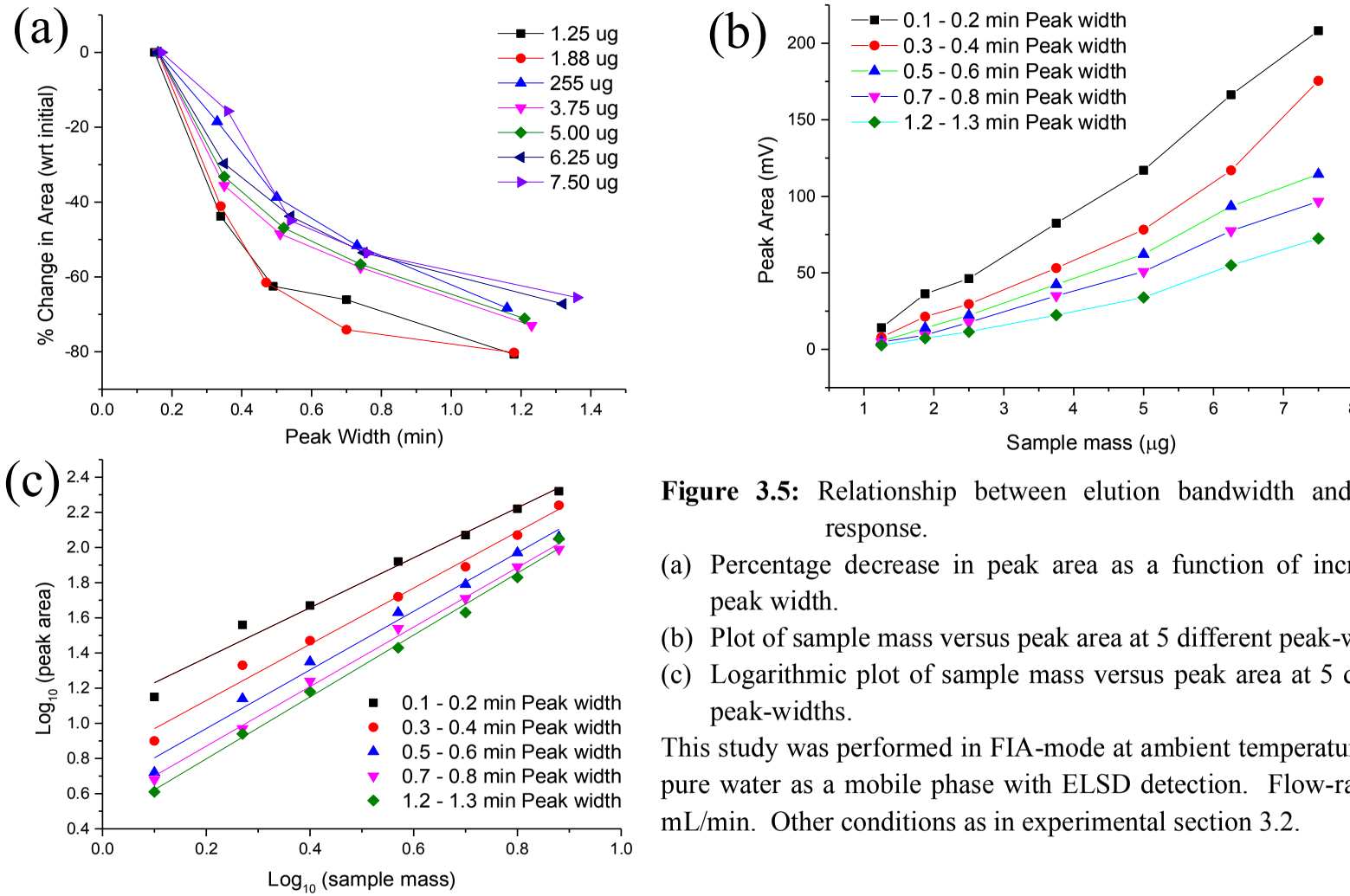

Figure 3.5: Relationship between elution bandwidth and ELSD response.

(a) Percentage decrease in peak area as a function of increase in peak width.

(b) Plot of sample mass versus peak area at 5 different peak-widths.

(c) Logarithmic plot of sample mass versus peak area at 5 different peak-widths.

This study was performed in FIA-mode at ambient temperature using pure water as a mobile phase with ELSD detection. Flow-rate - 0.5 mL/min. Other conditions as in experimental section 3.2.

Table 3.2: Relationship between elution bandwidth and ELSD response (Supporting information for fig-3. 5a&b)

Peak-width range (min)	Sample mass (µg)	1.3	1.9	2.5	3.8	5.0	6.3	7.5	Log C vs Log A curve equation
(0.1-0.2)	Width	0.15	0.16	0.16	0.16	0.16	0.16	0.17	Y = 1.45x + 1.07, R^2 = 0.984
	Area ± SD	14.09±0.26	36.26 ± 0.76	46.24 ±0.95	82.40 ± 1.8	117.01 ± 1.2	166.35 ± 1.7	208.18 ± 2.2	
	Log_{10}(A)	1.15	1.56	1.67	1.92	2. 07	2.22	2. 32	
(0.3-0.4)	Width	0.32	0.34	0. 33	0. 35	0. 35	0. 35	0. 36	Y = 1.63x + 0.79, R^2 = 0.988
	Area ± SD	7.92 ± 0.11	21.34 ± 0.50	29.56 ± 0.35	53.06 ± 0.22	78.20 ± 0.80	116.91 ± 0.94	175.50 ± 0.52	
	Log_{10}(A)	0.90	1.33	1.47	1.72	1.89	2.07	2.24	
(0.5-0.6)	Width	0.49	0.47	0.50	0.51	0.52	0.54	0.54	Y = 1.70x + 0.61, R^2 = 0.988
	Area ± SD	5.28 ± 0.08	13.94 ± 0.06	22.24 ± 0.20	42.42 ± 0.71	62.14 ± 0. 55	93.49 ± 1.2	114.41 ± 0.38	
	Log_{10}(A)	0.72	1.14	1.35	1.63	1.79	1.97	2.06	
(0.7-0.8)	Width	0.71	0.73	0.74	0.74	0.74	0. 75	0. 76	Y = 1.73x + 0.051 R^2 = 0.0.999
	Area ± SD	4.78 ± 0.06	9.38 ± 0.35	17.56 ± 0.46	34.99 ± 0.39	50.82 ± 0.20	77.42 ± 0.44	96.65 ± 0.39	
	Log_{10}(A)	0.68	0.97	1. 24	1. 54	1. 71	1. 89	1.99	
(1.1-1 4)	Width	1.18	1.18	1.16	1.23	1.21	1.32	1.36	Y = 1.80x + 0.30, R^2 = 0.992
	Area ± SD	2.72 ± 0.25	7.20 ± 0.02	11.50 ± 0.19	22.26 ± 0.48	33.83 ± 0.38	54.63 ± 0.30	71.76 ± 0.92	
	Log_{10}(A)	0.43	0.86	1.06	1.35	1.53	1.74	1.86	

and pass through the optics undetected due to Rayleigh scattering. Particles in the size range similar to the incident wavelength ($0.1 \leq (dp/\lambda) \geq 1$) lie in the Mie scattering domain, while particles much bigger than the incident wavelength ($dp/\lambda >> 1$) exhibit physical scattering by reflection and refraction mechanisms. Due to the highly polydisperse nature of the aerosol generated by conventional pneumatic nebulisers, the response of the ELSD results from a combination of different scattering mechanisms. This demonstrates the importance of the size of the dried solute particles in the response mechanism for the ELSD. The size of the solute particles reaching the optical unit depends on analyte concentration (C), density of analyte (ℓ_a) and the average size of the droplets (D_0) produced in the process of nebulisation [38].

$$d = D_0 (C/\ell_a)^{1/3} \qquad \text{(Equation-3.1)}$$

The number of droplets generated by the nebulisation of intake solvents remains unchanged under constant nebulisation parameters. However, the amount of solute in each droplet influences the process of size reduction in the vaporization process [20]. A narrow, symmetrical peak renders a compact and uniform plume of solute particles, whereas dispersed non-Gaussian peaks produce droplets containing a lower numbers of solute particles and hence disrupt the uniform size distribution of dried particles. Stolyhwo et al. [20] have reported the dependence of the ELSD response on solute mass flow-rate (M) and the analyte concentration at the peak maximum (C_m). Solute mass flow-rate at the peak maximum depends on the ratio of the product of the sample amount (m) and flow-rate (F), to peak-width (W) at the base.

$$M = C_m F = 4mF/\left(W/\sqrt{2\pi}\right) \qquad \text{(Equation-3.2)}$$

Using the Gaussian function Meeren et al. [39] derived an equation to calculate the solute concentration at the peak maximum:

$$C = \frac{X_0/10^9}{Q_l} \frac{\mathrm{Exp}[-(t_r - t)^2/2sd^2]}{(2\pi)^{1/2} sd} \qquad \text{(Equation-3.3)}$$

Where, X_0 is the sample loading (µg), Q_l is the volumetric flow-rate of the mobile phase, t_r is the retention time (s) and t corresponds to distance along the time axis. The standard deviation (sd) corresponds to the peak width at half height. According to this equation, the solute concentration (C) at the peak maximum depends on the sample load as well as the peak characteristics. The terms in the exponent in

Equation-3.3 determine the solute concentration per unit time, which in turn influences the droplet size distribution and the size of the dried solute particles. Their work was focussed on developing a simulation model to predict the effect of various operational parameters on ELSD response. It is important to note that peaks were assumed to be Gaussian to calculate the solute concentration at peak maximum. The effect of the elution bandwidth should therefore be more noticeable in isocratic separations, as late-eluting analytes exhibit a non-Gaussian peak profile. With an increase in separation temperature, elution bands become narrower and more symmetrical, which in turn influence the characteristics of the primary aerosol. A dense band of the droplets containing a higher concentration of analyte travels from the nebulisation chamber to the optical unit. Thus, the observed ELSD response enhancement in HTLC-ELSD can be attributed to the increased solute mass transport per unit time towards the optical unit of the ELSD.

3.3.3 Role of elution bandwidth

In isocratic separations, the longer the analyte spends inside the column the more it becomes dispersed, whereas in gradient separations, all the analytes tend to be eluted with approximately the same bandwidth. Since the elution bandwidth influences the response mechanism of the ELSD, the later eluted analytes in isocratic separations are likely to suffer underestimation (if using a universal calibrant) due to their dispersed peak geometry. In order to further support the relationship between peak width and ELSD response, and to illustrate the errors that may occur in quantitative analysis, a separation of test analytes with a wide range of retention factors was performed using aqueous HTLC. Linear van't Hoff curves were observed for all individual test probes (correlation coefficients in the range 0.993–0.999), indicating that the separation mechanism remained unchanged over the temperature range studied. A mixture of four test analytes was separated in an isocratic mode at four different temperatures and Fig. 3.6 shows the percentage change in peak area with the temperature for both ELSD (a) and C-CAD (b). It can be noted that the response enhancement varied between analytes and that the enhancement was more pronounced in ELSD detection compared to C-CAD. The former observation can be attributed to the retention order (glycine < sucrose < thymine < cytidine) because the later eluted peaks showed much larger reduction in retention time and peak widths as temperature increased than the earlier

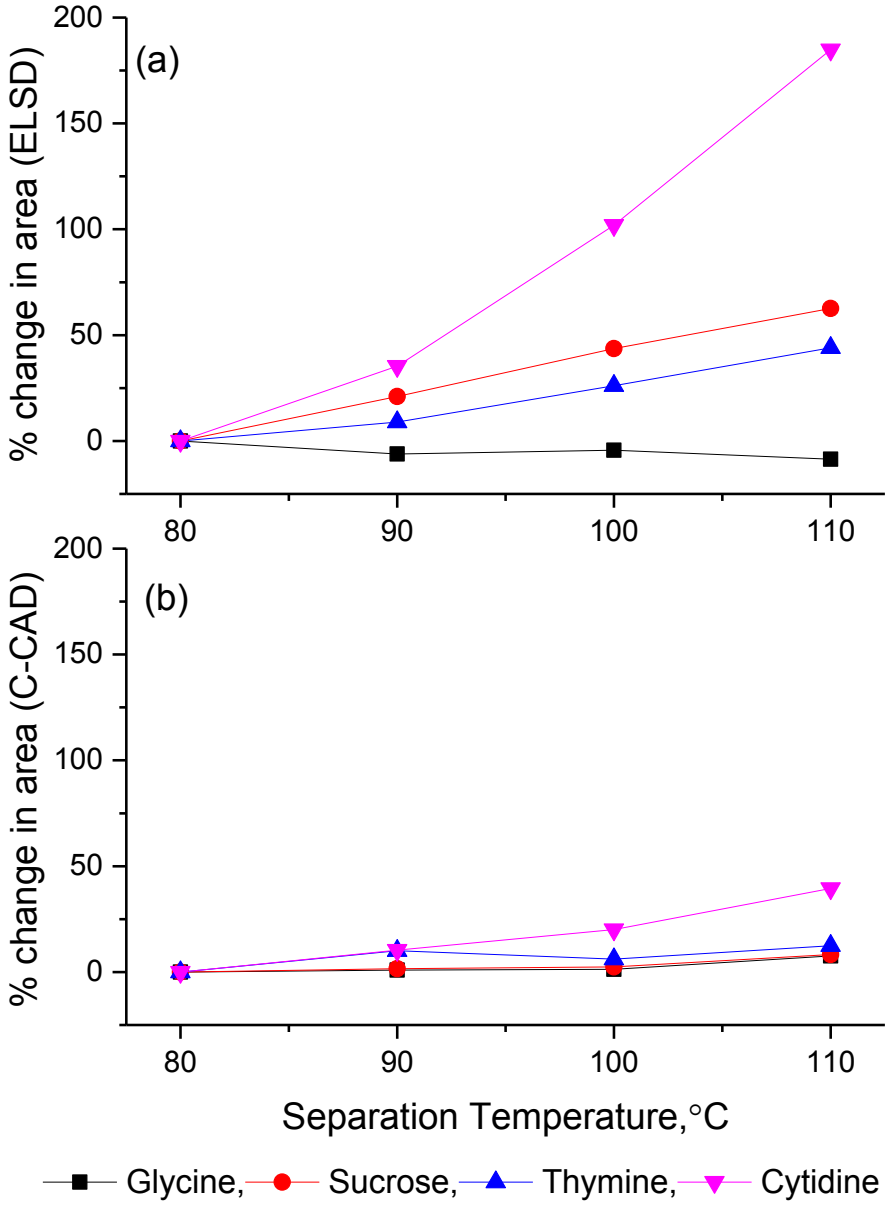

Figure 3.6: Comparison of percentage change in peak area of ELSD and C-CAD as a function of column temperature in an isocratic separation. Sample: mixture of glycine, sucrose, thymine and cytidine; sample concentration: 0.1 mg/mL of each; chromatographic conditions: column - Thermo Hypercarb*HT; mobile phase - water (100%); flow-rate - 0.5 mL/min; Injection volume - 25 µL; instrumental conditions as in experimental section 3.2.

eluted species. The latter observation is the result of the different detection mechanisms for the two detectors. In contrast to ELSD, which measures light scattering intensity exhibited by dried solute particles, the C-CAD involves electrical measurement of the current produced by the charged solute particles. In ELSD detection, particles with diameter less than 10 μm lie in the Rayleigh scattering domain and thereby limit the detection sensitivity; whereas in C-CAD, the Faraday cup electrometer generates a detectable signal from solute particles as small as 10 nm. As a result, tiny particles generated by the solute mass in the tailing ends of the broad-asymmetrical peaks go undetected in ELSD, giving a narrow peak, while under the identical conditions, C-CAD produces relatively broader peaks with higher response. This explains why the response alteration as a function of temperature induced peak compression was less pronounced in C-CAD, compared to ELSD.

A mixture of glycine, sucrose, uracil, thymine and cytidine was separated under the isocratic conditions at four different separation temperatures (Fig. 3.7) using the ELSD and C-CAD. The same set of analytes was also separated using the ELSD under isocratic conditions but with the addition of three different temperature gradient ramps (Fig. 3.8). Fig. 3.7 demonstrates that the largest change in both peak width and peak area occurred for the most strongly retained analyte, cytidine, whereas the least retained analyte (glycine) showed almost no change in either peak width or peak area. It is also evident from Fig. 3.7 that even at elevated temperature, the peak shapes for the more strongly retained peaks were asymmetrical. When a temperature gradient was applied (Fig. 3.8), the range of peak widths in the chromatogram was reduced very significantly and when the highest temperature gradient was used, the peak widths and detector responses were similar for all analytes. The use of a temperature gradient therefore provides optimal results for reduced separation time, consistent peak width, and consistent detector response.

3.4 Conclusion

HTLC separation and aerosol detectors complement each other. The mobile phase temperature only marginally influences the detector response, which makes effluent cooling unnecessary. At the same time, temperature-induced effects on retention and peak width can improve the detection response. Elution bandwidth was found to play a crucial role in the detector response for both ELSD and C-CAD, with

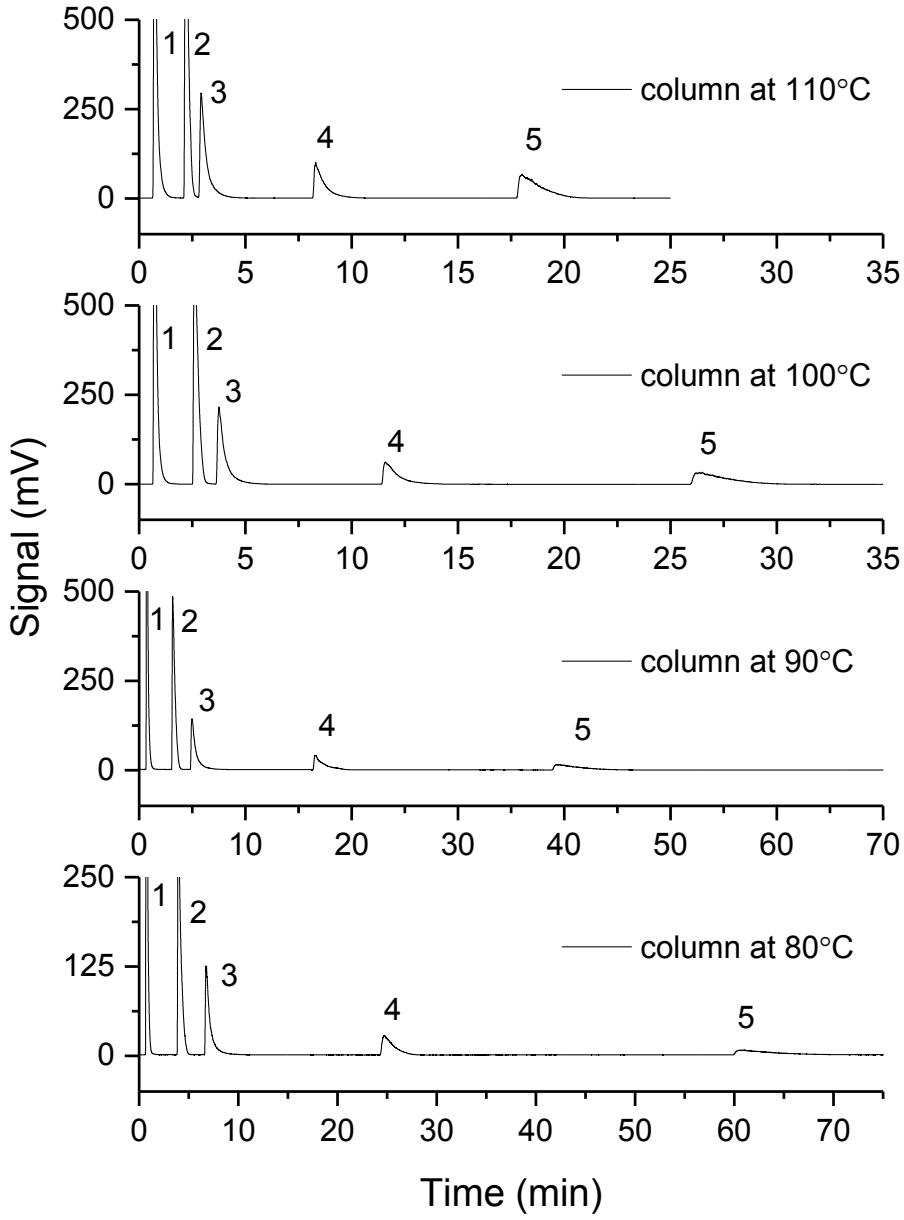

Figure 3.7: Isocratic-isothermal separation of a mixture of five analytes obtained at 4 different column temperatures using ELSD detection. Chromatographic conditions: Column - Thermo Hypercarb*HT, mobile phase: water (100%); flow-rate - 0.5 mL/min, sample concentration - 0.1 mg/mL of each analyte; Injection volume: 25 μL, elution order: (1) glycine, (2) sucrose, (3) uracil, (4) thymine, (5) cytidine; instrumental conditions as in experimental section 3.2.

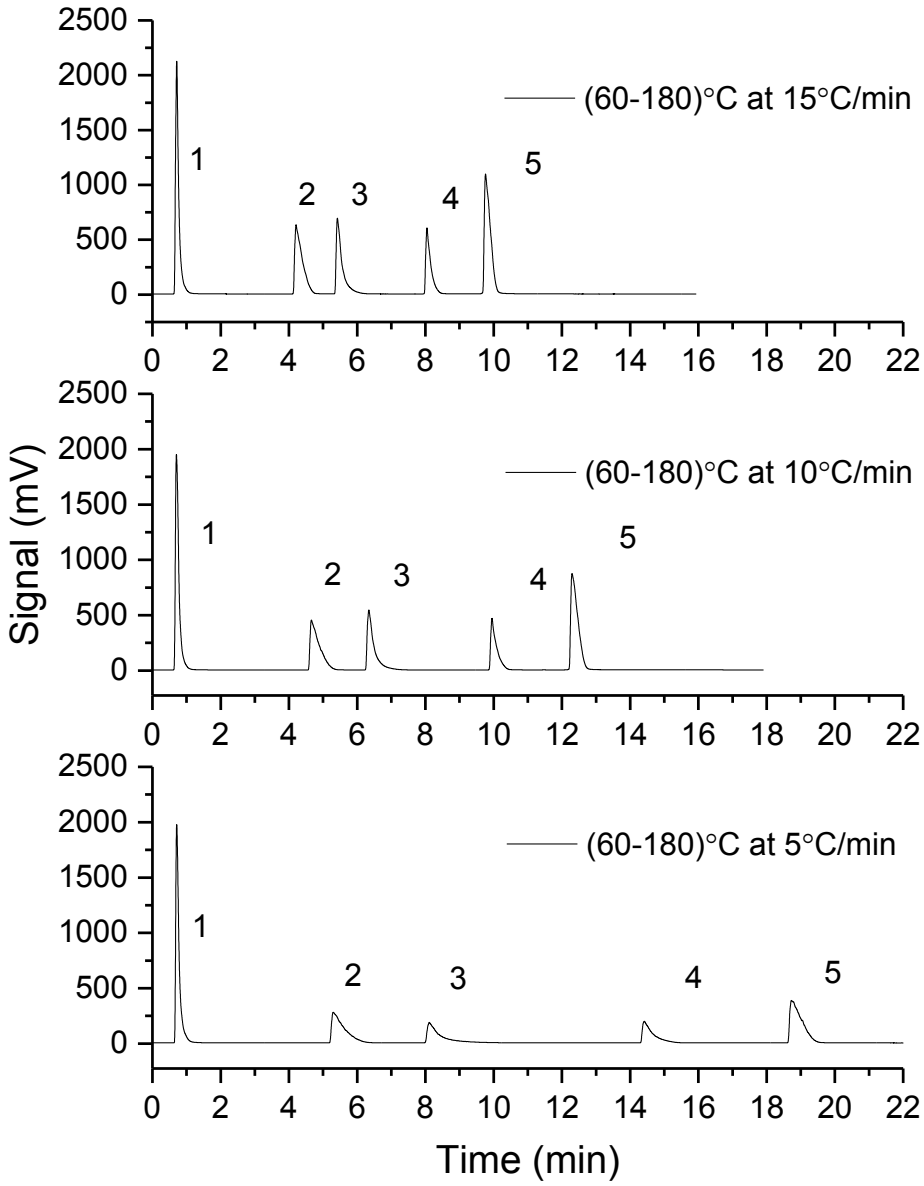

Figure 3.8: Isocratic-temperature gradient separation of a mixture of five analytes obtained by 3 different temperatures ramps using ELSD detection. Chromatographic conditions: Column - Thermo Hypercarb*HT, mobile phase - water (100%), flow-rate: 0.5 mL/min; sample concentration: 0.1 mg/mL of each; Injection volume: 25 µL, elution order: (1) glycine, (2) sucrose, (3) uracil, (4) thymine, (5) cytidine; instrumental conditions as in experimental section 3.2.

the ELSD showing the more pronounced effects. This necessitates careful consideration of elution bandwidth between peaks in a chromatogram if a normalised detection response for all analytes is to be achieved. The dependence of the response of the aerosol detectors on the size of the dried solute particles appears to be the origin of the observed inverse relationship between peak area and elution bandwidth. A limitation of the ELSD to detect Rayleigh scattering from very small particles makes it more susceptible to response alterations as a function of variation in elution bandwidth. The response of the C-CAD varies to a lesser extent with elution bandwidth due to a much lower limit of detectable particle size. Nevertheless, broader peaks compared to ELSD could be an issue in critical separations. Whilst the dependence of detector response on elution bandwidth complicates attaining universal detection in HTLC-ELSD analysis, the use of a temperature gradient provides more uniform response than isocratic-isothermal separations, even when the latter is performed at high temperature. Temperature gradients are therefore a useful alternative to solvent gradients with ELSD, which require the application of an inverse solvent gradient in order to stabilise the baseline. Further study needs to be undertaken to confirm the precise role of elution bandwidth in the response of aerosol detectors.

3.5 References

[1] T. Teutenberg, Potential of high temperature liquid chromatography for the improvement of separation efficiency - A review, Anal. Chim. Acta. 643 (2009) 1-12.

[2] S. Heinisch, J. L. Rocca, Sense and nonsense of high-tempearature liquid chromatography, J Chromatogr A. 1216 (2009) 642-658.

[3] C. McNeff, B. Yan, D. Stoll, R. Henry, Practice and theory of high temperature liquid chromatography, J Sep. Sci. 30 (2007) 1672-1685.

[4] H. A. Claessens, M. A. van Straten, Review on the chemical and thermal stability of stationary phases for reversed-phase liquid chromatography, J. Chromatogr. A 1060 (2004) 23-41.

[5] Y. Yang, Stationary phases for high-temperature liquid chromatography, LC GC EUR (2003) 37.

[6] L. Pereira, Porous graphitic carbon as a stationary phase in HPLC: Theory and applications, J. Liq. Chromatogr. Relat. Technol. 31 (2008) 1687-1731.

[7] J. Li, Y. Hu, P. W. Carr, Fast Separations at Elevated Temperatures on Polybutadiene-Coated Zirconia Reversed-Phase Material, Anal. Chem. 69 (1997) 3884-3888.

[8] G. Vanhoenacker, P. Sandra, Elevated temperature and temperature programming in conventional liquid chromatography--fundamentals and applications, J. Sep. Sci. 29 (2006) 1822-1835.

[9] R. Trones, A. Iveland, T. Greibrokk, High temperature liquid chromatography on packed capillary columns with nonaqueous mobile phases, J. Microcolumn. Sep. 7 (1995) 505-512.

[10] Y. Yang, T. Kondo, T. J. Kennedy, HPLC separations with micro-bore columns using high-temperature water and flame ionization detection, J. Chromatogr. Sci. 43 (2005) 518-521.

[11] T. S. Kephart, P. K. Dasgupta, Superheated water eluent capillary liquid chromatography, Talanta 56 (2002) 977-987.

[12] B. Gu, H. Cortes, J. Luong, M. Pursch, P. Eckerle, R. Mustacich, Low thermal mass liquid chromatography, Anal. Chem. 81 (2009) 1488-1495.

[13] A. Holm, P. Molander, E. Lundanes, T. Greibrokk, Novel column oven concept for cold spot large volume sample enrichment in high throughput temperature gradient capillary liquid chromatography, J. Sep. Sci. 26 (2003) 1147-1153.

[14] T. Teutenberg, H. J. Goetze, J. Tuerk, J. Ploeger, T. K. Kiffmeyer, K. G. Schmidt, W. Kohorst, T. Rohe, H. D. Jansen, H. Weber, Development and application of a specially designed heating system for temperature-programmed high-performance liquid chromatography using subcritical water as the mobile phase, J. Chromatogr. A 1114 (2006) 89-96.

[15] K. Peck, M. D. Morris, Optical errors in a liquid chromatography absorbance cell, J. Chromatogr. 448 (1988) 193-201.

[16] B. A. Jones, Temperature programmed liquid chromatography, J. Liq. Chromatogr. Relat. Technol. 27 (2004) 1331-1352.

[17] J. M. Charlesworth, Evaporative analyzer as a mass detector for liquid chromatography, Anal. Chem. 50 (1978) 1414 - 1420.

[18] T. Mourey, L. Oppenheimer, Principles of operation of an evaporative light scattering detector for liquid chromatography, Anal. Chem. 56 (1984) 2427-2434.

[19] R. W. Dixon, D. S. Peterson, Development and testing of a detection method for liquid chromatography based on aerosol charging, Anal. Chem. 74 (2002) 2930-2937.

[20] A. Stolyhwo, H. Colin, G. Guiochon, Use of Light Scattering as a detector principle in liquid chromatography, J. Chromatogr. 265 (1983) 1-18.

[21] D. Guillarme, S. Rudaz, C. Schelling, M. Dreux, J. L. Veuthey, Micro liquid chromatography coupled with evaporative light scattering detector at ambient and high temperature: Optimization of the nebulization cell geometry, J. Chromatogr. A. 1192 (2008) 103-112.

[22] B. T. Mathews, P. D. Higginson, R. Lyons, J. C. Mitchell, N. W. Sach, M. J. Snowden, M. R. Taylor, A. G. Wright, Improving quantitative measurements

for the evaporative light scattering detector, Chromatographia 60 (2004) 625 - 633.

[23] P. Molander, R. Trones, K. Haugland, T. Grebrokk, Aspects and applications of non-aqueous high temperature packed capillary liquid chromatography, Analyst 124 (1999) 1137-1141.

[24] K. Gaudin, P. Millet, F. Fawaz, P. Olliaro, N. J. White, C. Cassus-Coussere, U. Agbahoungha, J. P. Dubost, Investigation of porous graphite carbon at high temperature liquid chromatography with evaporative light scattering detection for the analysis of the drug combination artesunate - Azitrhomycine for the treatment of severe malaria, J. Chromatogr. A 1217 (2010) 75-81.

[25] A. Hazotte, D. Libong, P. Chaminade, High temperature micro liquid chromatography for lipid molecular species analysis with evaporative light scattering detection, J. Chromatogr. A 1140 (2007) 131-139.

[26] R. Trones, T. Andersen, T. Greibrokk, Impoved modification of a laser light scattering detector for the use in packed capillary high temperature liquid chromatography, J. High. Resolut. Chromatogr. 22 (1999) 283-286.

[27] R. Trones, T. Andersen, I. Hunnes, T. Greibrokk, Modified laser light scattering detector for use in high temperature micro liquid chromatography, J. Chromatogr. A 814 (1998) 55-61.

[28] S. Heinisch, G. Puy, M. P. Barrioulet, J. L. Rocca, Effect of temperature on the retention of ionizable compounds in reversed-phase liquid chromatography: Application to method development, J. Chromatogr. A 1118 (2006) 234-243.

[29] T. Teutenberg, S. Wiese, P. Wagner, J. Gmehling, High temperature liquid chromatography Part-II: Determination of the viscocities of the binary solvent mixtures - implications for liquid chromatographic separations, J. Chromatogr. A 1216 (2009) 8470-8479.

[30] T. Teutenberg, P. Wagner, J. Gmehling, High-temperature liquid chromatography. Part I: Determination of the vapour pressure of binary mixtures-implications for liquid chromatography separations, J. Chromatogr. A 1216 (2009) 6471-6480.

[31] T. Andersen, I. L. Skuland, A. Holm, R. Trones, T. Greibrokk, Temperature - programmed packed capillary liquid chromatography coupled to evaporative light scattering detection and electrospray ionization time of flight mass spectrometry for characterization of high molecular -mass hindered amine light stabilizers, J. Chromatogr. A 1029 (2004) 49-56.

[32] B. Merelli, M. D. Person, P. Favetta, M. Lafosse, Analysis of triacylglycerols on porous carbon by high temperature liquid chromatography, J. Chromatogr. A 1157 (2007) 462-466.

[33] L. C. Heinz, T. Macko, H. Pasch, High temperature liquid chromatography at critical conditions: Separation of polystyrene from blends with polyethylene and ethylene-styrene block copolymers, Int. J. Polymer Anal. Char. 11 (2006).

[34] R. Trones, T. Andersen, T. Greibrokk, D. R. Hegna, Hindered amine stabilizers investigated by the use of packed capillary temperature programmed liquid chromatography J. Chromatogr. A 874 (2000) 65-71.

[35] A. Hazotte, D. Libong, M. Matoga, P. Chaminade, Comparison of universal detectors for high temperature liquid chromatography, J. Chromatogr. A 1170 (2007) 52-61.

[36] US EPA [2012], Estimation Programs Interface Suite™ for Microsoft® Windows, v 4.11]. United States Environmental Protection Agency, Washington, DC, USA http://www.epa.gov/opptintr/exposure/pubs/episuitedl. html, [2012].

[37] S. Nukiyama, Y. Tanasawa, On the droplet-size distribution in an atomized jet, Trans. Soc. Mech. Eng. Jpn. 5 (1939) 62-67.

[38] M. Righezza, G. Guiochon, Effects of the Nature of the Solvent and Solutes on the Response of a Light Scattering Detector, J. Liq. Chromatogr. 11 (1988) 1967 - 2004.

[39] P. Van der Meeren, J. Vanderdeelen, L. Baert, Simulation of the mass response of the evaporative light scattering detector, Anal. Chem. 64 (1992) 1056-1062.

Chapter 4

Assessment of the complementarity of temperature and flow-rate for response normalisation of C-CAD

4.1 Introduction

Aerosol-based liquid chromatography detectors, such as the ELSD and the C-CAD, are regarded widely as quasi-universal detectors. These detectors have been proven useful for quantitative analysis of non-volatile analytes since they provide detection response irrespective of the optical absorption properties of the analyte and mobile phase. Nevertheless, non-linearity of the response with sample concentration and solvent dependency of detection response are major concerns, which limit the widespread acceptance of these detection techniques. Log-normalization is generally used to relate the detection response to sample concentration and it works well under isocratic conditions. However, with solvent gradient separation, response correction requires multiple calibration curves, since the response of aerosol detectors varies with the mobile phase composition. This poses practical difficulties in quantification, and it is highly desirable to have single calibrant quantification.

Relative uniformity of response is an attractive goal, especially for impurity testing in the pharmaceutical industry. In this case, a calibration plot prepared for the active pharmaceutical ingredient could be used to determine the levels of impurities without the need for standards or calibration plots for these impurities. As discussed earlier (section 1.3.2.2), many different approaches to mitigate the solvent effect have evolved recently [1-5]. All these approaches involve correcting the response variations resulting from the solvent gradient separation. One potential solution to the non-uniformity of response of aerosol detectors would be to avoid the solvent gradient altogether and to optimize the separation under isocratic conditions. This might be achievable using alternate separation tools such as temperature or flow-rate variation, which facilitates a comparable elution profile to that obtained using solvent gradient elution.

In the present study, the possibility of achieving relatively uniform detection response of the C-CAD for different analytes by employing isocratic separation with temperature and mobile phase-flow rate variation as optimization tools has been investigated. The capability of HTLC to meet the ever-increasing requirements for separation throughput and control of separation selectivity has been investigated by many researchers. In recent times, several aspects of HTLC, including retention mechanism and principles, range of applications from analytical to capillary scale separations, challenges in broader acceptance and consequent developments in instrumentation have been published [6-9]. It is well documented that with an increase in temperature, viscosity, surface tension and the dielectric constant of water and aqueous-organic binary solvent mixtures drop significantly and approach the properties of the pure organic solvents [6,7,10]. It is noteworthy that an increase in temperature by 4-5℃ is required to achieve an effect comparable to a 1% change in the amount of organic solvent (ACN or methanol) present in the mobile phase. However, for chromatographic separations employing water-rich eluents, variation of temperature alone may not be sufficient to achieve elutropic strength comparable to a solvent gradient. Different strategies such as the use of isocratic binary solvent mixtures containing higher amount of organic solvents coupled with a high temperature ramp [9,11,12] or temperature pulsing [13], have been reported to improve the performance of HTLC separations. Thus, isocratic-temperature gradients can replace the use of solvent gradients in many instances and thereby complement aerosol detectors by minimizing the contribution of solvent effects on non-uniformity of the response. Nevertheless, the majority of the published work related to the use of temperature gradient separations has been limited to separations involving UV-detection. Even after quite intensive research in HTLC, the use of temperature gradients is not considered a mainstream approach for chromatographic optimization. This is due primarily to potential practical limitations of temperature gradients, such as slow heat transfer in liquids, high thermal mass of analytical scale columns, and lack of a suitable heating device providing a sufficiently wide temperature range and a suitably steep temperature ramp. In view of these limitations, some combination of temperature gradients with additional optimization parameters becomes inevitable.

Although the use of mobile phase flow-rate variation for improving the separation speed and peak efficiency has been investigated before [14-18], the risk of

high column backpressure in a conventional high performance liquid chromatography set-up has deterred the widespread implementation of flow-rate programming. The dependence of column backpressure *(*ΔP) on the viscosity (η) and linear velocity (u) of the fluid is commonly described by Darcy's equation:

$$\Delta P = \beta_0 \cdot \eta \cdot u \cdot L \qquad \text{(Equation-4.1)}$$

Where, β_0 is the resistance factor and L is the length of the column.

Column backpressure alters in direct proportion to viscosity and the linear velocity of the mobile phase. In HTLC separation, a temperature-induced decrease in solvent viscosity results in much lower column backpressure, permitting separations to be performed at a high flow-rate. Variations in mobile phase flow-rate can be utilised as a means to improve efficiency and speed of HTLC separations. In HTLC separations, because of the reduced viscosity of the mobile phase, the diffusion coefficient alters significantly and thereby improves the inter-phase solute mass transfer, allowing separations to be performed at solvent velocities greater than the optimal Van Deemter value without significantly affecting efficiency. Therefore, isothermal-HTLC separations are normally performed at higher flow-rates. However, in temperature gradient separations, the column backpressure varies across the length of the temperature ramp. Therefore, for optimal resolution and separation speed, a simultaneous alteration in linear velocity becomes necessary. In order to fully realise the separation benefits of a temperature gradient, optimal mobile phase linear velocity needs to be maintained throughout the chromatographic run. Moreover, flow-rate programming can help to reduce the run time in a temperature gradient separation. Thus, a flow-rate gradient perfectly complements the use of a temperature gradient. Previous studies [14-18] involving simultaneous variation in column temperature and mobile phase flow-rate have been focused on separation throughput and were performed using a conventional UV-detector. In this study, the suitability of these separation strategies for response normalization in aerosol detectors has been investigated.

4.2 Experimental

The general experimental details (instrumentation and chemicals) are given in chapter 2. Stock solutions of individual analytes were prepared at a concentration of 2 mg/mL in ACN/water (1:1 v/v) and stored in a refrigerator at 4°C.

A Dionex Ultimate 3300 UHPLC system equipped with dual gradient pumps, auto-sampler, column heater, photodiode array detector (PDA) and Chromeleon (version 7.1) chromatography data processing software was used. 130 µm × 1100 cm capillary tubing was used to connect the inverse gradient pump to the mixing tee-piece. The outlet of the mixing tee-piece was further connected to the C-CAD detector inlet using 130 µm × 45 cm viper-fit stainless steel tubing. Throughout this study, the ELSD parameters employed were: nebulisation and evaporation temperatures - 60°C; gas flow-rate - 1.6 SLM, and a gain factor of 4. The C-CAD was used with the manufacturer's recommended setting of 35±0.2 psi for the gas flow at 30°C nebuliser temperature.

4.2.1 Flow-injection analysis (FIA)

The possible role of mobile phase flow-rate and solvent composition in detection response of the ELSD and C-CAD was evaluated using FIA. Caffeine and sucrose solution (0.2 mg/ml in water) were injected in triplicate at 5 different mobile phase compositions (5/95 (v/v), 20/80 (v/v) 50/50 (v/v) 80/20 (v/v) and 95/5 (v/v) ACN/Water). In addition, the mobile phase flow-rate varied from 0.2-2.0 mL/min for each mobile phase composition.

4.2.2 Chromatographic separations

Separations were carried out using a Dionex Acclaim RSLC 120, C18, 2.2-µm Analytical (2.1 × 100 mm) column purchased from Thermo Fisher Scientific, Scoresby, Vic., Australia. To minimise the band dispersion resulting from extra-column volume and thermal mismatch, the column was connected to the injector using the Polaratherm mobile phase pre-heating coil (120µm × 50mm SS-tubing). This coil has a volume of ~5.6 µL and typical early-eluted peaks exhibited a volume of ~90 µL, suggesting that the adverse effects of extra-column dispersion should be negligible. The ELSD or C-CAD inlet was connected to the column outlet using stainless steel tubing (130 µm × 45 cm of 1/16' (o.d.)) bent into a serpentine shape. The eluents used throughout this study were: mobile phase-A: 10 mM NH_4OAc (pH-5.5), mobile phase-B: ACN. For the inverse gradient approach (Section 3.3), the composition of the secondary solvent stream must be maintained exactly opposite to that of the column effluent. Therefore, a delay time of the inverse gradient program was used so that throughout the gradient segment, the composition of the secondary stream arriving at the mixing tee-piece

remained exactly opposite to that of the column effluent. Furthermore, experiments similar to that described by de Villiers et al. [5] were performed to confirm the synchronization of the two gradients.

An equimass mixture of 8 analytes was separated at an eluent flow-rate of 0.3 mL/min, using the following solvent gradient program: pump-1: 0-1 min 20% B, 1-8 min 20-80% B, 8-10 min 80% B, 10-13 min 80-20% B followed by equilibration for 7 min. Solvent gradient compensation was performed using following inverse gradient program: pump-2: 0-1.8 min 80% B, 1.8-9.8 min 80-20% B, 9.8-11 min 20% B, 11-13 min 20-80% B followed by equilibration for 7 min. Temperature gradient separation was achieved under isocratic mobile phase conditions (ACN / 10 mM NH_4OAc at pH 5.5, 20:80, v/v) at a flow-rate of 0.3 mL/min, using the following temperature gradient program: 0-0.5 min 30°C, 0.5-10.5 min temperature gradient (30-80° at heating rate of 5°C/min), 10.5-16 min 80°C, 16-20 min 80-30°C (at the rate of 30°C/min), followed by equilibration at 30°C for 5 min. As discussed in section 4.3.2, in order to enhance detection response, a secondary stream of 100% ACN (at 0.3 mL/min) was mixed with the column effluent using a post-column mixing tee-piece. Separation was also performed using a mobile phase flow-rate gradient superimposed on the temperature gradient described above. The flow-rate gradient used for pump-A was: 0-3 min 0.3 mL/min, 3-4 min 0.5 mL/min, 4-5 min 0.5 mL/min, 5-6 min 0.7 mL/min, 6-16 min 0.7 mL/min, 16-19 min 0.3 mL/min and 19-25 min 0.3 mL/min. As discussed in section 4.3.2 a secondary stream of mobile phase (from pump-B) was mixed with the column effluent to compensate the baseline elevation resulting from the flow-rate variation. The flow-rate gradient program for pump-B was: 0-3 min 0.6 mL/min, 3-4 min 0.4 mL/min, 4-5 min 0.4 mL/min, 5-6 min 0.2 mL/min, 6-16min 0.2 mL/min, 16-19 min 0.6 mL/min and 19-25 min 0.6 mL/min.

4.3 Results and discussion

4.3.1 Effect of mobile phase composition and flow-rate on response of aerosol detectors (FIA)

To assess the practicality of using a flow-rate gradient, the effect of solvent composition and eluent flow-rate variation on the response of aerosol detectors was examined by FIA. As shown in Fig. 4.1(a), the response of both the detectors (ELSD

and C-CAD) was enhanced with an increase in ACN up to 80%, which is in accordance with the commonly reported solvent-composition dependency of aerosol detection response. Effects of mobile phase flow-rate on the detection response have been investigated previously. While the responses of ELSD and C-CAD are often reported to have an inverse relationship with the mobile phase flow-rate, some authors have reported contradictory observations. For instance, one of the frequently cited ELSD papers [19] has reported a gradual increase in ELSD response with increases in mobile phase flow-rate from 0.1-1.0 mL/min. Novakova et al. [20] observed a marginal decrease (about 25%) in C-CAD response with an increase in mobile phase flow-rate from 0.4-1.0 mL/min. In contrast, Hutchinson et al. [21] reported that an increase in mobile phase flow-rate from 0.2-2.0 mL/min caused an increase in the response of the C-CAD. It is worth noting that variations in instrument design and physical properties of solvents used for particular studies may significantly influence these reported trends. Clearly, understanding the effects of flow-rate variation on detection response of ELSD and C-CAD is important for hyphenation of these detectors with a flow-rate gradient. As shown in Fig. 4.1(b), in experiments involving eluent flow-rate variation, the two detectors responded in a different manner. Regardless of the mobile phase composition, a sharp decrease in the ELSD response was observed with an increase in the flow-rate above 0.2 mL/min, but response for both detectors was relatively constant for flow-rates greater than 1.0 mL/min. A significant increase in the C-CAD detection response was observed for eluents containing >80% ACN when the flow-rate was changed from 0.2 to 0.4 mL/min. A possible explanation for this observation is that while the ELSD and C-CAD both use a concentric nebuliser to introduce the sample, the C-CAD operates at much higher gas velocity than the ELSD [22]. Under constant nebulising gas parameters, the response depends strongly on the viscosity, surface tension and density of the eluent. An increase in the percentage of ACN in the eluent dramatically influences the droplet distribution and evaporation process, leading to the production of a higher concentration of fine solute particles and therefore a higher response. Moreover, at constant eluent composition the relative velocities of the nebulising gas and eluent streams dominate the aerosol transport efficiency. The relationship between nebulising gas and eluent flow-rates in ELSD detection has been widely studied [23-25] and it is commonly reported that relative velocities of the gas and liquid streams need to be maintained in the sonic velocity range to achieve optimum detection response [23,26]. Similar data have not yet been reported for the C-CAD, but it is likely that at

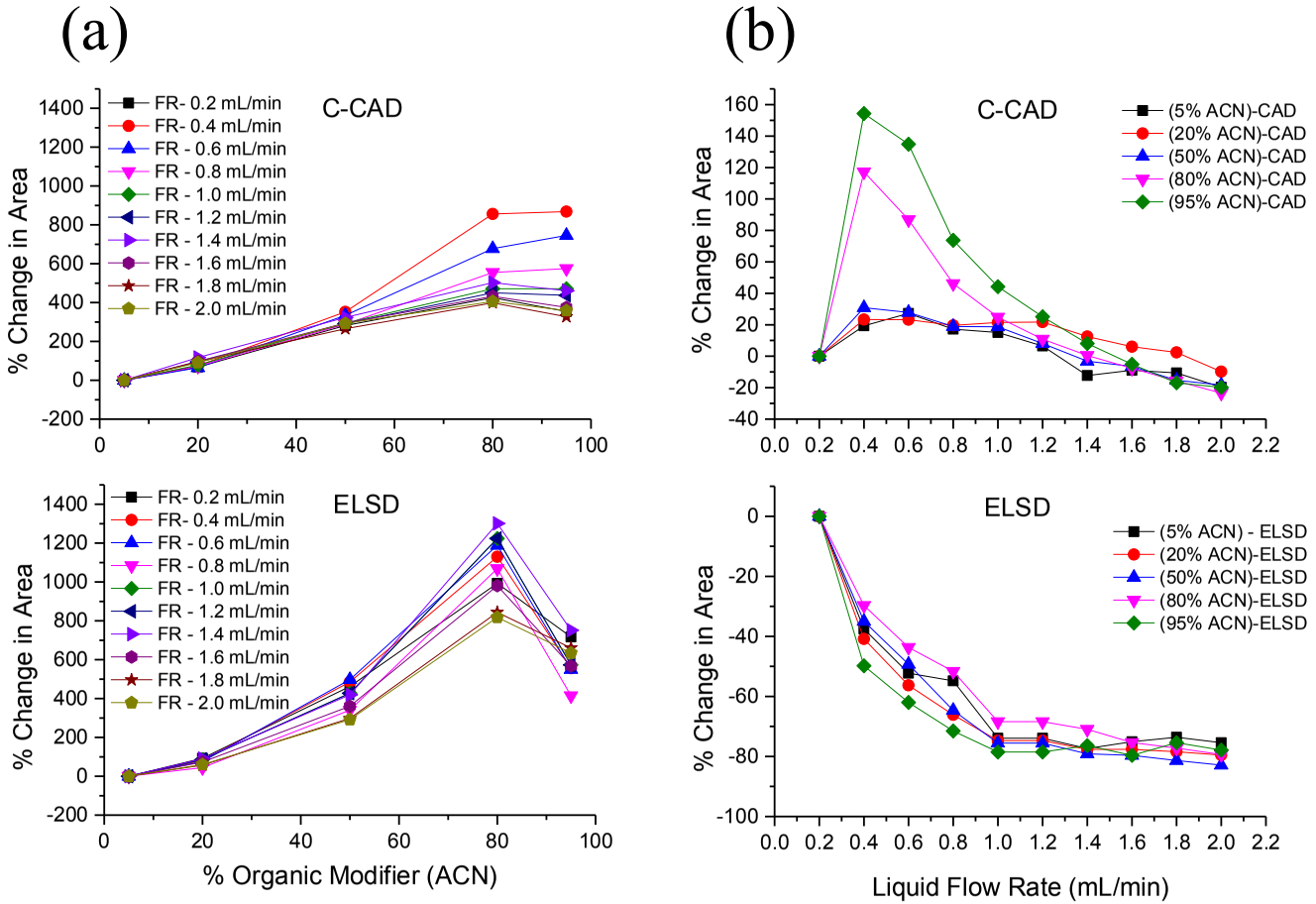

Figure 4.1: Flow injection analysis. The effect of (a) mobile phase flow-rate variation and (b) mobile phase composition on response of C-CAD and ELSD, Flow-injection conditions and instrumental parameters are detailed in experimental section 4.2

low eluent flow-rates (< 0.2 mL/min) an increase in gas-to-liquid velocities produces coarse droplets, leading to a very low and inconsistent response. The data points shown at 0.2 mL/min in Fig 4.1(b) are therefore likely to be unreliable. However, for the eluents containing less than 50% ACN, the response of the C-CAD was found to remain relatively unaffected (within 20% of peak area) with an increase in flow-rate from 0.2-2.0mL/min. In particular, flow-rate variation in the range of 0.4-1.2 mL/min was found to be most appropriate for implementation of a flow-rate gradient using C-CAD.

4.3.2 Utilising temperature and flow-rate gradients to achieve separation under isocratic conditions

To demonstrate the effect of mobile phase composition on the C-CAD response an equimass mixture of 8 analytes was separated by a linear solvent gradient method over the range 20-80% ACN. Response variation as a function of mobile phase solvent composition is clearly seen in Fig. 4.2, where the response (in terms of peak area) varied considerably across the chromatogram, with the analytes being eluted in a more solvent-rich part of the chromatogram (analytes 7 and 8) showing highest response, as predicted from the C-CAD plot in Fig. 4.1 (a). Fig. 4.3 represents a temperature gradient approach in which separation of the same test mixture was carried out using a linear temperature gradient from 30-80^{0}C under isocratic conditions (ACN/ 10 mM NH_4OAc, 20:80 v/v). Results published from chapter-3 [27] revealed that eluent temperature had only a marginal effect on the response (area counts) of aerosol detectors, therefore, relatively uniform response can be achieved by isocratic-temperature programming instead of conventional solvent gradient separation. The peak areas for all the 8 analytes in Fig. 4.3 are very similar (percentage relative standard deviation (%RSD < 5%). An alternative approach involving simultaneous variation in column temperature and eluent flow-rate is shown in Fig. 4.4. Bearing in mind the limitation of a temperature gradient in achieving an elutropic strength variation comparable to a solvent gradient, and the column backpressure restrictions on flow rate-variation, a combination of temperature and flow-rate gradients was considered complementary. Uniform response for all the 8 analyte was obtained (RSD<3%) and the overall analysis time was reduced. Thus, as shown in Figs. 4.3 & 4.4, the variable detection response of a C-CAD caused by the use of a solvent gradient can be overcome by performing the separation under isocratic mobile phase conditions but with the use of temperature and flow-rate gradients.

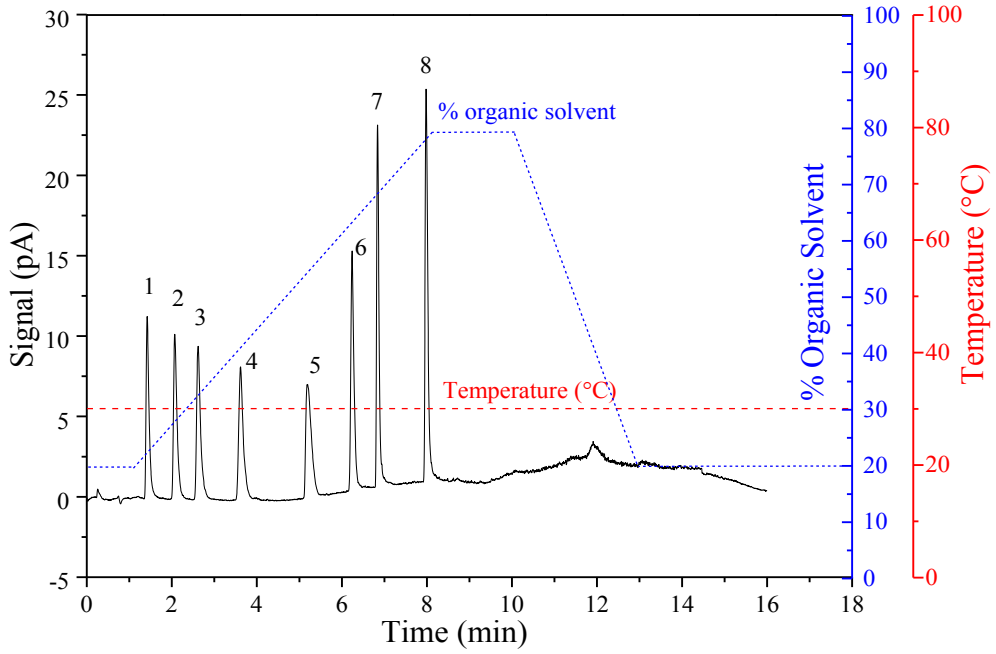

Figure 4.2: Solvent gradient separation of equimass mixture of 8 analytes Elution order: (1) Sufamerazine, (2) sulfamethamine, (3) sulfamethizole, (4) sulfamethoxazole, (5) sulfamethoxine, (6) furosemide, (7) prednisolone and (8) indapamide. For chromatographic conditions, refer experimental section 4.2

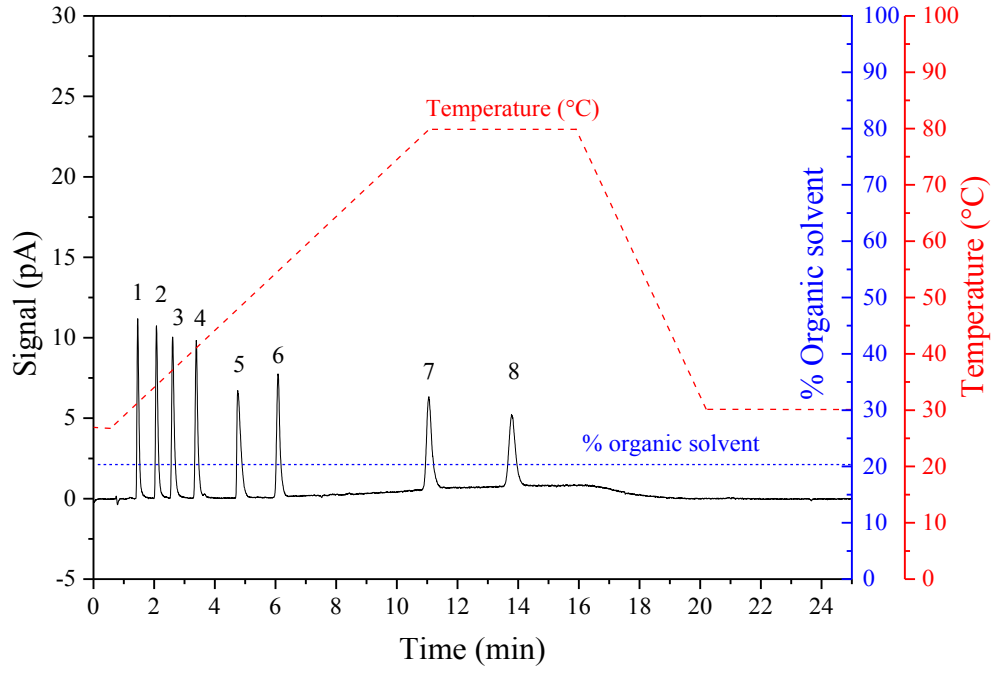

Figure 4.3: isocratic-temperature gradient separation of equimass mixture of 8 analytes. Elution order same as Figure 4.2. For chromatographic conditions, refer experimental section 4.2.

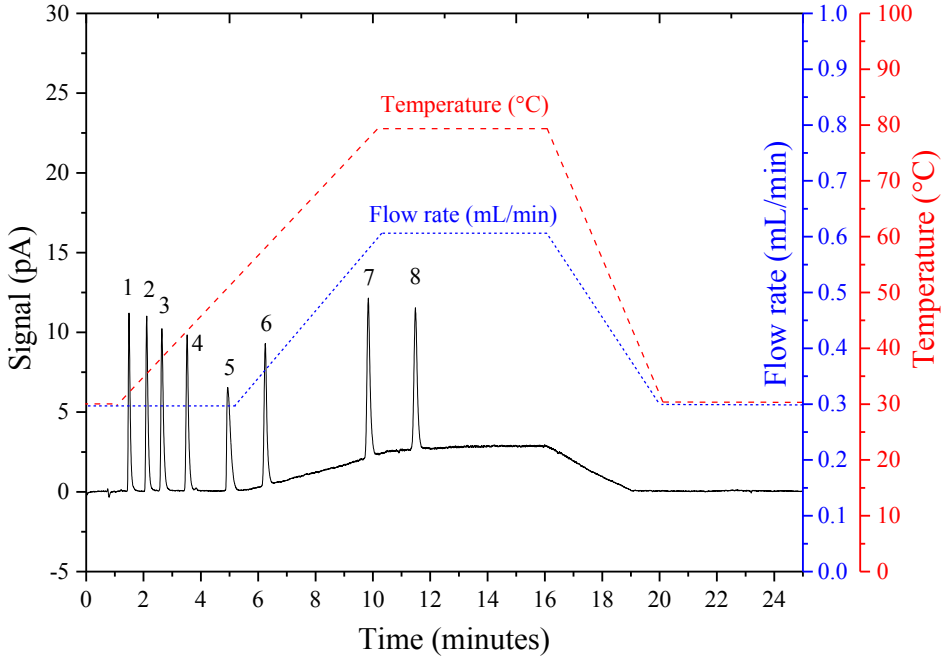

Figure 4.4: Isocratic separation of an equimass mixture of 8 analytes, using combination of temperature and flow-rate gradient. Elution order same as Figure 4.2. For chromatographic conditions, refer experimental section 4.2

Although the latter two approaches (Figs. 4.3 & 4.4) provided uniform response in comparison to the solvent gradient separation, the overall response for these two approaches was reduced due to the relatively low amount of organic solvent (20% v/v) in the eluent. Moreover, baseline elevation observed with increase in the eluent flow-rate was another issue with the flow-rate gradient approach (Fig. 4.3). Therefore, the feasibility of improving these two approaches by the post-column addition of a secondary solvent stream was investigated (Figs. 4.5 & 4.6). These investigations were focused on two aspects: first, the enhancement of response by the addition of an organic solvent (ACN) after the temperature gradient separation, and second, baseline correction by compensating the flow-rate variation by means of post-column flow-rate make-up to introduce a constant flow- rate into the C-CAD.

According to the Nukiyama-Tanasawa equation [28], at constant nebulisation parameters, solvent surface tension and viscosity of the liquid stream influence the process of evaporation. This indicates that in an isocratic temperature gradient separation, response enhancement of the C-CAD can be achieved by mixing the column effluent with a secondary stream of ACN. The flow-rate of the secondary stream was varied over the range 0.1-0.6 mL/min to change the mixing ratio with the column effluent from 3:1 to 1:2. Typically, the surface tension of aqueous-organic solvent mixtures decreases in a non-linear manner and the decrease in surface tension is more significant for the initial regions when the organic solvent is added to water [29,30]. This could be the reason that incrementing the flow-rate of the secondary stream above 0.3 mL/min showed no noticeable response enhancement. However, when the second pump was set to deliver ACN at the same flow-rate as used in the chromatographic separation (i.e. 0.3 mL/min), a 3-fold response enhancement was achieved (Fig. 4.7 (a)), albeit with some increase in baseline noise and baseline instability). Fig. 4.7 (b) shows the effects of flow-rate compensation utilized with a flow-rate gradient. The baseline stability is clearly improved when flow-rate compensation was used. Without this compensation, the baseline reflects each step in the flow-rate gradient profile, which could lead to interferences in the quantification of peak areas.

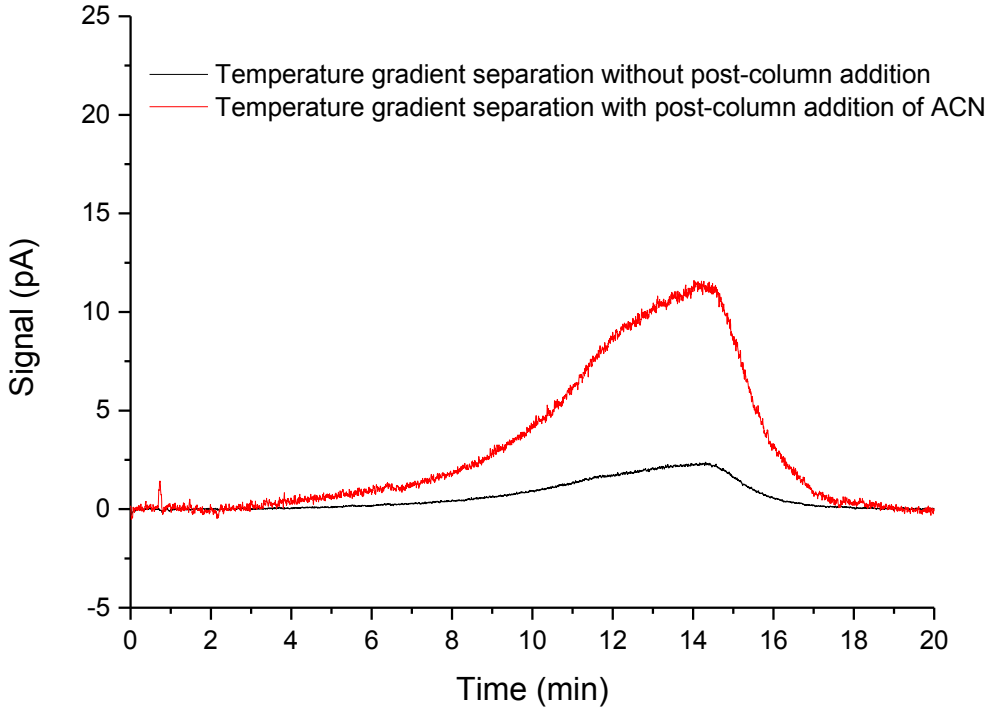

Figure 4.5: Effects of post-column solvent addition on baseline in isocratic-temperature gradient. Temperature ramp: 30-180°C at 5°C/min, flow-rate: 0.3 mL/min. Secondary stream mixed with column effluent at 0.6 mL/min

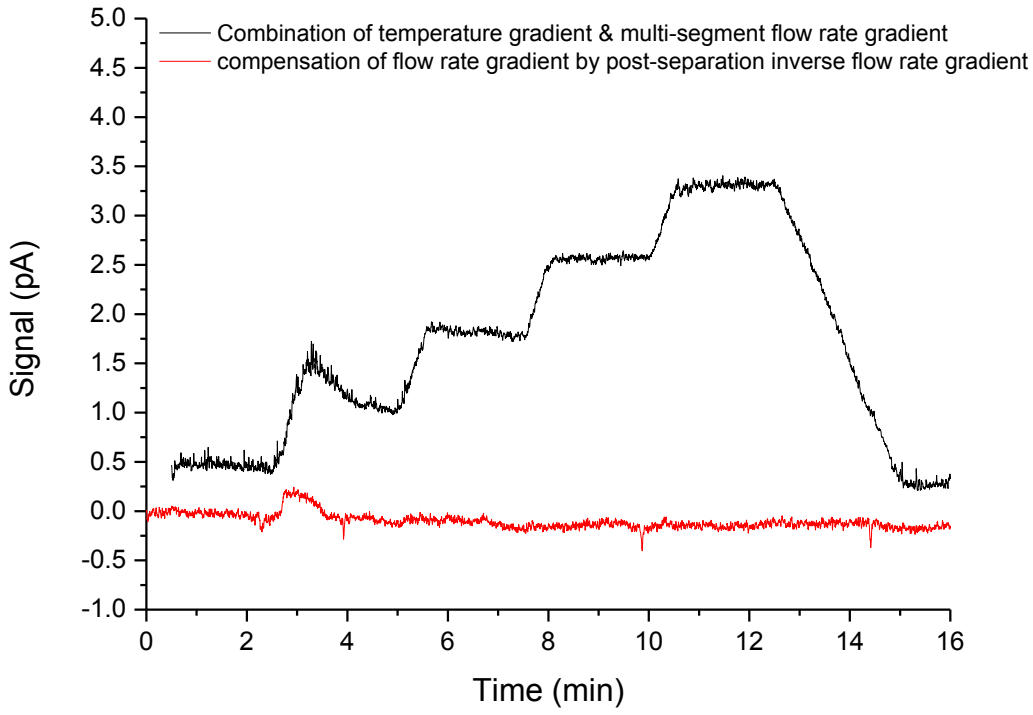

Figure 4.6: Effects of post-column solvent addition on baseline in isocratic-temperature + flow-rate gradient. Temperature ramp: 30-180°C at 5°C/min. Nebuliser feed maintained at a constant flow-rate by means of inverse flow-rate gradient of the secondary stream.

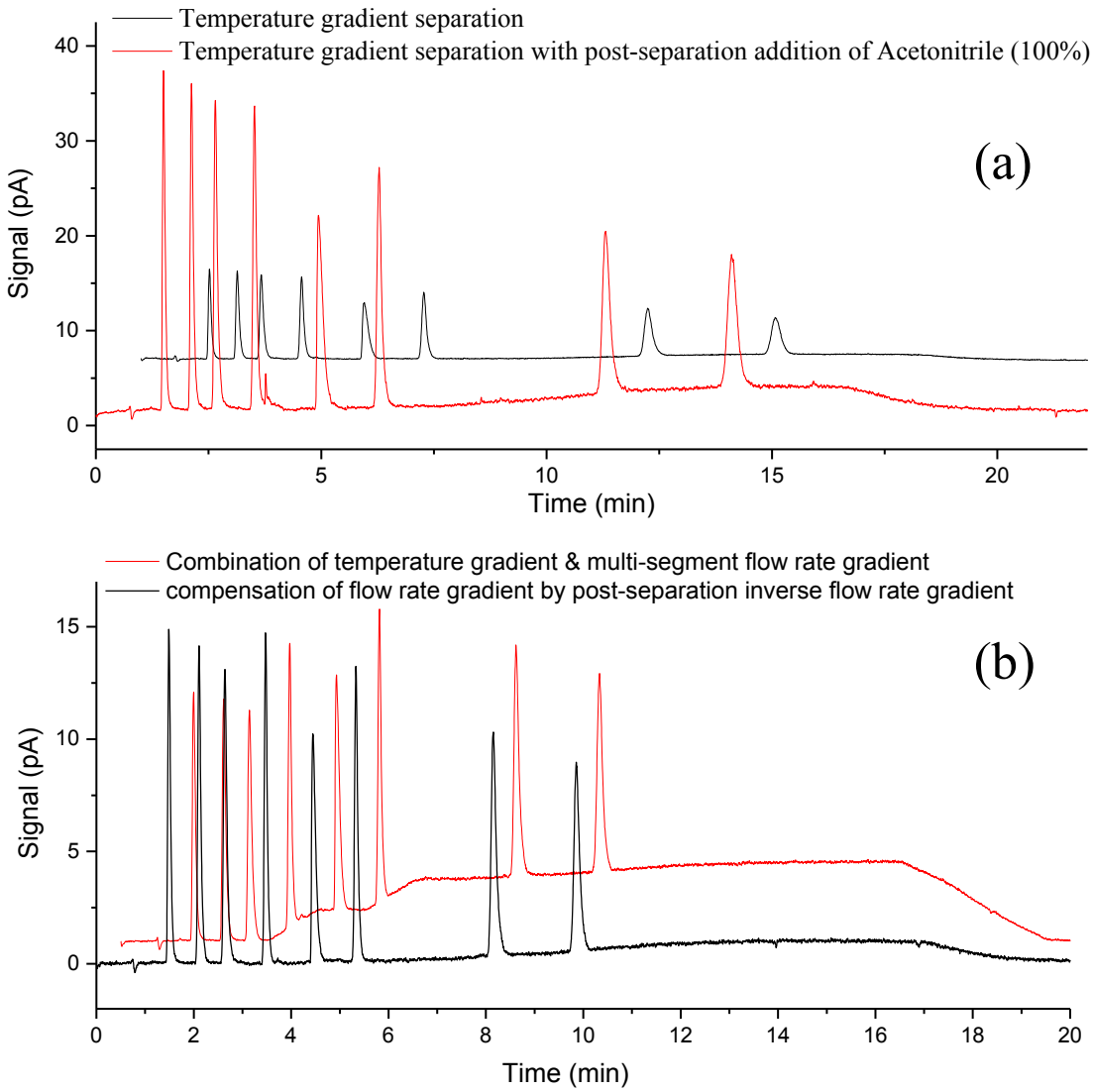

Figure 4.7: Separation of a mixture of 8 analytes by (a) Approach-I: Isocratic – temperature gradient separation (3-fold response enhancement achieved by mixing pure ACN with column effluent), (b) Approach-II: Separation under isocratic conditions using a combination of a temperature gradient and a flow-rate gradient. Baseline instability resulting from continuous flow-rate variation was compensated by mixing a secondary stream of mobile phase with the column effluent. Elution order is the same as Fig 2. Experimental conditions detailed in section 2.1.4

4.3.3 Comparative evaluation of approaches to C-CAD response normalisation

C-CAD response normalisation was assessed by comparing a traditional solvent gradient, a solvent gradient with inverse gradient compensation, an isocratic-temperature gradient with post-column ACN addition, and a combination of temperature and eluent flow-rate gradients with flow-rate make-up. Each of the latter three approaches provided excellent reproducibility in peak areas (RSD <3%, n=3) and retention times (RSD < 2 %, n=3) of all 8 analytes. Fig. 4.8 depicts the response homogeneity achieved by the four approaches, using two sample loading levels (0.1 and 0.5 µg). The conventional solvent gradient method gave a wide variation in response (RSD 33.5% averaged over the two sample loading levels studied) between the analytes (Fig. 4.8 (a)), although this variation was reduced considerably (to an average RSD of 6.5%) when the inverse gradient solvent compensation was applied (Fig. 4.8 (b)). The average % RSD values were 4.8% and 4.5% for the temperature gradient and flow-rate gradient methods (Figs. 4.8 (c) and 4.8 (d)), respectively. Moreover, the isocratic-temperature gradient approach with post-column solvent addition (Fig. 4.8 (c)) showed the highest response factors. Calibration curves for all the tested analytes were obtained over the sample mass range 0.1-7.0 µg using the three separation approaches. Log transformed values of the peak area of all 8 analytes were plotted against log (sample mass). All three approaches showed good linear correlation with R^2>0.99 (Figs. 4.10 (b), 4.11 (b) & 4.12 (b)) with the calibration plots for all analytes being almost superimposable, indicating improved uniformity in response.

To demonstrate the potential utility of these approaches for uniform detection response in pharmaceutical analysis, a typical drug impurity profiling application was mimicked by separation of a standard mixture containing 5 mg/mL of prednisolone and 5mg/L (i.e. 0.1% with respect to prednisolone) of the remaining seven compounds in the test mixture. The peak area (corrected using logarithmic regression) for a 0.1 mg/mL prednisolone standard was used for the quantification of the peaks corresponding to the known compounds. Signal-to-noise ratio (S/N) for the individual peaks were obtained by comparison with corresponding blank chromatograms. Chromatograms are shown in Fig. 4.13 and performance data are listed in Table 4.1. The accuracies observed for the temperature gradient method with post-column solvent addition and for the combination of temperature and flow-rate gradients were superior to that observed for the inverse gradient solvent compensation method.

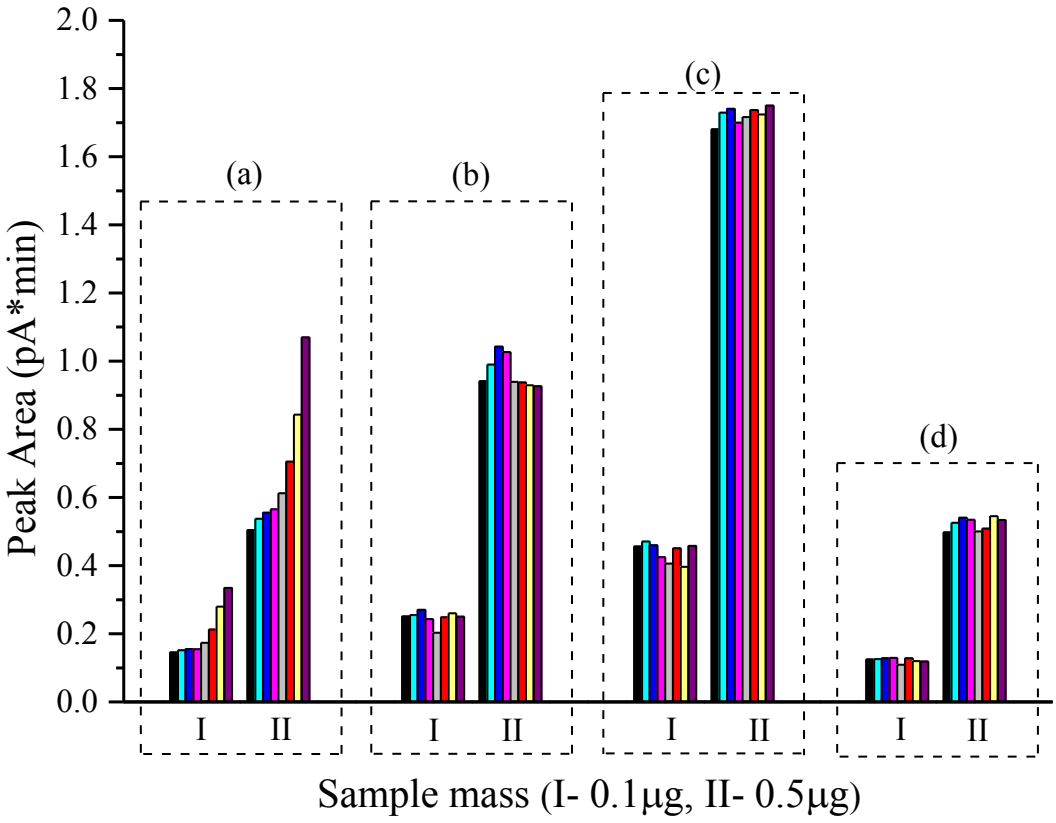

Figure 4.8: Effectiveness of different approaches for C-CAD response normalisation. (a) Solvent gradient, (b) inverse gradient solvent compensation, (c) isocratic-temperature gradient separation with post-column solvent addition, (d) combination of temperature and flow rate gradients with post-column flow-rate make-up. Column order (left to right): Sulfamerazine > sulfamethazine > sulfamethizole > sulfamethoxazole > sulfamethoxine > furosemide > prednisolone > indapamide. Each column represents average area (RSD < 3, n=3) of the respective compound. Experimental conditions detailed in section 4.2

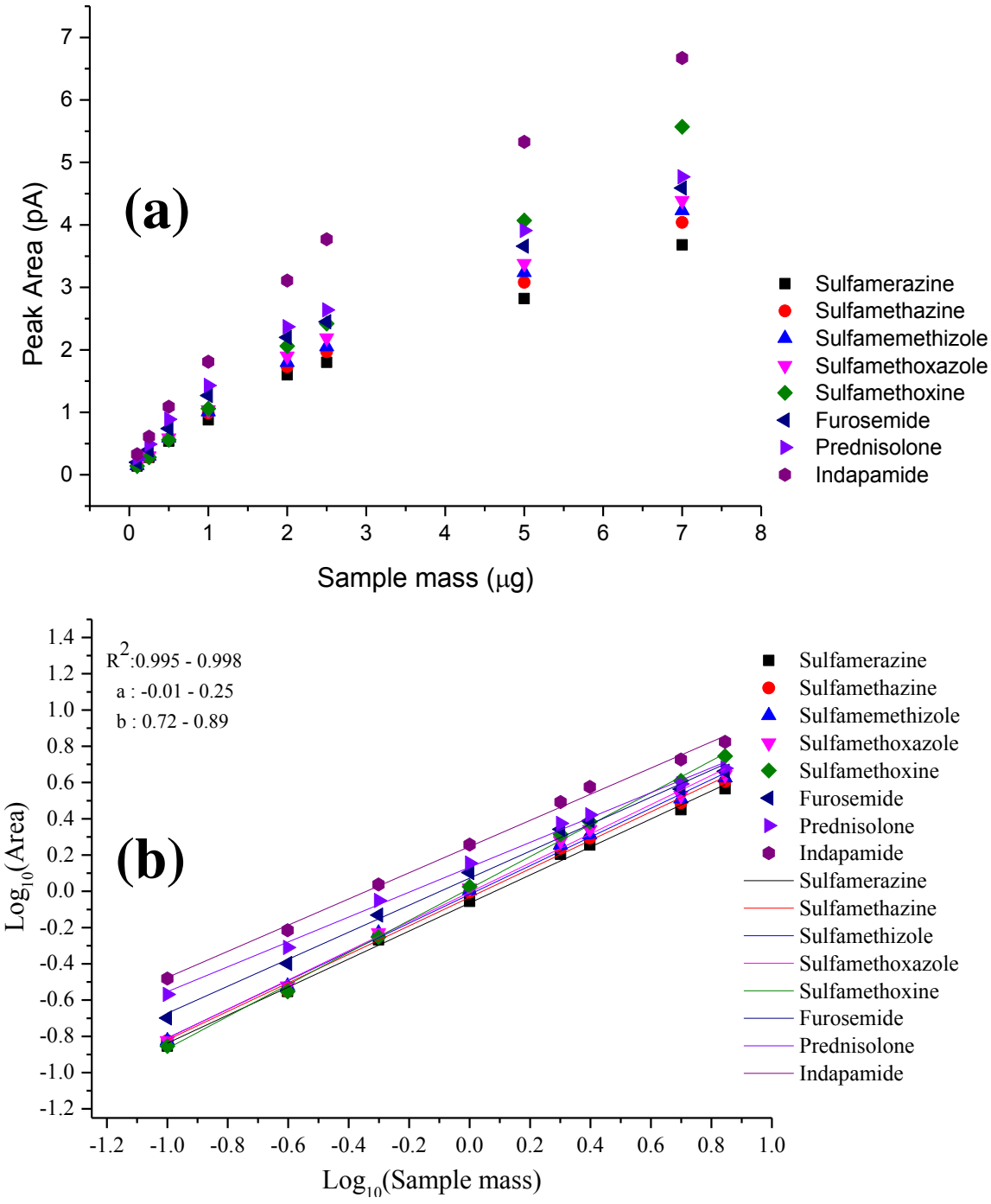

Figure 4.9: Average calibration curves obtained for 8 analytes separated by solvent gradient- (a) Non-logarithmic coordinates (b) Logarithmic coordinates.

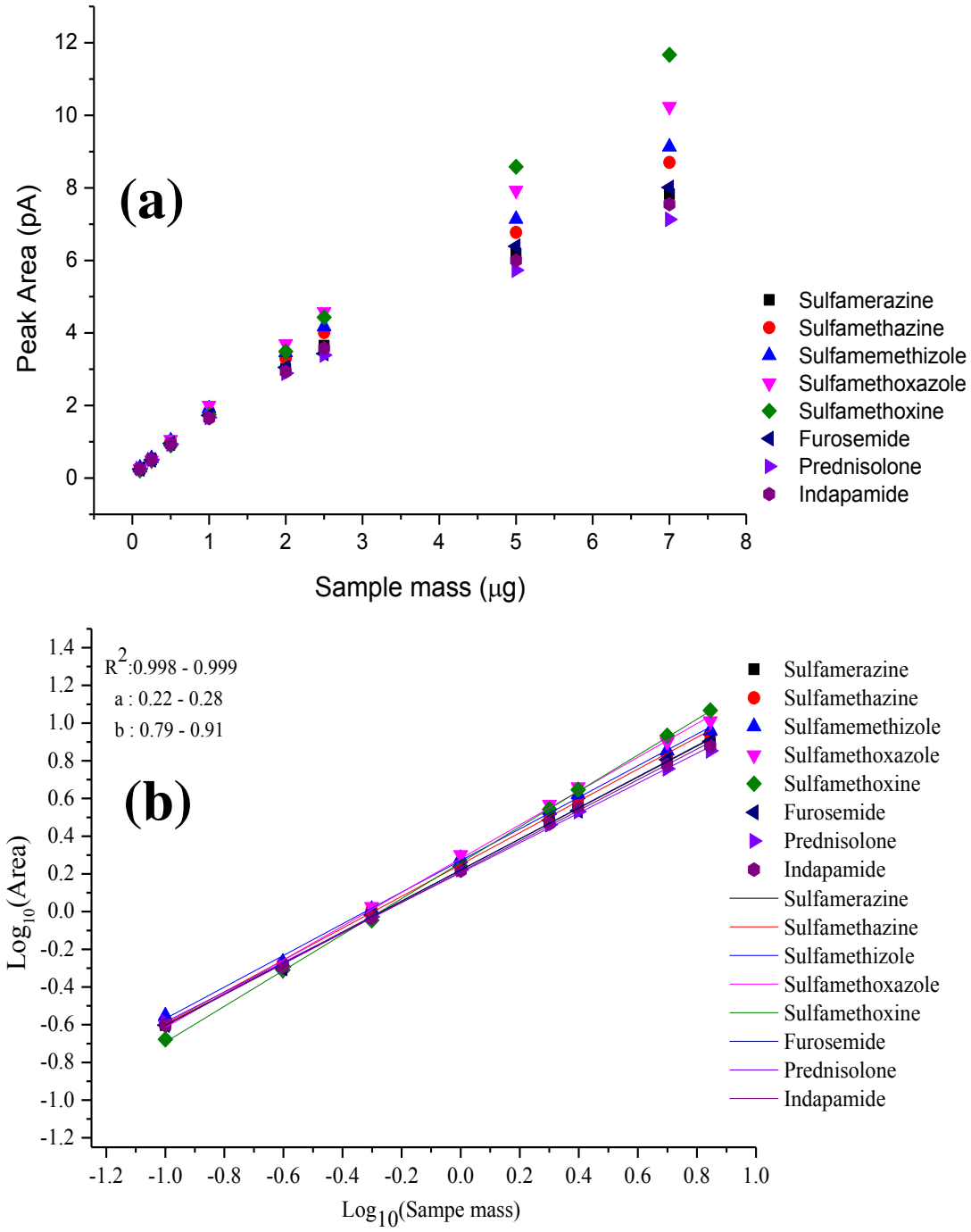

Figure 4.10: Average calibration curves obtained for 8 analytes separated by inverse gradient solvent compensation technique- (a) Non-logarithmic coordinates (b) Logarithmic coordinates.

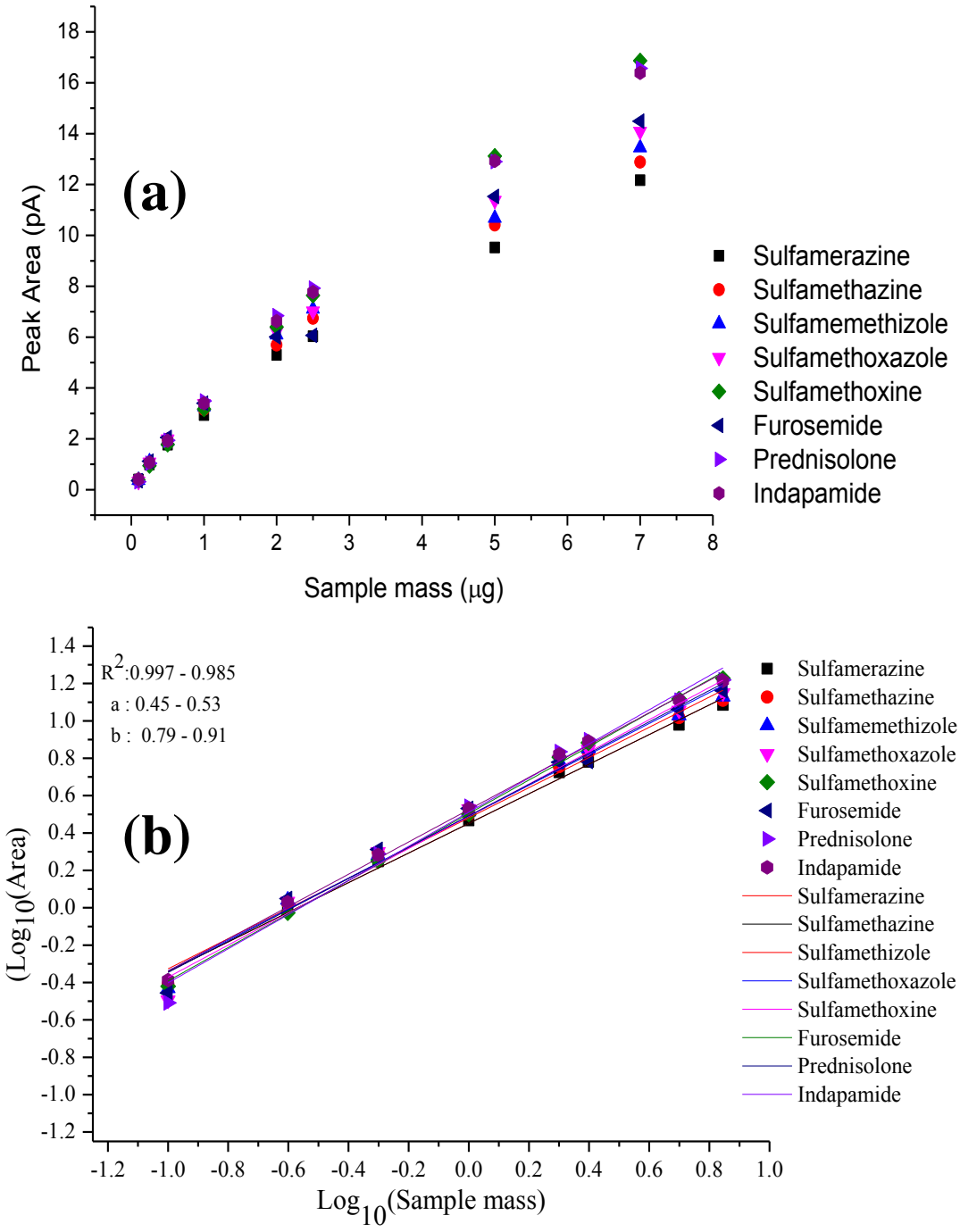

Figure 4.11: Average calibration curves obtained for 8 analytes separated using isocratic-temperature gradient with post-column solvent addition- (a) Non-logarithmic coordinates (b) Logarithmic coordinates.

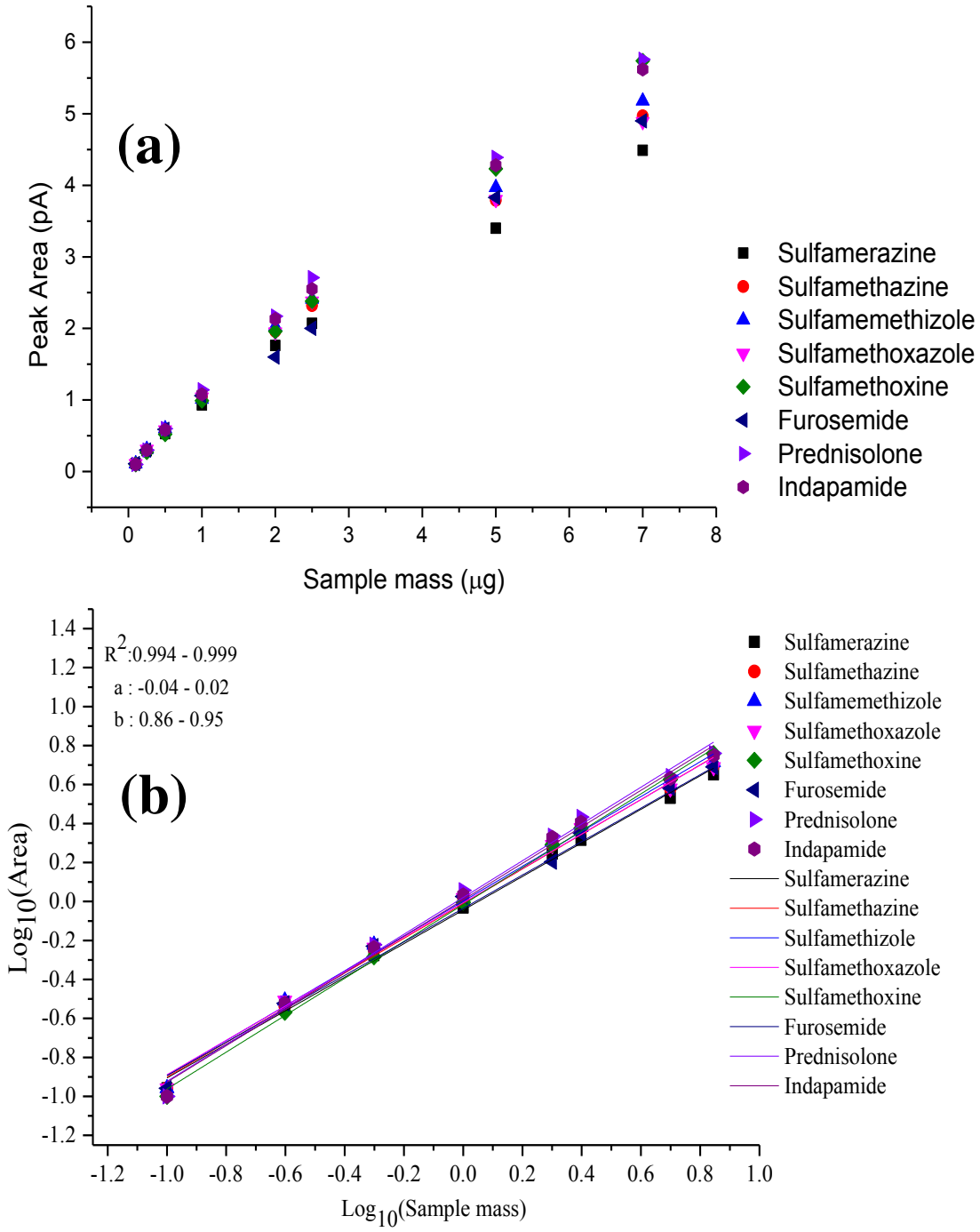

Figure 4.12: Average calibration curves obtained for 8 analytes using a combination of isocratic-temperature and flow-rate gradient with post-separation flow-rate make-up (a) Non-logarithmic coordinates (b) Logarithmic coordinates.

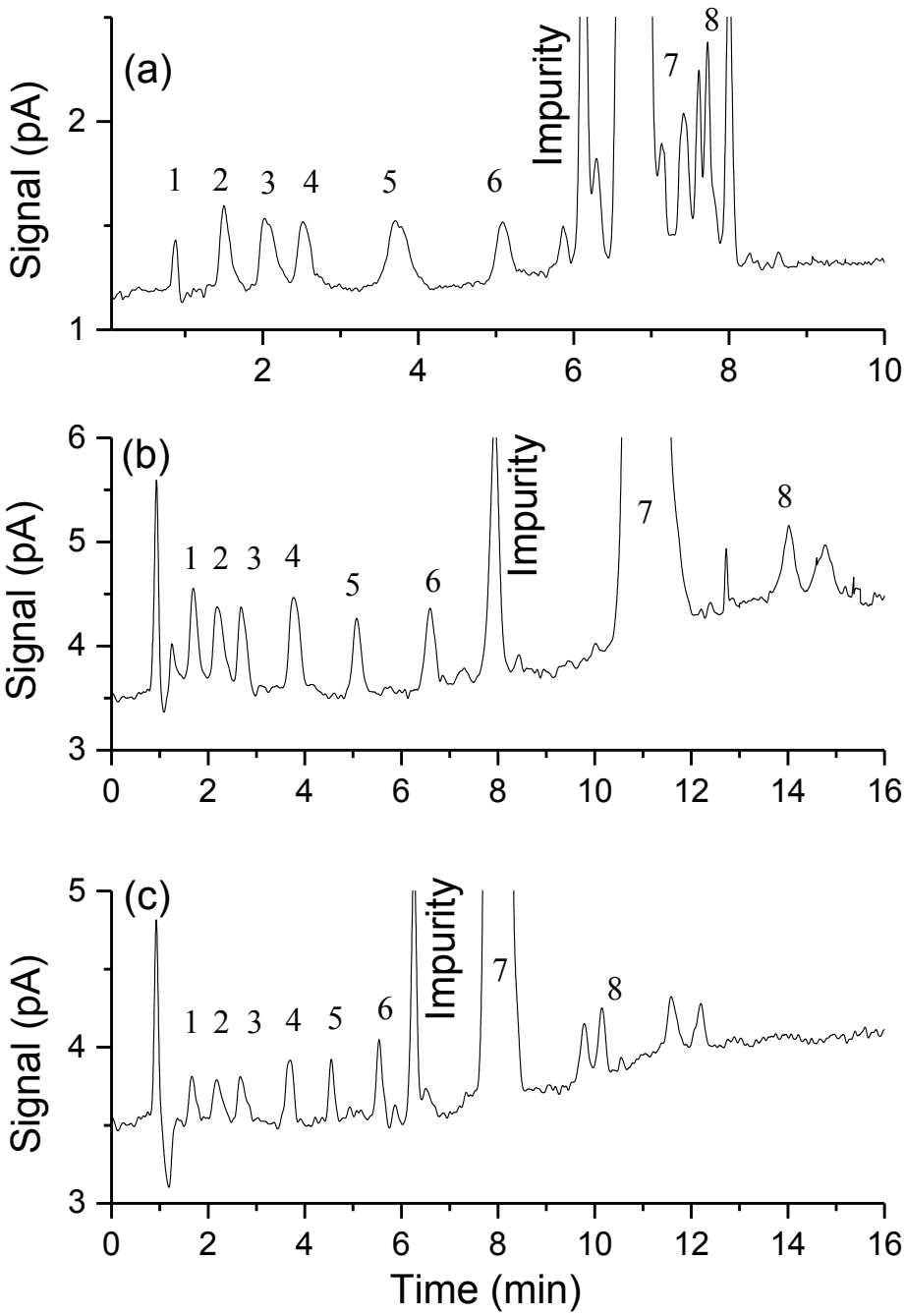

Figure 4.13: Separation of a test solution containing 5 mg/mL of prednisolone and 5 mg/L each of remaining 7 compounds, by 3 different gradient approaches. (a) inverse gradient solvent compensation, (b) isocratic-temperature gradient with post-column addition of ACN and (c) combination of temperature and flow-rate gradients with post-column flow-rate make-up using mobile phase. For peak identities, refer Fig-2. Experimental conditions detailed in experimental section 4.2.

Table-4.1: Comparison of different separation approaches for quantitative analysis using C-CAD:

Peak	C (µg/mL)	Temperature Gradient with Post-column Solvent Addition		Combination of Temperature and Flow-rate Gadient		Inverse Gradient Solvent Compensation	
		C* (µg/mL)	Accuracy (Mean ± RSD)	C* (µg/mL)	Accuracy (Mean ± RSD)	C* (µg/mL)	Accuracy (Mean ± RSD)
Sulfamerazine	5.00	4.51	90.2 ± 1.8	4.32	86.4 ± 2.8	3.91	78.2 ± 3.2
Sulfamethazine	5.00	4.59	92.0 ± 3.5	4.66	93.2 ± 2.6	5.32	106.5 ± 3.8
Sulphamethizole	5.00	3.88	77.8 ± 3.1	4.83	96.6 ± 4.9	4.09	81.8 ± 6.2
Sulfamethaxazole	5.00	5.71	114.3 ± 3.8	5.51	110.3 ± 4.4	4.13	82.7 ± 10.7
Sulphamethoxine	5.00	4.06	81.4 ± 6.5	4.57	91.5 ± 5.3	4.76	95.4 ± 4.1
Furosemide	5.00	5.08	101.7 ± 6.8	5.77	115.5 ± 4.2	3.43	68.5 ± 3.5
Prednisolone impurity	_	16.54	_	16.94	_	15.91	_
Indapamide	5.00	5.75	115.1 ± 6.5	5.94	110.3 ± 6.6	4.72	94.5 ± 9.6

C – Theoretical concentration, C* - concentration calculated using a calibration curve of Prednisolone.

Log_{10} (peak area) vs Log_{10} (Sample mass) curve equations for Prednisolone:

1) Isocratic-temperature gradient: $Y = 0.914X + 0.512$, $R^2 = 0.989$,

2) Isocratic-temperature flow rate gradient: $Y = 0.943X + 0.021$, $R^2 = 0.994$ and

3) Inverse gradient solvent compensation: $Y = 0.792 + 0.207$, $R^2 = 0.991$

In addition, it is important to note that, in the pharmaceutical industry, speed and accuracy requirements of chromatographic methods vary depending on the stage of the drug development process at which the analysis is performed. As most drug substances are synthesized by multi-step chemical reactions, process samples contain structurally diverse compounds. Moreover, organic solvents used for reaction quenching and purification processes are often present in high amounts in process samples. Therefore, process sample analysis poses significant challenges to the ability of chromatographic methods to provide semi-quantitative information about reaction conversion rates and the presence of major by-products. There has been a continued quest for an easy to operate and economical detector that can provide a uniform response for all the sample components. Considering these facts, the approaches proposed in the current study can be beneficial for chromatographic analysis in early stage drug development.

4.4 Conclusions

The present study investigated the compatibility and complementarities of separation modes involving simultaneous variation in eluent temperature and flow-rate, for use with C-CAD. The response of the C-CAD was found to remain relatively unaffected by the temperature and flow-rate variations, which reaffirms the ability of the C-CAD to provide truly mass dependent detection response. Both temperature and flow-rate gradients have their own limitations when applied separately, but in combination, these approaches complement each other to improve chromatographic performance. Based on these findings, two approaches have been proposed as alternatives to the conventional solvent gradient separation. An isocratic temperature gradient separation employing water-rich eluents can show significant response enhancement by post-column mixing of the column effluent with a secondary stream of the pure organic solvent. This process does not affect the response homogeneity of the C-CAD. A second approach demonstrates the utility of the C-CAD with a dual gradient of temperature and mobile phase flow-rate. This appears to be a simple and practical approach to enhance the temperature gradient separation.

Both of the proposed approaches minimize the necessity of use of a solvent gradient and thereby facilitate significant improvement in the response homogeneity of the C-CAD. The response homogeneity, detection limit and the separation

reproducibility achieved by the proposed approaches were found to be equal or superior to those obtained with the inverse gradient solvent compensation approach [4]. Additionally, the proposed approaches can be applied successfully in micro-scale separations to extend the utility of C-CAD for low flow-rate without requiring a special nebulizer.

.

4.5 References

[1] B. T. Mathews, P. D. Higginson, R. Lyons, J. C. Mitchell, N. W. Sach, M. J. Snowden, M. R. Taylor, A. G. Wright, Improving quantitative measurements for the evaporative light scattering detector, Chromatographia 60 (2004) 625 - 633.

[2] J. P. Hutchinson, J. Li, W. Farrell, E. Groeber, R. Szucs, G. Dicinoski, P. R. Haddad, Universal response model for a corona charged aerosol detector, J. Chromatogr. A 1217 (2010) 7418-7427.

[3] S. Ball, I. Agilent Technologies, Universal quantifi cation using the Agilent 385-ELSD Evaporative Light Scattering Detector., http://www.chem.agilent.com/Library/technicaloverviews/Public/5990-9159EN.pdf / accessed on 9 January 2014.

[4] T. Gorecki, F. Lynen, R. Szucs, P. Sandra, Universal response in liquid chromatography using charged aerosol detection, Anal. Chem. 78 (2006) 3186-3192.

[5] A. de. Villiers, T. Gorecki, F. Lynen, R. Szucs, P. Sandra, Improving the universal response of evaporative light scattering detection by mobile phase compensation, J. Chromatogr. A 1161 (2007) 183-191.

[6] S. Heinisch, J. L. Rocca, Sense and nonsense of high-tempearature liquid chromatography, J. Chromatogr. A 1216 (2009) 642-658.

[7] T. Teutenberg, Potential of high temperature liquid chromatography for the improvement of separation efficiency - A review, Anal. Chim. Acta 643 (2009) 1-12.

[8] C. McNeff, B. Yan, D. Stoll, R. Henry, Practice and theory of high temperature liquid chromatography, J. Sep. Sci. 30 (2007) 1672-1685.

[9] G. Vanhoenacker, P. Sandra, Elevated temperature and temperature programming in conventional liquid chromatography - fundamentals and applications, J. Sep. Sci. 29 (2006) 1822-1835.

[10] Y. Yang, Subcritical water chromatography: A green approach to high-temperature liquid chromatography, J. Sep. Sci. 30 (2007) 1131-1140.

[11] S. Wiese, T. Teutenberg, T. C. Schmidt, General strategy for performing temperature programming in high performance liquid chromatography: prediction of linear temperature gradients, Anal. Chem. 83 (2011) 2227-2233.

[12] S. Wiese, T. Teutenberg, T. C. Schmidt, A general strategy for performing temperature-programming in high performance liquid chromatography--further improvements in the accuracy of retention time predictions of segmented temperature gradients, J. Chromatogr. A 1222 (2012) 71-80.

[13] T. J. Causon, H. J. Cortes, R. A. Shellie, E. F. Hilder, Temperature Pulsing for Controlling Chromatographic Resolution in Capillary Liquid Chromatography, Anal. Chem. 84 (2012) 3362-3368.

[14] F. Houdiere, P. W. J. Fowler, N. M. Djordjevic, Combination of Column Temperature Gradient and Mobile Phase Flow Gradient in Microcolumn and Capillary Column High-Performance Liquid Chromatography, Anal. Chem. 69 (1997) 2589-2593.

[15] L. K. Moore, R. E. Synovec, Axial thermal gradient microbore liquid chromatography by flow programming, Anal. Chem. 65 (1993) 2663-2670.

[16] L. R. Snyder, Comparisons of Normal Elution, Coupled-Columns, and Solvent, Flow or Temperature Programming in Liquid Chromatography, J. Chromatogr. Sci. 8 (1970) 692-706.

[17] S. El Deeb, U. Schepers, H. Wätzig, Fast HPLC method for the determination of glimepiride, glibenclamide, and related substances using monolithic column and flow program, J. Sep. Sci. 29 (2006) 1571-1577.

[18] P. N. Nesterenko, M. A. Rybalko, Separation of homologues of organic compounds using the gradient of the eluent flow rate on a monolithic porous column, J. Anal. Chem. 60 (2005) 349-354.

[19] M. Righezza, G. Guiochon, Effects of the Nature of the Solvent and Solutes on the Response of a Light Scattering Detector, J. Liq. Chromatogr. 11 (1988) 1967 - 2004.

[20] L. Novakova, S. Lopez, D. Solichova, D. Satinsky, B. Kulichova, P. Solich, Comparison of UV and charged aerosol detection approach in pharmaceutical analysis of statins, Talanta 78 (2009) 834-839.

[21] J. P. Hutchinson, J. Li, W. Farrell, E. Groeber, R. Szucs, G. Dicinoski, P. R. Haddad, Comparison of the response of four aerosol detectors used with ultra high pressure liquid chromatography, J. Chromatogr. A 1218 (2011) 1646-1655.

[22] R. W. Dixon, D. S. Peterson, Development and testing of a detection method for liquid chromatography based on aerosol charging, Anal. Chem. 74 (2002) 2930-2937.

[23] G. Guiochon, A. Moysan, C. Holley, Influence of Various Parameters on the Response Factors of the Evaporative Scattering Detector For a Number of Non-Volatile Compounds, J. Liq. Chromatogr. Relat. Technol. 11 (1988) 2547-2570.

[24] J. Shaodong, W. J. Lee, J. W. Ee, J. H. Park, S. W. Kwon, J. Lee, Comparison of ultraviolet detection, evaporative light scattering detection and charged aerosol detection methods for liquid-chromatographic determination of anti-diabetic drugs, J. Pharm. Biomed. Anal. 51 (2010) 973-978.

[25] A. Stolyhwo, H. Colin, G. Guiochon, Use of Light Scattering as a detector principle in liquid chromatography, J. Chromatogr. 265 (1983) 1-18.

[26] T. Mourey, L. Oppenheimer, Principles of operation of an evaporative light scattering detector for liquid chromatography, Anal. Chem. 56 (1984) 2427-2434.

[27] M. M. Khandagale, J. P. Hutchinson, G. W. Dicinoski, P. R. Haddad, Effects of eluent temperature and elution bandwidth on detection response for aerosol-based detectors, J. Chromatogr. A 1308 (2013) 96-103.

[28] S. Nukiyama, Y. Tanasawa, Experiments on the atomization of liquids in an air stream. Report3: on the droplet-size distribution in an atomized jet, Trans. Soc. Mech. Eng., Japan, 1939.

[29] Y. Yang, M. Belghazi, A. Lagadec, D. J. Miller, S. B. Hawthorne, Elution of organic solutes from different polarity sorbents using subcritical water, J. Chromatogr. A 810 (1998) 149-159.

[30] G. Vazquez, E. Alvarez, J. M. Navaza, Surface Tension of Alcohol Water + Water from 20 to 50 .degree.C, J. Chem. Eng. Data 40 (1995) 611-614.

Chapter 5

Investigating strategies to improve performance of ELSD

5.1 Introduction

This chapter investigates a range of strategies to improve the analytical performance of ELSD. Variation in elution bandwidth and solvent composition of the column effluent significantly deteriorates the response uniformity of ELSD. As discussed in previous chapters, various approaches have been devised so far to counter the solvent effects. However real time control of the nebuliser gas flow-rate [1] has largely been uninvestigated. Nebuliser gas assists in the generation of the primary aerosol with a transfer of its kinetic energy to the liquid stream to overcome the surface tension and cohesive forces holding the liquid together. In addition, it also determines the droplet residence time, vapour saturation in the evaporator tube and thus influences the tertiary aerosol characteristics. Therefore, in ELSD method development, nebuliser gas flow-rate is selected according to the physical properties and volumetric flow-rate of the eluents and is generally kept constant throughout the separation.

As discussed previously, the process of aerosol generation and transport towards the detection zone determines the response characteristics of aerosol-based detectors. According to the NT-equation, at a constant ratio of volumetric flow-rates of the gas and liquid streams, the physical properties of the liquid dominate the response [2]. A simultaneous alteration in the ratio of volumetric flow-rates of the gas and liquid streams therefore appears to be a rational solution to compensate for the solvent effects observed in solvent gradient separations. The effect of the gas flow-rate on ELSD response has been investigated previously [3,4]. For optimum ELSD response, the gas to liquid flow-rate ratio needs to be maintained in the sonic region. In 2009, Agilent introduced software which enables real time control of the nebuliser gas flow-rate and is claimed to compensate for the solvent gradient effects on ELSD response [1]. However, this approach has seldom been reported in literature. Therefore, the potential utility of the nebuliser gas flow-rate control approach was investigated in the present study. Commercial C-CAD detectors operate at constant gas flow-rate, therefore this approach was not investigated in the previous chapter. On the other hand, most

ELSDs allow nebulising gas flow-rate variation over a wide range. Therefore, experiments were performed to assess the feasibility of using real time gas flow-rate control for compensating the solvent effects. In addition, the applicability of inverse gradient solvent compensation [5,6] and temperature gradient approaches [7] for improving the performance of ELSD was also assessed.

Strategies to counter elution bandwidth issues have also been investigated. The effect of elution bandwidth variation, as observed in isocratic-isothermal separation conditions, can be resolved to some extent by applying a temperature gradient [8]. However, implementation of a temperature gradient is restricted by the limited choice of stationary phases that can withstand high temperature (>100°C) and the practical limitations in applying a steep temperature ramp. In particular, these limitations become more apparent in temperature gradient separation of the samples containing compounds with a wide range of polarity. Therefore, the feasibility of applying flow-rate modulation approaches to alleviate the elution bandwidth effects was investigated.

In comprehensive multidimensional analysis, transferring primary peaks into the second dimension as a narrow band, in a rapid and repetitive manner, is of crucial importance to maintain the 1^{st} dimension separation performance and to achieve optimal detection sensitivity. A device interfacing the two dimensions plays an active role in sampling and transfer of the 1^{st} dimension effluent and hence it is normally called a modulator. Different aspects of GC×GC modulators, such as the modulation mechanism, operational parameters and consequential influence on the separation and detection performance in the 2^{nd} dimension have been reviewed extensively [9-11]. GC modulators are broadly classified into thermal and valve-based modulators. The present investigation mimics flow-based modulation approaches that lead to peak compression-in-time [12]. In the GCXGC approach, the entire 1^{st} dimension effluent is sampled into two storage loops at regular intervals and then flushed into the 2^{nd} dimension column using high velocity auxiliary gas. The period of modulation depends mainly on the width of the 1^{st} dimension peak. A high flow differential (flush:fill flow-rate ratio > 20) [12] is used to transfer a sample pulse of constant width into the 2^{nd} dimension. This is a relatively simple approach for the bandwidth modulation. To some extent this approach has similarity with comprehensive LC×LC [13,14]. Because the physical properties of the eluents used in LC are fundamentally different to those used in GC

analysis, flow modulation in LC cannot be expected to provide band-compression and a high level of signal enhancement. However, the purpose of the present study was to evaluate whether introducing a sample peak into the ELSD in the form of a series of peak slices of equal width can alleviate the bandwidth issues identified earlier in this thesis.

5.2 Experimental

The general experimental details (instrumentation and chemicals) are given in Chapter 2. The test analytes used in this study were of analytical grade and purchased from Sigma-Aldrich. Stock solutions of individual analytes were prepared at a concentration of 1 mg/mL in water and stored in a refrigerator at 4°C. Nitrogen gas obtained from an in-house nitrogen generator was used as the nebuliser gas for the ELSD. Except for the FIA investigation related to the gas flow-rate programming approach, throughout this study the ELSD parameters employed were: nebulisation and evaporation temperatures, 60°C; gas flow-rate 1.6 Standard litres per minute (SLM), and a gain factor of 4.

5.2.1 Flow-injection analysis (FIA)

The effect of nebuliser gas flow-rate and eluent composition on the ELSD response was examined by FIA. To ensure Gaussian peak shape and minimal band dispersion, the injector outlet was connected to the ELSD using SS-tubing (130 μm × 45 cm) bent in a serpentine shape. Caffeine and sucrose solutions (0.2 mg/mL in water) were injected in triplicate at different eluent compositions (5/95, 20/80, 50/50, 80/20 and 95/5 of ACN/water, v/v) and nebuliser gas flow-rates (1.0, 1.2, 1.4, 1.6, 1.8 and 2.2 SLM) by changing one parameter at a time. Measurements were made at three eluent flow-rates (0.4, 0.8 and 1.2 mL/min). The data generated from these experiments were plotted as a 3D-surface to visualise the ELSD response variation as a function of nebuliser gas flow-rate and organic solvent content of the eluent.

5.2.2 Chromatographic separations

Two different chromatographic separations were performed to assess the effectiveness of the inverse gradient solvent compensation approach. Hypercarb*HT (2.1 × 100 mm, 3 μm) and Dionex Acclaim C18 Analytical (2.1 × 100 mm, 3 μm)

columns purchased from Thermo Fisher Scientific, Scoresby, Vic., Australia were used for the studies described in sections 5.3.1 and 5.3.2. Chromatographic separation of an equimass mixture of 5 analytes (0.2 mg/mL of each) was performed at an eluent flow-rate of 0.3 mL/min using a gradient of water (mobile phase-A) and acetonitrile (mobile phase-B). The solvent gradient programme used was: (pump-A) 0-1 min 100% A, 1-13 min 0-55% B, 15-16 min 55-0% B followed by equilibration for 3 min. A solvent gradient compensation was performed using the following inverse gradient program: (pump-B) 0-1.8 min 100% B, 1.8-15.8 min 100-45% B, 15.8–16.8 min 100% B, followed by an equilibration step. Chromatographic separation of an equimass mixture of 8 analytes (0.1 mg/mL of each) was performed at an eluent flow-rate of 0.3 mL/min, using a gradient of 10 mM NH_4OAc buffer (mobile phase-A) and acetonitrile (mobile phase-B). The solvent gradient programme used was as follows: (pump-A) 0-1 min 20% B, 1-8 min 20-80% B, 8-10 min 80% B, 10-13 min 80-20%, B followed by equilibration for 7 min. A solvent gradient compensation was performed using the following inverse gradient program: pump-B: 0-1.8 min 80% B, 1.8-9.8 min 80-20% B, 9.8-11 min 20% B, 11-13 min 20-80% B, followed by equilibration for 7 min. The experimental set-up for the inverse gradient separation was the same as in section 4.2.4.

5.2.3 Flow modulation experiments

A two position, 10-port Cheminert switching valve (Vici, Houston, TX, USA) configured with a Dionex Ultimate 3300 UHPLC dual gradient system was used for these experiments. The valve modulation was controlled using an Arduino UNO R3 microcontroller board. A flow schematic is shown in Fig. 5.1. The effect of flow modulation on the response of the ELSD was examined by FIA of a set of sucrose solutions within the concentration range of 0.05–0.3 mg/ mL. For the conventional FIA (without modulation), the valve was kept in position-A and port-10 (waste) was connected to the detector. In the post-valve solvent mixing experiments, the effluent from port-10 was mixed with a secondary stream of liquid using a T-connector and then introduced into the detector. For the chromatograms shown in section 5.3.4, an Agilent 1290 infinity 2-dimensional LC instrument equipped with 2 position / 8 port, dual sample loop (40 µL volume) configuration was used. The ELSD signal was acquired using an Agilent 35900E dual channel interface. An Agilent OpenLab CDS Chemstation (Rev. C.01.04) Software was used to control the instrument operation.

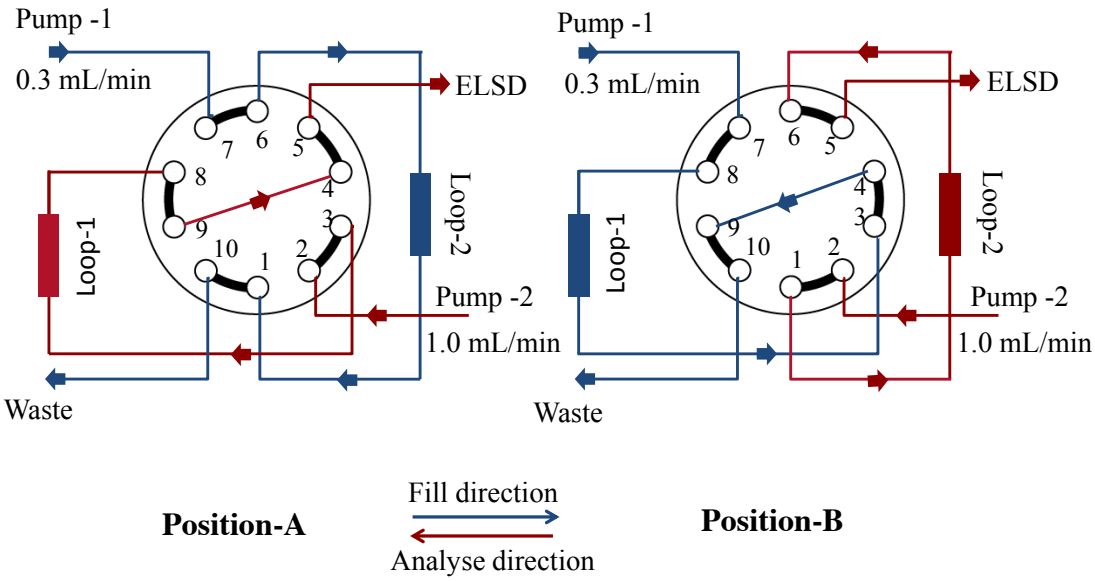

Figure 5.1: Schematic diagram of the valve configuration used for flow-rate modulation experiments

5.3 Results and discussion

5.3.1 Effects of nebuliser gas flow-rate variation

The 3D-surface plots generated by FIA (Fig. 5.2) represent the individual and cumulative effects of variation in the nebuliser gas flow-rate and solvent composition on the response of the ELSD. From these 3D-surface plots, some trends in ELSD response are clearly visible. It shows that, at a constant gas flow-rate, response increases with an increase in organic solvent content up to a maximum and then drops down on further increase in organic solvent content. At constant eluent composition, the response increases with a decrease in nebuliser gas flow-rate. The effect of eluent composition and gas flow-rate was studied at three different liquid flow-rates (0.4, 0.8 and 1.2 mL/min). As can be seen in Fig. 5.2 the response maximum shifted towards higher percentage of organic solvents with an increase in liquid flow-rate from 0.4 to 1.2 mL/min. These observations are in agreement with previous reports [3,4]. The NT-equation has commonly been used to explain these effects (see Chapter 1).

Variation in nebuliser gas flow-rate can be used to compensate the solvent effects, however, as shown by the contour lines in Figs. 5.2 (a-c) this approach caused significant decrease in detection response. Response enhancement by gas flow-rate programming is usually much lower when water-rich eluents are employed. For these eluents, a decrease in the gas flow-rate contributes to an increase in droplet size ($D_{3,2}$) by coagulation of droplets. Coarser droplets thus formed undergo partial evaporation only and therefore cause a decrease in signal with an increase in noise. When eluents containing a high amount of volatile organic solvents are used, high nebuliser gas flow-rate produces a mist of fine droplets. The fine mist thus formed evaporates rapidly to form tiny solute particles that fall in the Rayleigh region and exit the detection unit undetected. Thus, gas flow-rate programming results in a significant drop in the detection response. Fig. 5.3, which has been extracted from the Agilent technical note describing gas flow-rate programming [1], illustrates the effectiveness of the real time gas flow-rate programming for reducing the solvent gradient effects. For the sake of discussion, the original figure has been modified with peak annotations showing approximate peak areas of 5-fluorocytosin (5-FC). It shows that response of 5-FC

Liquid flow-rate: 0.4 mL/min

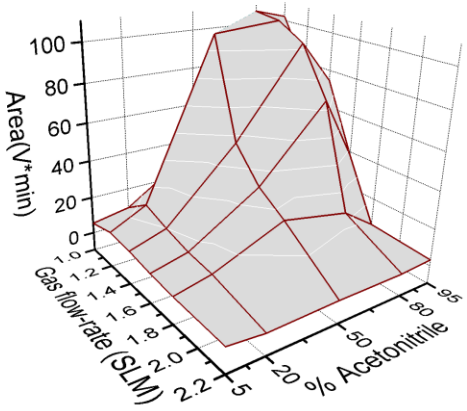

Liquid flow-rate: 0.8 mL/min

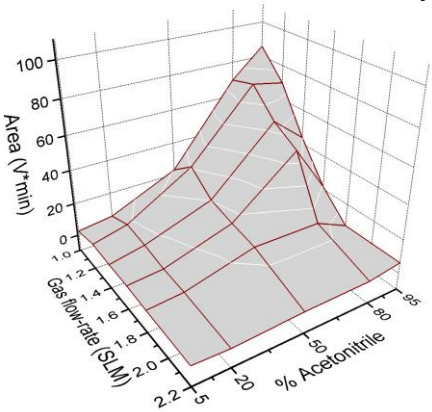

Liquid flow-rate: 1.2 mL/min

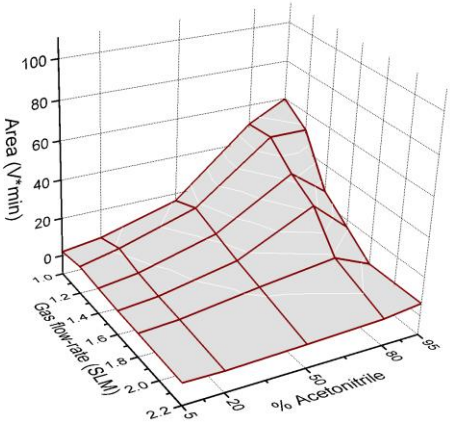

Figure-5.2: 3D surface diagrams showing ELSD response (peak area) as a function of nebulising gas flow-rate and organic solvent content of the eluent.

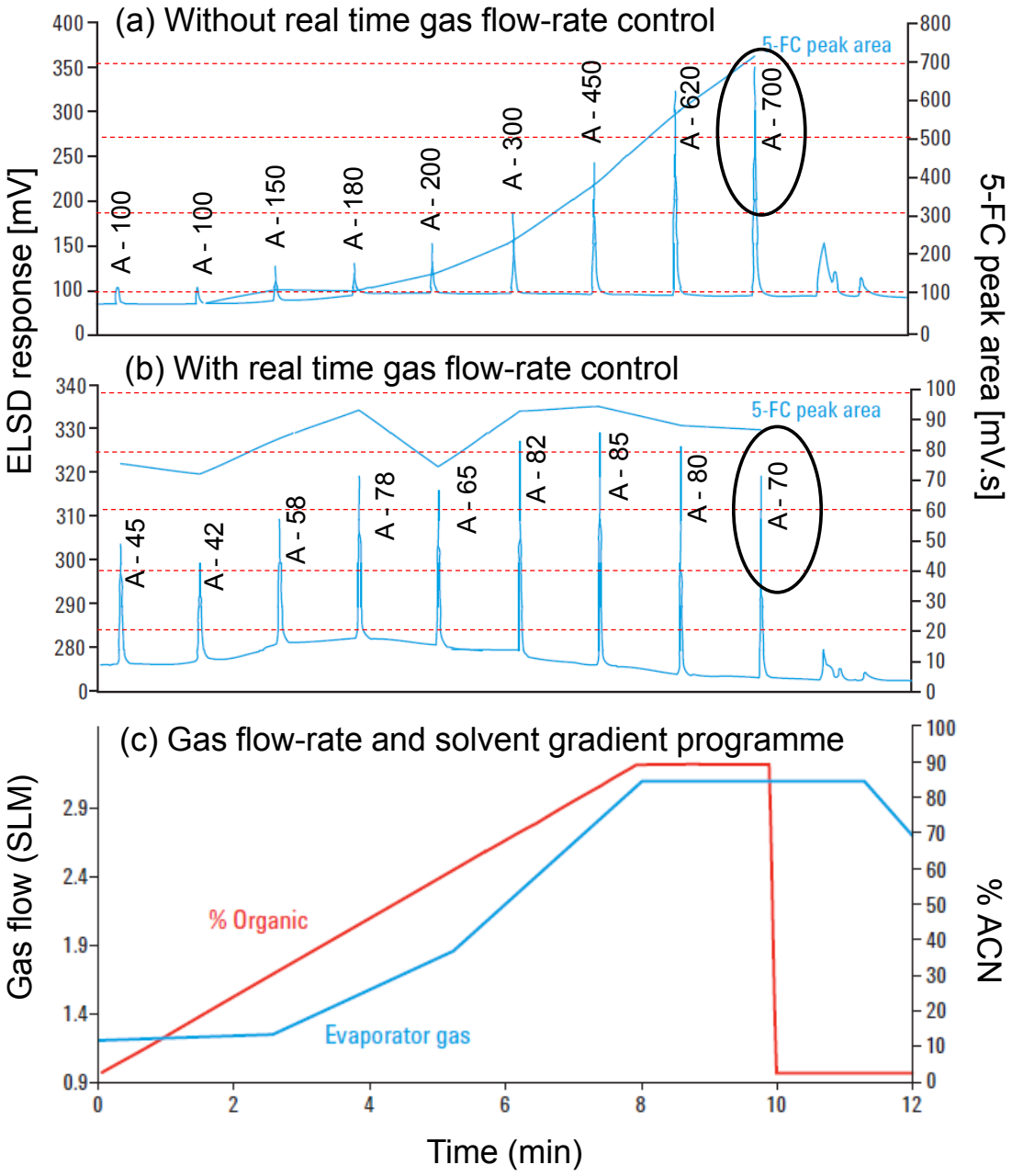

Figure 5.3: Real-time gas control to minimise solvent effects on ELSD response (a) 5-FC response across solvent gradient without real time gas flow-rate control, (b) 5-FC response across solvent gradient with real time gas flow-rate control, (c) nebuliser gas flow-rate and solvent gradient programme. Peak annotation A- an approximate peak area of 5-FC, determined from the grid lines [Figure has been modified from ref. [1]]

deviates by 72.8% (% RSD of peak areas) across the gradient of 5-95%. By step increment gas flow- rate control, response deviation was brought down to 23.8% (% RSD of peak areas). This indicated that nebuliser gas programming can help to overcome the negative effects of solvent gradient. Nevertheless, it is important to note that this approach causes a significant loss in sensitivity. As discussed before, loss in sensitivity as a function of the increase in gas flow-rate becomes pronounced with an increase in organic solvent content of the eluent. As shown in Fig. 5.3(b), the response of the 5- fluorocytosin peak, which is eluted at 95% of ACN, was decreased by about 10-fold as a result of the increase in gas flow-rate. Clearly, the real-time gas flow-rate programming approach deteriorates the sensitivity and thus has limited practical applicability.

5.3.2 Evaluation of inverse gradient solvent compensation approach

Applying an inverse solvent gradient [5] is a more elegant approach to minimise solvent gradient effects. This approach was originally developed to ameliorate response changes in C-CAD. The inclusion of an inverse gradient solvent causes a 2-fold increase in the liquid feed of the nebuliser as it requires post-separation mixing of the column effluent with a secondary stream of liquid. Previous studies have shown that the ELSD responses vary inversely with the eluent flow-rate [3,4,7,15]. It was, therefore, not surprising to find that the inverse gradient compensation significantly lowered ELSD response (see Fig.-5.4 which shows results for two groups of analytes). de Villiers et al. [6] used inverse gradient solvent compensation for LC-ELSD separation of sulphonamides. They showed that despite the reduced sensitivity, this approach can provide a uniform ELSD response at 0.05% concentration of analyte. The effectiveness of this approach for obtaining uniform ELSD response under solvent gradient conditions was therefore assessed in the current study. As expected, the solvent gradient separations shown in Fig. 5.4(a) and (b) yielded considerably high response variation (peak area % RSD = 67.8% and 30.6%, respectively). By applying the inverse solvent gradient, this deviation was reduced to 18.2% and 25.5% (Figs. 5.4(a) and (b), respectively). Thus, the inverse gradient approach appears to be less effective for minimising ELSD response deviation.

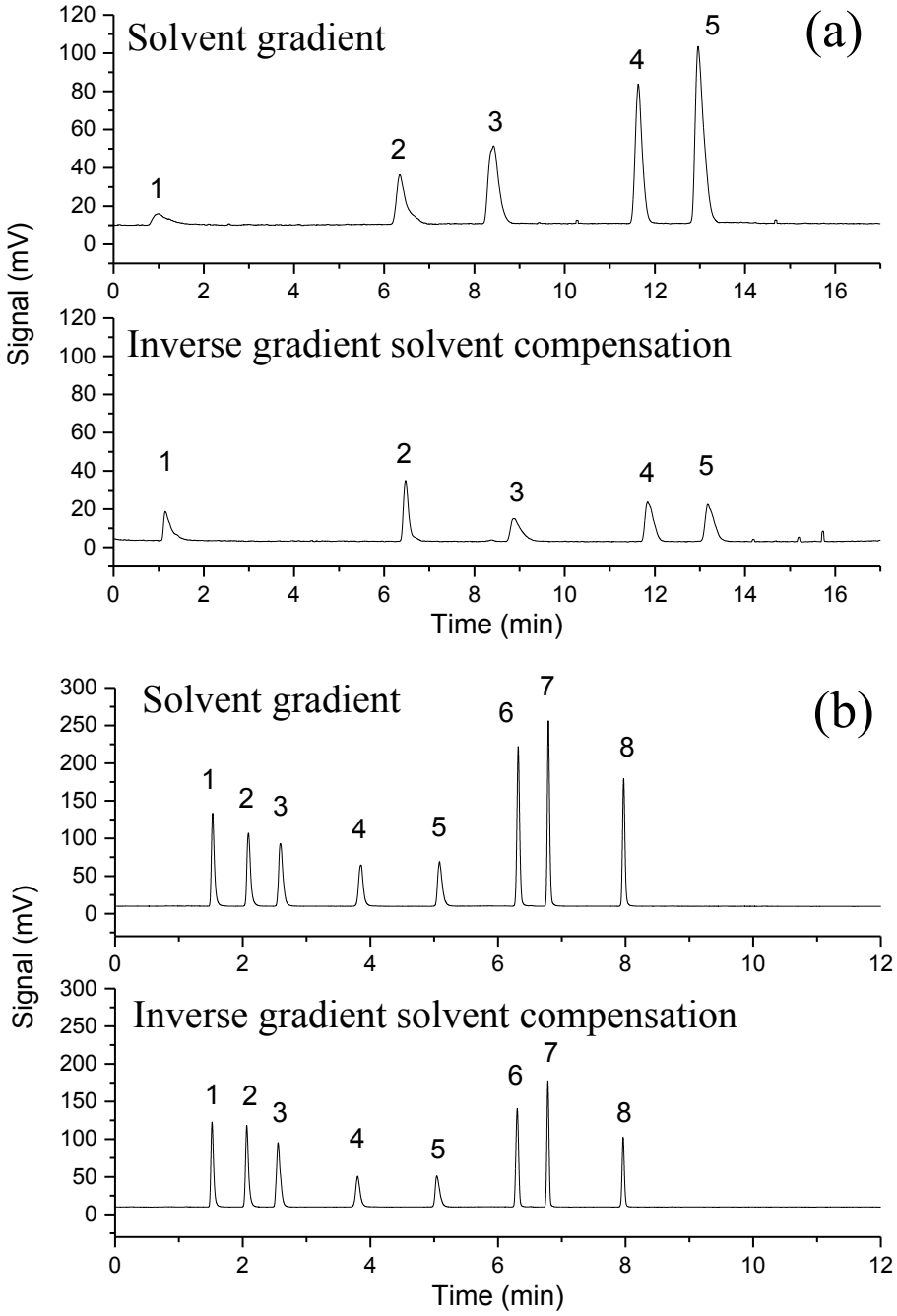

Figure 5.4 (a): Separation of an equimass mixture of 5 analytes by (a) solvent gradient and (b) Inverse solvent gradient. Elution order: 1 - glycine, 2 - sucrose, 3 - uracil, 4 - thymine and 5 - cytidine. **(b)** Separation of an equimass mixture of 8 analytes by (a) solvent gradient and (b) inverse solvent gradient. Elution order: 1 - Sufamerazine, 2 - sulfamethamine, 3 - sulfamethizole, 4 - sulfamethoxazole, 5 - sulfamethoxine, 6 - furosemide, 7 - prednisolone and 8 - indapamide. For chromatographic conditions refer to experimental section 5.2

Fig. 5.5 shows data for peak width and percentage changes in peak area after application of the inverse solvent gradient for each analyte in the separations shown in Fig. 5.4. A dotted red line represents an ideal response that would be expected for individual analytes, if ELSD provided uniform detection response. For instance, in a chromatogram showing separation of an equimass mixture of 5 anlytes, each individual peak would be expected to exhibit 20% of the the total peak areas if all analytes gave identical detector responses. Similarly, in the separation of an equimass mixture of 8 analytes, the area percent contribution of each peak should be 12.5%. In this figure, a clear inverse correlation exists between elution bandwidth and ELSD response, which explains why even with solvent compensation there is a considerable variation in response between analytes. It is noteworthy that under identical conditions, variation of the C-CAD response was found to reduce from 33.5% RSD for a conventional solvent gradient to 6.5% RSD by applying an inverse gradient solvent compensation (see section 4.3.3). Elution bandwidth variation and increase in flow-rate were found to have marginal effects on the response of C-CAD. However, for ELSD, it is necessary to minimise the contributions from elution bandwidth variation to realise the benefits of an inverse gradient for improved response homogeneity. Replacing the solvent gradient with a temperature gradient separation under isocratic conditions can minimise these solvent effects. It also helps to reduce the bandwidth variation to some extent. Since C-CAD is a mass sensitive detector, flow-rate variation does not influence the detection response. Hence, it allowed implementation of post-separation solvent addition to minimise the negative effects of the solvent gradient. However, similar approaches cannot be used with ELSD. This prompted further investigations into alternate ways to modulate the elution bandwidth in order to obtain response homogeneity.

5.3.3 Effect of flow modulation on response of ELSD

5.3.3.1 Flow injection analysis (FIA)

The effect of flow modulation on the response of the ELSD was studied in the flow injection mode. To obtain peak widths comparable to those observed in typical chromatographic separations, sample loops made from SS-tubings of different i.d. and length were connected between the injector and the valve inlet. To minimise the peak dispersion, all fluid connections were made using low i.d. capillaries. Figure 5.1

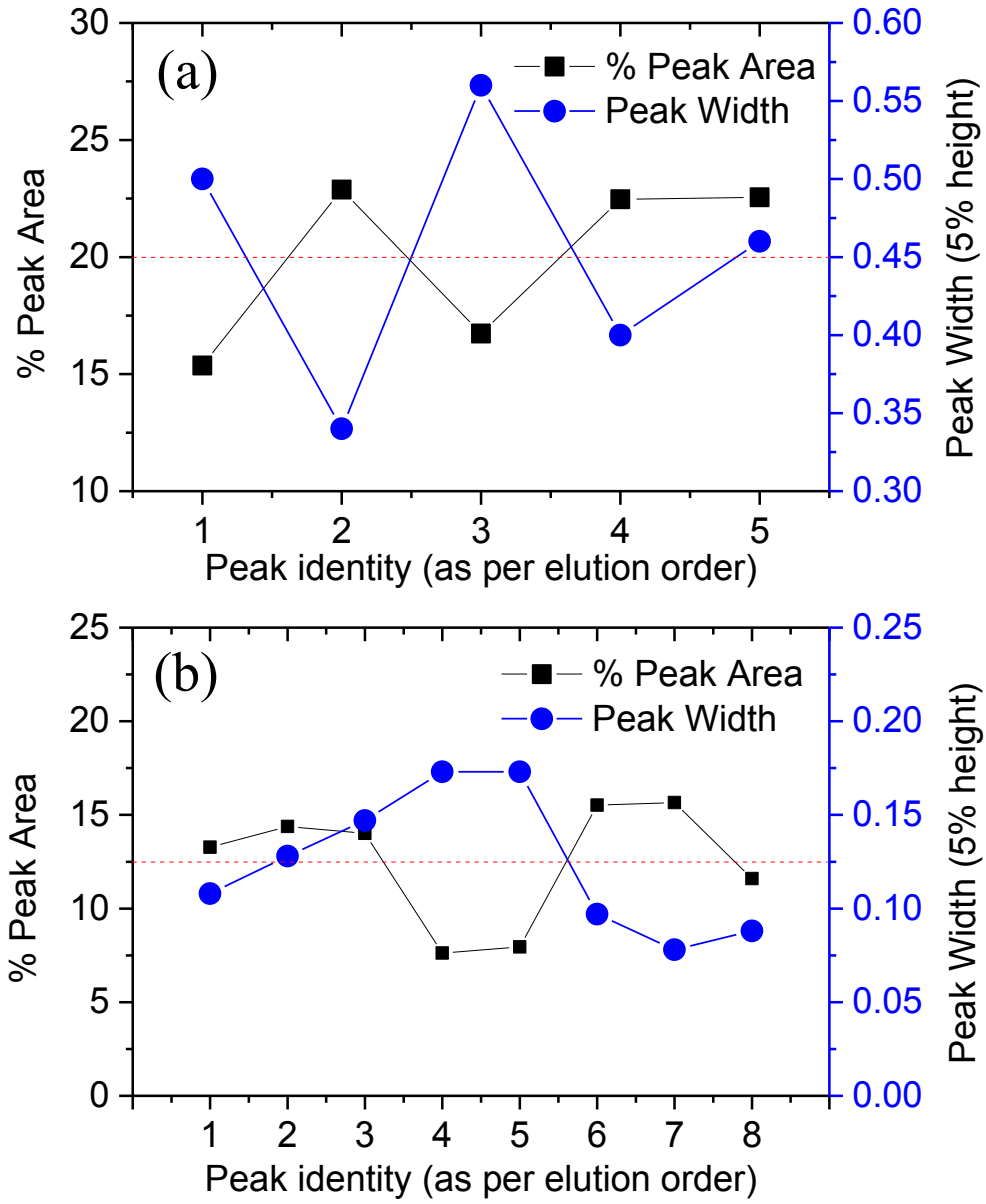

Figure 5.5: Relationship between peak area and peak-width deviation for inverse gradient separations of (a) An equimass mixture containing 1- glycine, 2- sucrose, 3- uracil, 4- thymine and 5- cytidine and (b) An equimass mixture containing 1- Sufamerazine, 2- sulfamethamine, 3- sulfamethizole, 4- sulfamethoxazole, 5- sulfamethoxine, 6- furosemide, 7- prednisolone and 8- indapamide. For chromatographic conditions refer experimental section 5.2.

illustrates the valve configuration used in these experiments. The valve was equipped with two 40 μL sample storage loops. As shown in the schematic diagram, while one loop is being filled with the primary eluent, the second loop is backflushed at a high flow-rate of a secondary eluent, towards the ELSD inlet. The outcome of this process is that the peak entering the valve is sliced into a series of individual segments of constant peak width, depending on the switching frequency of the valve. For GCXGC flow modulation, it is necessary to maintain a high flow differential between the carrier gas flow-rate and that of the gas used to empty the loop [12,16]. However, in the system used in the present study, because of the non-compressible nature of liquids and adverse effects of high flow-rate on ELSD response, maintaining a flow differential as high as that used in GC×GC analysis is not appropriate. In the present study, the primary eluent flow-rate was kept at 0.3 mL/min while the secondary eluent was pumped at 1.0 mL/min. The modulation was controlled by switching the valve position continuously at 5 second intervals, so as to obtain a minimum of three peak slices for each primary peak.

Fig. 5.6 represents the effect of flow modulation on ELSD response. These experiments were performed in the FIA mode, by injecting sucrose solutions within the concentration range of 0.05 – 0.3 mg/mL. The width of the analyte band arriving at valve inlet was adjusted to 0.7 min ($W_{5\%height}$). However, as can be seen by careful inspection of the peaks in Fig. 5.6 (a) and (b), peak width varied in the range of 0.6 – 0.8 min ($W_{5\%height}$). This characteristic feature of ELSD response was also observed previously (section 3.3.2). At a low concentration, tiny solute particle formed from the tailing and fronting ends of the peak pass through the optics undetected and therefore peak-width appears to be narrower compared to those at high concentration. To adjust for the peak dilution caused by flow-rate modulation, the detector liquid feed was adjusted to 1.0 mL/min by post-valve mixing with a secondary stream of the same eluent. An inverse relationship between ELSD response and the eluent flow-rate was observed in both post-valve solvent mixing (Figs. 5.6 (b)) as well as for flow-rate modulation (Fig. 5.6 (c)), however the decrease in peak area as a result of sample dilution was less significant in the latter. Notably, despite more than a 3-fold sample dilution, the peak amplitude of the modulated peaks was found to be comparable to the corresponding principal peaks. This indicates increased solute concentration at the peak

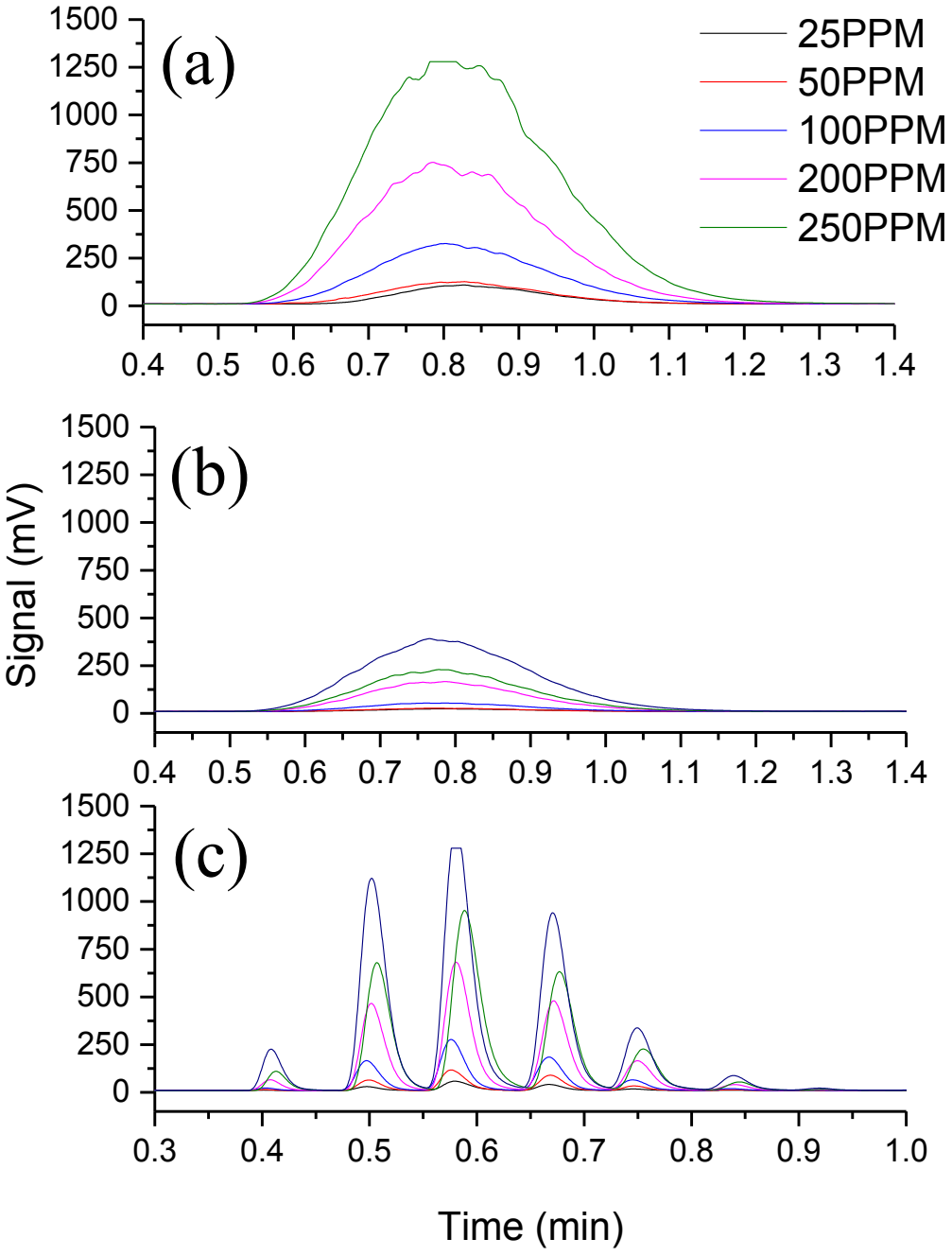

Figure 5.6: Effect of flow modulation of ELSD response: (a) Without flow modulation (primary stream at 0.3 mL/min), (b) Without modulation (liquid feed of ELSD was adjusted to 1.0 mL/min by post-valve mixing of second stream of the same eluent), (c) Flow modulation (primary stream – 0.3 mL/min and second stream – 1.0 mL/min), volume of loop-1 and 2 – 40 µL, modulation period – 5 sec.

apex as a result of improved solute mass transport [8,17]. As explained by equation 3.2, in mass sensitive detectors, peak amplitude depends on solute mass flow-rate and solute concentration at the peak apex. Solute mass at the peak apex alters in direct relation with the flow-rate.

The same set of experiments as described above for a constant peak width was then performed for peak widths varied over the range of 0.2-0.7 min ($W_{5\%height}$). Linear calibration curves were then obtained using log transformed values of the sample mass and peak areas. Results from these experiments have been summarised in Table 5.1. Fig. 5.7 (a) represents the calibration curves obtained without modulation using a 0.3 mL/min eluent flow-rate. Table 5.1 and Figures 5.7 (a) and (b) show clearly that the slope and intercept values of the calibration curves were altered significantly with a decrease in peak width from 0.7 to 0.3 min. In effect, a completely new calibration plot applies when the peak width is altered. An increase in flow-rate produces larger aerosol droplets [8,15] and because of the lower solute concentration per droplet, the process of evaporation and transportation yields tiny solute particles. Thus, the lower calibration plot intercept values obtained in the post-valve mixing experiments can be interpreted as a gradual shift of light scattering towards the Rayleigh region [15,18].

By contrast, the effects of variation on analyte peak width on the calibration plots shown in Fig 5.7 (c) were found to be negligible for the flow modulation approach. The calibration plots for the different peak widths tested were almost identical. The flow modulation process cuts each peak at regular intervals and transfers a sample plug of constant width into the detector, using a high flow-rate of the secondary eluent. Additionally, the high flow-rate of the secondary eluent assists in faster mass transfer and thus reduces dispersion in the evaporator tube. These findings were encouraging as they suggest that applying flow modulation to an isocratic separation could resolve the negative effects of bandwidth variability. Therefore, further investigations were focused on applying this approach to chromatographic separations.

5.3.3.2 Chromatographic separation with flow modulation

To confirm the effects of modulation on peak response uniformity, on-column separations were performed. In these experiments uracil solution (0.2 mg/mL) was

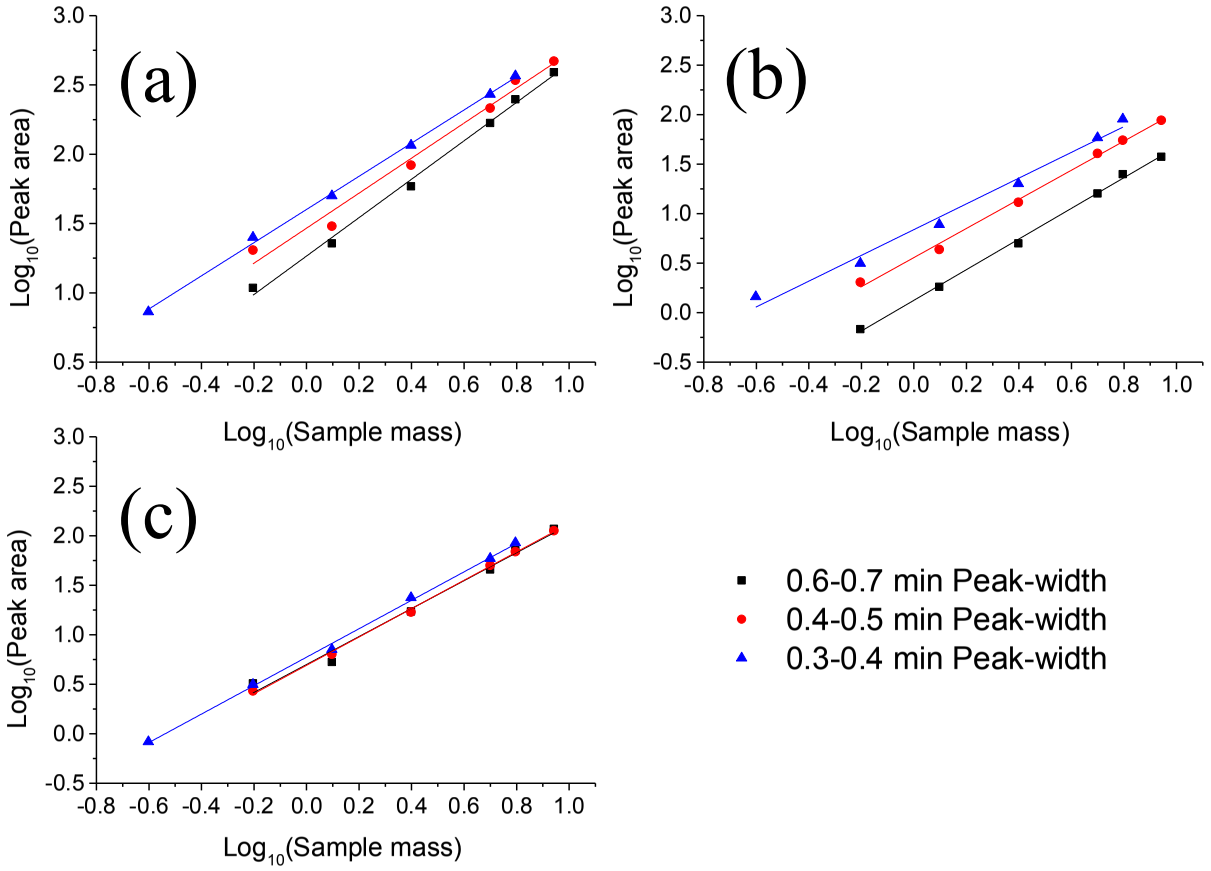

Figure 5.7: Effect of flow modulation of ELSD response. (a) Without flow modulation (primary stream at 0.3 mL/min), (b) Without modulation (liquid feed of ELSD was adjusted to 1.0 mL/min by post-valve mixing of the second stream of the same eluent), (c) Flow modulation (primary stream: 0.3 mL/min and second stream: 1.0 mL/min), modulation period- 5 sec.

Table 5.1: Effect of flow modulation on ELSD response (supporting information for Fig. 5.7)

Peak Areas (Average, n=3)								
Sampe mass (µg)	0.25	0.625	1.25	2.5	5.0	6.25	8.75	Regression equation
Width (at 5% height)				Without modulation (Flow rate - 0.3 mL/min)				
0.2 - 0.4 min	7.3	25.12	50.08	116.20	270.51	367.92	_	1.197x + 1.602, R^2= 0.999
0.4 - 0.5 min	_	20.32	30.20	83.33	214.81	342.08	469.66	1.264x + 1.467, R^2= 0.982
0.6 - 0.7 min	_	10.86	22.72	55.73	167.85	249.36	390.01	1.386x + 1.265, R^2= 0.996
				Without modulation (Flow rate adjusted to 1.0 mL/min)				
0.2 - 0.4 min	1.45	3.15	7.74	20.04	58.35	90.35	_	1.301x + 0.839, R^2= 0.987
0.4 - 0.5 min	_	2.03	4.34	13.01	40.59	55.04	87.5	1.476x + 0.553, R^2= 0.997
0.6 - 0.7 min	_	0.68	1.82	5.00	15.98	25.05	37.6	1.549x + 0.125, R^2= 0.998
				With flow modulation (Flow rate- 1.0 mL/min)				
0.2 - 0.4 min	0.83	3.15	7.11	23.71	58.95	85.02	_	1.437x + 0.774, R^2= 0.998
0.4 - 0.5 min	_	2.70	5.36	16.91	50.3	68.94	112.51	1.432x + 0.691, R^2= 0.998
0.6 - 0.7 min	_	3.22	5.30	17.20	45.65	71.25	117.32	1.413x + 0.669, R^2= 0.987

injected onto a Hypercarb*HT column maintained at different temperatures (90, 120, 150 and 180°C) in order to obtain different retention times and also different elution bandwidths of uracil. Results are presented in Fig 5.8 for constant flow-rates of 0.3 and 1.0 mL/min, as well as for flow modulation. Note that the area of each peak is recorded next to that peak. In this way, peaks for the same analyte (and therefore constant detector response characteristics) were presented to the detector with different bandwidths but in the same eluent (water). The primary eluent flow-rate was set at 0.3 mL/min. For post-separation flow-rate make-up experiments, the switching valve was kept in position-A and the effluent from port-10 was directed to the ELSD inlet via a T-connector. The detector feed was adjusted to 1.0 mL/min by mixing the column effluent with a secondary stream of water. For flow-modulation experiments, the modulation period was set to 10 sec.

Although the detector liquid feed was the same (1.0 mL/min) in both the modulation (Fig. 5.8 (b)) and post-column mixing (Fig. 5.8 (c)) experiments, the amplitude of the modulated peaks was about 3-fold higher than those in post-column mixing. The chromatogram obtained by separation without modulation showed a 66.1% change in peak area with an increase in elution bandwidth from 0.4 min at 180°C to 1.4 min at 90°C. However, Figure 5.8 (b) shows that in contrast to the findings from the FIA study (5.3.3.1), chromatograms obtained using modulation displayed a considerable change in peak area (59.6%) as the peak width was varied. These results point towards the possible role of the symmetry of the principal peak in modulation and the likelihood that some of the segments from the leading and tailing parts of the broader peaks do not lead to significant particle formation in the evaporator tube and are therefore, not detected.

The flow modulation approach was then applied to an isocratic separation of an equimass mixture of glycine, sucrose, uracil and thymine (0.2 mg/mL each in water). Separation was performed on a Hypercarb*T column using pure water as a mobile phase (flow-rate - 0.3 mL/min). These analytes all have melting points higher than 100°C and they can be expected to provide uniform ELSD response at constant elution bandwidth (chapter 3, section 3.3.3).

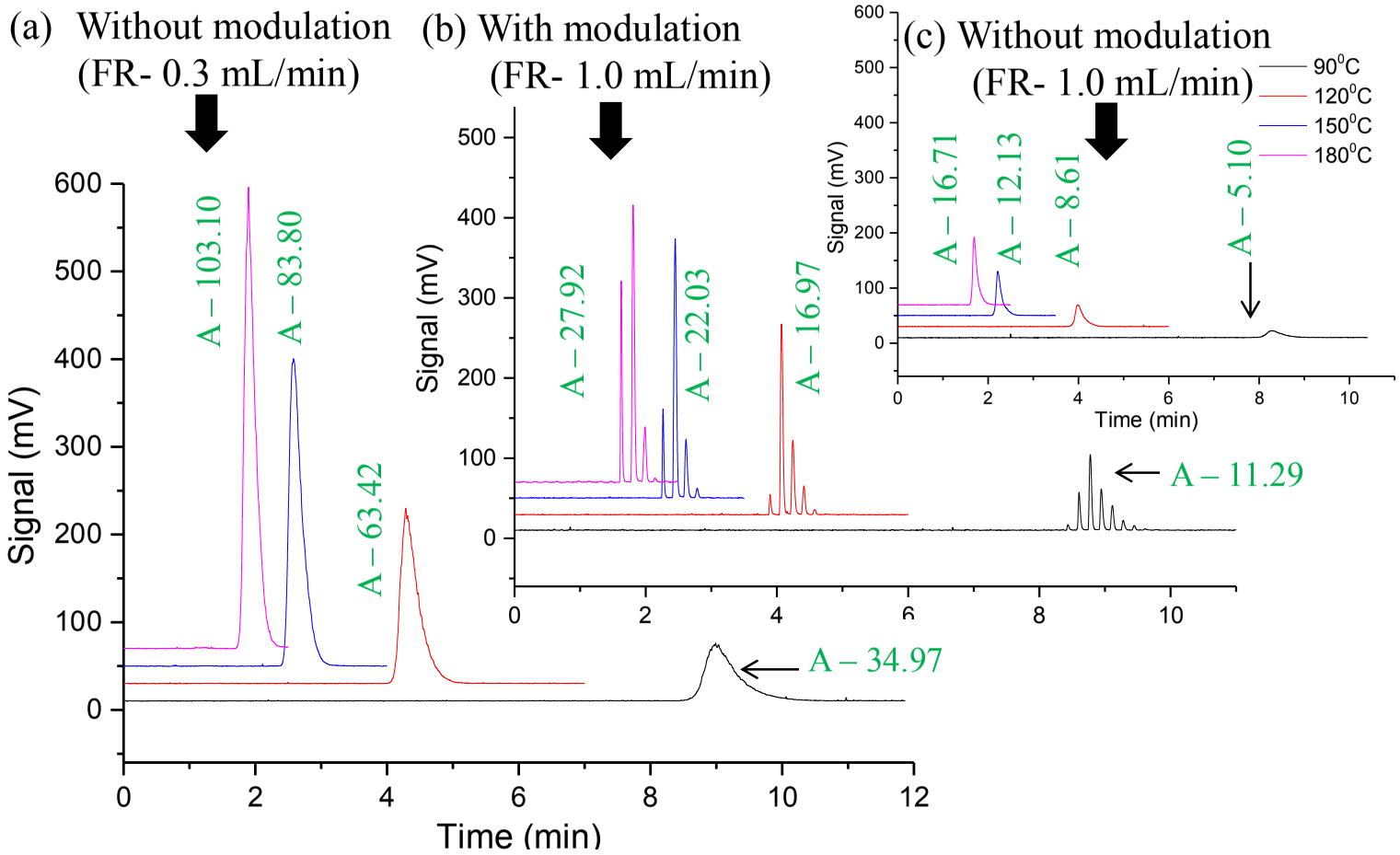

Figure 5.8: Effect of post-column flow-rate modulation on peak amplitude in ELSD after on-column separation. Peak annotation: Area, for experimental details refer section 5.3.3.2

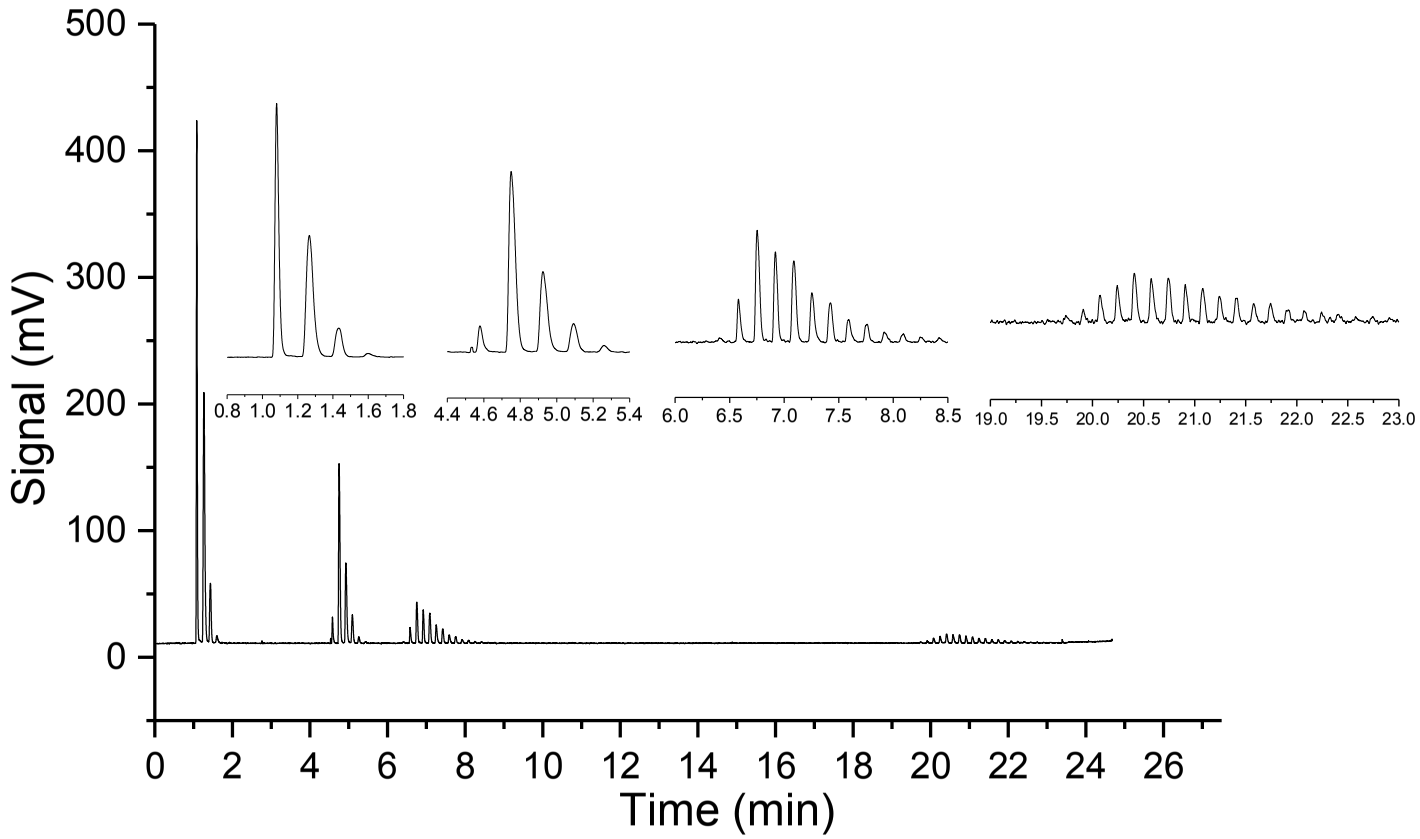

Figure 5.9: Isocratic separation of equimass mixture of 4 analytes using post-separation pulsed flow modulation. (Top part of the figure shows enlarged individual paeaks). Chromatographic conditions: column – Hypercarb*HT (100 × 2.1mm, i.d.), column temperature - 100°C, MP – water, flow-rate - 0.3 mL/min, injection volume - 10 µL, modulation period - 10 sec, volume of the loop 1 and 2- 80 µL, secondary stream - pure water at 1.0 mL/min

In Fig. 5.9 an increase in peak width as a function of retention time caused a significant response deviation (peak area % RSD = 73.3%), in contrast to the FIA experiments reported in Fig. 5.7. These contradictory results can be explained by the non-Gaussian peak shape and much larger widths of the late eluting peaks in Fig. 5.9 compared to those examined in FIA [17]. The response of ELSD changes non-linearly with the solute concentration and variations in linearity and response become more pronounced with an increase in peak width (chapter-3, Fig. 3.5). In particular, the tailing ends of the non-Gaussian peaks in Fig. 5.9 contain very low solute concentrations compared to the peak apexes. Therefore, the droplets formed from this low concentration region, produce tiny solute particles and consequently pass through the optics undetected. With flow modulation, this effect becomes more pronounced as a result of the peak dilution and this could be the reason for the failure of the flow modulation approach to demonstrate the desired degree of uniformity of analyte response.

5.3.3.3 Calibration method for flow modulation

As discussed, peak dilution and the resultant concentration non-linearity of ELSD response constitutes a major hurdle in obtaining a uniform response in flow modulation. Since in flow modulation, solute mass corresponding to the principal peak is conserved into narrow peak slices, response correction of individual slices should reduce the response deviation. Therefore, FIA experiments were performed using sucrose solutions as primary eluent to obtain a true detection response for each individual peak slice. All other conditions were identical to the flow modulation experiments shown in Fig. 5.9. At 0.3 mL/min flow rate, use of an 80 µL sample loop allowed ~62.5% filling in 10 sec modulation period. The theoretical sample mass corresponding to an individual peak slice was calculated according to the concentration and the volume of the sucrose solutions sampled into the loops. The ELSD response curve was then obtained using log-transformed values of theoretical sample mass and area (average, n = 10) of modulated sucrose peaks. Data from these experiments is shown in Fig. 5.10. A regression equation (Fig. 5.10 (c)) was then used to calculate the solute mass of the individual analyte peaks shown in Fig. 5.9. Chromatographic separation was performed by injecting 20 µL of an equimass mixture of 4 analytes (0.2 mg/mL of each), which accounts to a theoretical sample load of 4 µg. Sample masses

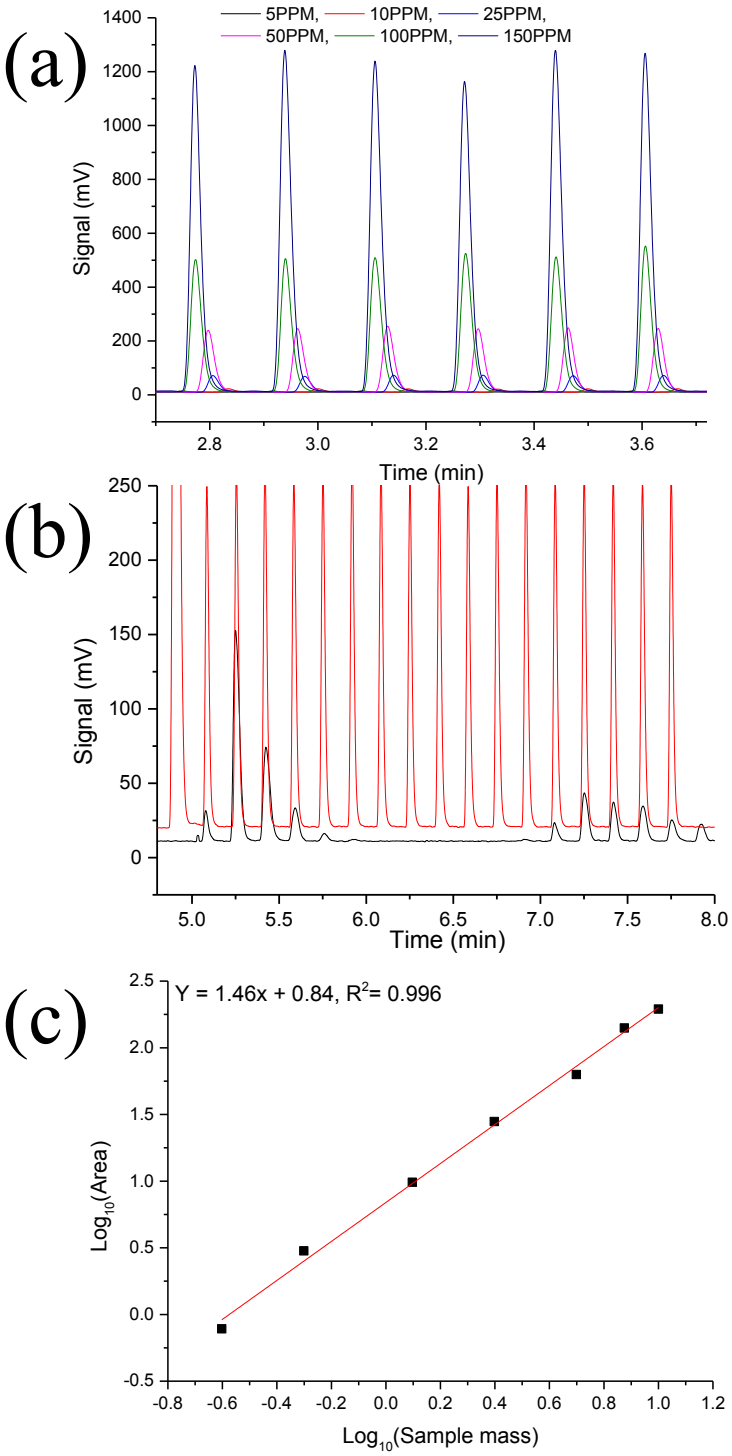

Figure 5.10: FIA experiments using sucrose solutions as an eluent. (a) Modulated peaks for the sucrose solution within the concentration 0.05 – 0.3 mg/mL. (b) FIA modulated peak slices overlaid on the chromatogram in Fig. 5.9 (c) Plot of Log_{10}Peak Area v/s Log_{10} Sample mass.

calculated using the calibration curve were 3.18, 2.10, 1.90 and 1.24 µg for glycine, sucrose, uracil and thymine, respectively. Thus the response deviation was reduced from 60.2% for unmodulated (deviation from mean mass of 4 analytes)) to 38.3% by response correction. Although this indicates some improvement in response uniformity, it is certainly not sufficient for quantitative analysis. A careful examination of the results showed that the calculated sample masses corresponding to the peak slices generated from the fronting and tailing ends of the principal peak lie well below the lower end concentration of the calibration curve. The relatively high limit of detection of ELSD (about 0.25 µg/mL) therefore poses practical difficulty in obtaining a calibration curve that can cover the lower concentrations necessary for effective performance of the flow modulation approach. These findings also point towards the possibility of error in calculating sample mass introduced into the detector. Dispersion of a sample plug to be flushed into the detector can alter the calculated mass introduced into a detector, determined by calibration. This may lead to overestimation of the sample mass in principal peaks. There is further need to understand the influence of the primary elution conditions on modulation and ELSD response.

5.3.3.4 Flow modulation for temperature and solvent gradient separations

As demonstrated in chapter 4, replacing a solvent gradient by an isocratic temperature gradient separation can improve the response uniformity of C-CAD. It was also shown that post-separation addition of an organic solvent can be used to compensate the negative effects of water-rich solvents used in temperature gradient separations. The previous section has shown that despite more than a 3-fold sample dilution, flow modulation provided peak amplitudes comparable to those observed in primary separation. Therefore, experiments were performed to assess the feasibility of using flow modulation to improve ELSD response in isocratic temperature gradient separations when an organic solvent was used to transfer the loop contents to the detector. A temperature gradient separation of an equimass mixture of 8 analytes (the analyte set was the same as in Fig. 5.4 (b)) was performed on a Dionex Acclaim RSLC C18 column, using a temperature gradient (Fig. 5.11 (a)) with NH_4OAc (10 mM) / ACN (80:20 v/v) as eluent. Because the separation was performed under isocratic

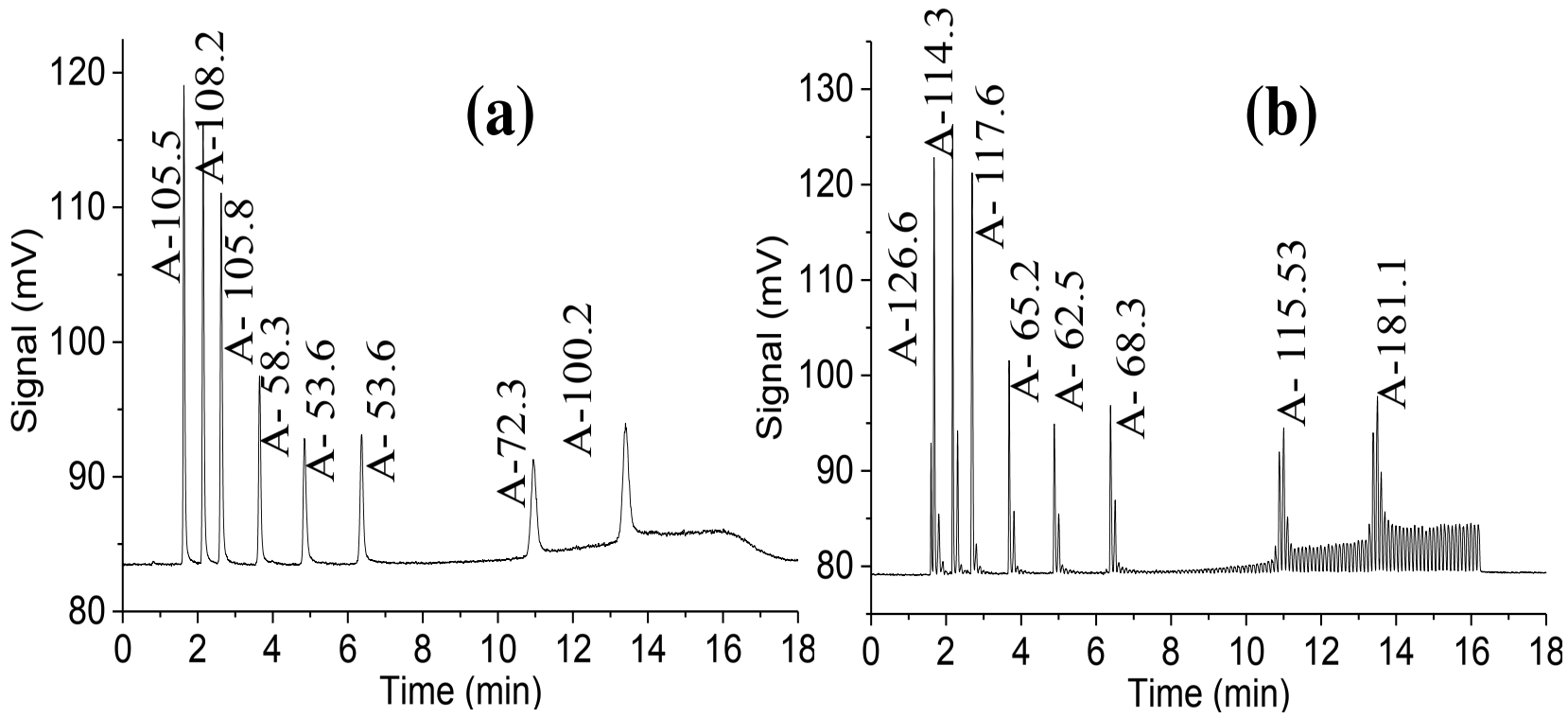

Figure 5.11: Flow modulation to improve response uniformity of ELSD in temperature gradient separation (a) Temperature gradient separation without modulation, (b) Post-separation flow-rate modulation using pure ACN. Temperature gradient – 30 - 80°C from 1 – 13 min at 5°C / min, injection volume – 5 µL, volume of loop-1 and 2 – 40 µL, modulation period - 0.1 min

conditions, the increase in elution bandwidth as a function of retention time caused about 30% response variation (Fig. 5.11 (a)). Considering that better peak symmetry and narrower peak-widths compared to those in Fig. 5.9 were observed in Fig. 5.11(a), post-separation flow modulation was expected to improve the response homogeneity. First, flow modulation experiments were performed using a secondary eluent with a solvent composition the same as the primary eluent. This caused a significant drop in detection response, so in further trials, a pure organic solvent (100% ACN) was used as the secondary eluent in flow modulation. As can be seen from Fig. 5.11(b), flow modulation using pure ACN caused significant baseline noise at the high temperature region (i.e. longer retention times) of the chromatogram, making it difficult to accurately measure peak areas of all peaks. This increase in noise is perhaps related to solvent mixing issues between the disparate primary and secondary eluents at high temperature.

Further experiments were then carried out to see if flow modulation can be used as a peak sampling device to eliminate the negative effects observed with use of a solvent gradient. In these experiments a mixture of glycine, sucrose, uracil, thymine and cytidine (0.2 mg/ mL) was separated on a Hypercarb*HT column using a solvent gradient of water and ACN (0-55% ACN from 1.5 – 13 min). As shown in Fig. 5.12 (a), increase in ACN from 0 to 55% caused a 51.6% variation in response between these analytes. Similar to the solvent gradient experiments described in section 5.2, the response deviation in solvent gradient was found to be associated with solvent effects as well as elution bandwidth variability. Flow modulation was then applied to sample each peak at regular intervals, with transfer into the ELSD being performed using pure ACN. As shown in Fig. 5.12 (b), flow modulation using pure ACN reduced the response deviation to 15.7%, which indicated that post-separation solvent mixing using switching valve can, to a considerable extent, compensate solvent gradient effects. Improved response homogeneity could be a combined effect of the high volume ratio of the organic solvent that was used to transfer analyte band into the ELSD, compared to the volume of each modulation segment. Chromatogram 5.12 (b) also shows high baseline noise and poor resolution between modulated peaks. Therefore, it is necessary to further investigate the effect of primary elution conditions on modulation performance.

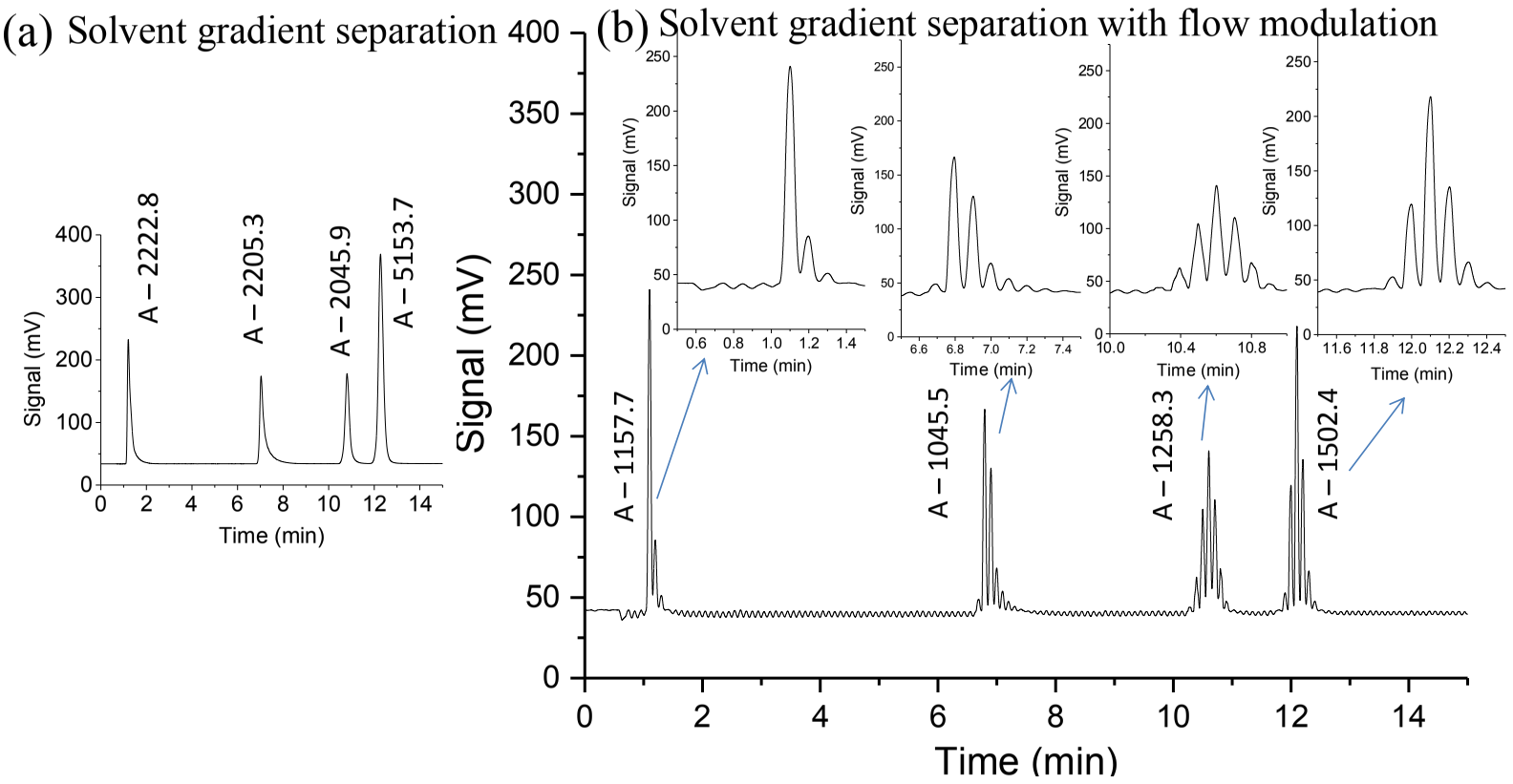

Figure 5.12: Flow modulation to improve response uniformity of ELSD in solvent gradient (a) Solvent gradient separation without modulation (b) Post-separation flow-rate modulation using pure ACN as a secondary eluent. A mixture of 8 analytes was separated on Hypercarb*HT column using solvent gradient of water and ACN (0-55% ACN from 1.5 – 13 min). Volume of loop-1 and 2 – 40 µL, modulation period – 0.1 min.

5.4 Conclusions

Different approaches to overcome the effects of solvent gradient and elution bandwidth variation on ELSD response were investigated. The FIA study showed that variation in the nebuliser gas flow-rate can be used to reduce solvent effects, but this comes at a cost of significant loss in sensitivity. Use of an inverse gradient is a relatively simple and more efficient approach to compensate the solvent gradient effects. However, bandwidth variation across the separation deteriorated the benefits of solvent compensation. In an attempt to overcome bandwidth variability issues, flow modulation experiments were conducted. FIA study showed that transferring peaks into the ELSD as pulses of constant width can provide uniform response, irrespective of the bandwidth of the original peak. Despite an increase in flow-rate caused by the modulation process, the amplitude of the modulated peaks was found to be comparable to unmodulated peaks. However, when applied to broad asymmetric peaks obtained under isocratic conditions, flow modulation showed no improvement in response uniformity. The response of the modulated peaks was found to be dependent on the characteristics of the principal peak.

Therefore, an accurate calibration method to compensate for peak dilution and resultant concentration non-linearity needs to be further investigated. Investigations also showed that implementation of flow modulation in LC using ELSD has some constraints, such as difficulty in maintaining high flow-rate differential and mechanical limitations in switching valve position at high frequency. Moreover, increasing the flow-rate of the secondary eluent to maintain a high flow-rate differential is not recommended because of the adverse effects of high liquid intake on ELSD response. In comparison, valve based peak sampling in conventional solvent gradient and isocratic-temperature tuned separation, appears to be a practical way to achieve uniform response and therefore utility of switching valve as a peak sampling device is worth investigating further. Separation at low flow-rate using micro/capillary scale columns and a low primary eluent flow-rates allows use of a sufficiently high flow-rate differential but at the same time modulation of narrow peaks would require high valve switching frequency.

5.5 References

[1] S. Ball, I. Agilent Technologies, Universal quantifi cation using the Agilent 385-ELSD Evaporative Light Scattering Detector., http://www.chem.agilent.com/Library/technicaloverviews/Public/5990-9159EN.pdf / accessed on 9 January 2014.

[2] S. Nukiyama, Y. Tanasawa, Experiments on the atomization of liquids in an air stream. Report3: on the droplet-size distribution in an atomized jet, Trans. Soc. Mech. Eng., Japan, 1939.

[3] M. Righezza, G. Guiochon, Effects of the Nature of the Solvent and Solutes on the Response of a Light Scattering Detector, J. Liq. Chromatogr. 11 (1988) 1967 - 2004.

[4] J. M. Charlesworth, Evaporative analyzer as a mass detector for liquid chromatography, Anal. Chem. 50 (1978) 1414 - 1420.

[5] T. Gorecki, F. Lynen, R. Szucs, P. Sandra, Universal response in liquid chromatography using charged aerosol detection, Anal. Chem. 78 (2006) 3186-3192.

[6] A. de. Villiers, T. Gorecki, F. Lynen, R. Szucs, P. Sandra, Improving the universal response of evaporative light scattering detection by mobile phase compensation, J. Chromatogr. A 1161 (2007) 183-191.

[7] M. M. Khandagale, E. F. Hilder, R. A. Shellie, P. R. Haddad, Assessment of the complementarity of temperature and flow-rate for response normalisation of aerosol-based detectors, J Chromatogr A 1356 (2014) 180-187.

[8] M. M. Khandagale, J. P. Hutchinson, G. W. Dicinoski, P. R. Haddad, Effects of eluent temperature and elution bandwidth on detection response for aerosol-based detectors, J. Chromatogr. A 1308 (2013) 96-103.

[9] M. Pursch, K. Sun, B. Winniford, H. Cortes, A. Weber, T. McCabe, J. Luong, Modulation techniques and applications in comprehensive two-dimensional gas chromatography (GC x GC), Anal. Bioanal. Chem. 373 (2002) 356-367.

[10] P. Q. Tranchida, G. Purcaro, P. Dugo, L. Mondello, G. Purcaro, Modulators for comprehensive two-dimensional gas chromatography, TrAC Trends in Analytical Chemistry 30 (2011) 1437-1461.

[11] J. V. Seeley, Recent advances in flow-controlled multidimensional gas chromatography, Journal of Chromatography A 1255 (2012) 24-37.

[12] J. V. Seeley, F. Kramp, C. J. Hicks, Comprehensive Two-Dimensional Gas Chromatography via Differential Flow Modulation, Analytical Chemistry 72 (2000) 4346-4352.

[13] P. Jandera, Column selectivity for two-dimensional liquid chromatography, J Sep Sci 29 (2006) 1763-1783.

[14] I. Francois, K. Sandra, P. Sandra, Comprehensive liquid chromatography: fundamental aspects and practical considerations--a review, Anal. Chim. Acta 641 (2009) 14-31.

[15] A. Stolyhwo, H. Colin, M. Martin, G. Guiochon, Study of the qualitative and quantitative properties of the light-scattering detector., J Chromatogr. 288 (1984) 253-215.

[16] P. M. Harvey, R. A. Shellie, P. R. Haddad, Design Considerations For Pulsed-Flow Comprehensive Two-Dimensional GC: Dynamic Flow Model Approach, J. Chromatogr. Sci. 48 (2010) 245-250, 212A.

[17] P. Van der Meeren, J. Vanderdeelen, L. Baert, Simulation of the Mass Response of the Evaporative Light Scattering Detector, Anal Chem. 64 (1992) 1056-1062.

[18] T. Mourey, L. Oppenheimer, Principles of operation of an evaporative light scattering detector for liquid chromatography, Anal. Chem. 56 (1984) 2427-2434.

Chapter 6

General conclusions and future work

The overall aim of this thesis has been to improve the analytical performance of ELSD and C-CAD and to expand their field of applicability. Investigations have been focussed on reducing quantification errors caused by response irregularities of aerosol-based detectors by coupling with relatively unconventional separation techniques. In this chapter, general conclusions based on the findings, the strengths and limitations of the studies presented in this thesis and suggestions for future work are presented.

6.1 Conclusions

Hyphenation with HTLC is one of the major recent trends in the usage of ELSD and C-CAD. Various aspects of HTLC separation and their benefits for specific applications have always remained a prime focus. Therefore, the central aim of the studies presented in chapter 3 was to examine the effects of HTLC conditions on the response of ELSD and C-CAD. The results from the present study showed that eluent temperature influence the response of these detectors only marginally and thus makes eluent cooling unnecessary. This suggested that the response homogeneity of ELSD and C-CAD can be improved by replacing solvent gradient with isocratic-HTLC separation. In chromatographic separations, temperature-induced alterations in elution bandwidth were found to influence the peak area produced by ELSD significantly. Further investigations revealed that an inverse relationship existed between elution bandwidth and ELSD response. The origin of this issue lies in the fact that the elution bandwidth dominates the size distribution of the tertiary aerosol reaching the optical unit and consequently alters the mechanism of light scattering. The ELSD response variability as a function of elution bandwidth becomes most pronounced in isocratic separations. Application of a temperature gradient to an isocratic separation reduced the elution bandwidth variation across the chromatographic separation and thus

improved the response uniformity of ELSD. In contrast to ELSD, a variation in elution bandwidth had little effect on peak area obtained with a C-CAD. Since C-CAD provided a uniform response independent of elution bandwidth, it was selected for further investigations. The primary aim of the studies described in chapter 4 was to assess the feasibility of replacing solvent gradient separation by isocratic separation methods employing a simultaneous variation in temperature and flow-rate, so that uniform C-CAD response could be achieved. Results from FIA studies showed that C-CAD was relatively insensitive to the changes in eluent temperature and flow-rate when water-rich eluents were used. Nevertheless, for optimum signal-to-noise ratio, it was necessary to consider the eluent composition while selecting the range of flow-rate variation. Based on these findings two separation approaches were developed. The first approach demonstrated that the temperature gradient applied to an isocratic water-rich mobile phase could be used to replace a solvent gradient separation. The sensitivity loss resulting from water-rich eluents in isocratic-temperature gradient separation can be compensated by post-separation addition of a secondary stream of pure organic solvent. The secondary eluent must be selected based on miscibility with the primary eluent and the solubility of the sample constituents.

The second approach involved simultaneous variation in temperature and flow-rate. Baseline disturbances resulting from the backpressure changes produced in a flow-rate gradient were compensated by post-column flow-rate make-up using an inverse flow-rate gradient of the eluent. This study has shown that temperature gradients suffered from low elutropic strength, resulting in broadening of late eluting peaks when elution was performed at a constant flow-rate, whereas a flow-rate gradient under isothermal conditions posed risk of high back-pressure. Combining a temperature gradient with a simultaneous flow-rate variation allowed use of the high flow-rate changes required for the flow-rate gradient, improved the separation speed and reduced the elution bandwidth variability across the separation. The proposed approaches, as well as use of an inverse gradient, allowed quantification at 5 mg/L level. Considering the wide dynamic range of the C-CAD, quantification of impurities present at lower concentration levels can be achieved by increasing the sample mass per injection. The approaches described in the present study minimise the necessity of solvent gradients and thus reduce the response deviation across the separation.

Moreover, these approaches offer flexibility in the use of C-CAD for relatively unconventional separation modes and thereby contribute to extend its universality. The proposed approaches do have some limitations, such as a limited choice of thermo-stable stationary phases, the difficulty in applying a high temperature ramp, slow thermal equilibration due to the high thermal mass of the analytical scale columns, and the risk of high backpressure in maintaining a sufficiently high flow-rate range in flow-rate gradients. These limitations are particularly characteristic of conventional analytical scale separations. It should be noted this is proof-of-concept work and potential future work in instrument development could resolve these issues. Moreover, these approaches could be further extended to micro and capillary scale separations.

The studies in chapter 5 investigated different strategies to overcome response irregularities of the ELSD. It was shown that real time gas flow-rate programming can be used to compensate partially for response variations resulting from solvent gradient effects. However, significant loss in sensitivity is one of the major concerns in the implementation of this approach. A lack of commercially available software to precisely control gas flow-rate is another constraint, as Agilent Technologies Inc. is the only provider of the real time gas programming software for ELSD and has recently discontinued the development and sale of this software. Although use of an inverse solvent gradient helped to maintain constant composition of the eluent entering into the ELSD, bandwidth variability across the separation still contributed to response deviation. The temperature and flow-rate gradient approaches discussed earlier can help alleviate this issue, but are not recommended for ELSD as they employ water-rich eluents and cause sample dilution because of post-column solvent mixing. These findings reiterated the urgent need to reduce bandwidth variability for uniform response using ELSD.

The possibility of using valve-based post-separation flow-rate modulation to control the width of the analyte band entering the ELSD was investigated. Although flow-rate modulation causes a decrease in peak area, the amplitude of the modulated peaks remained comparable to those obtained without modulation. The results from a FIA study showed that the slope and intercept values of the ELSD response curves (logarithmic scale) obtained by flow-rate modulation remained relatively unaltered irrespective of elution bandwidth. This implied that flow-rate modulation improved the

analyte mass transport and thus could be used to overcome the bandwidth variability issue. However, when applied to isocratic separation, flow-modulation showed only a marginal improvement in response uniformity. Although flow-modulation is a conceptually interesting approach, it has some limitations. It requires a high flow-rate differential for optimum modulation, but at the same time, the resultant sample dilution significantly lowered the ELSD response. Experiments showed that the performance of flow-rate modulation depended strongly on the characteristics of the principal peak. Because of the wide molar mass distribution across the broad chromatographic peaks, response correction was required for individual peak slices generated by modulation. Considering the complexity of the light scattering mechanisms in ELSD and its high detection limit, flow-rate modulation appears not, at this stage of its development, to be a practical solution to response irregularities of ELSD.

6.2 Future work

- Application of the proposed temperature and flow-rate gradient approaches to real analytical problems, especially in the area of pharmaceutical impurity analysis, is an obvious area of further research.
- As pointed out, the use of temperature gradients and flow-rate gradients have some constraints in terms of suitable stationary phases, slow thermal equilibration of the analytical scale columns, and the risk of high backpressure in maintaining sufficiently a flow-rate gradient. These limitations are particularly characteristic of conventional analytical scale separations. In contrast, capillary-micro scale columns allow faster thermal equilibration because of their low thermal mass. Recently introduced low thermal mass (LTM) heating modules enable heating ramps up to 1800°C/min or cooling at 100-200°C/min for capillary scale columns. Since micro-capillary scale separations employ very low flow-rates, it would be possible to maintain a high linear velocity differential of the eluent as required for the flow-rate gradient. A temperature and flow-rate tuned separation under isocratic condition can also benefit from capillary scale separations to overcome issues related to the solvent gradient mixing and save on time required for re-equilibration of the column. Previous studies on hyphenation of ELSD with capillary scale separations have

reported the necessity of a micro-scale nebuliser to minimise band dispersion induced by the nebuliser cell. It would be interesting to see whether the approaches proposed in this study allow use of commercially available ELSD and C-CAD, without any nebuliser cell modification. Considering these facts, the best way forward with the proposed approaches would be to optimise separation using capillary or micro-scale columns using water-rich eluents.

- It is also possible to overcome pH-gradient limitations of C-CAD. According to the manufacturer's recommendations, mobile phases of pH level > 7.5 should not be introduced into the C-CAD. This possibly could be due to the dependence of the charge deposition process on the surrounding atmosphere. There has been growing interest in pH-gradient separations. In addition, some of the high temperature stationary phases such as zirconia-PBD require eluents of high pH level to suppress the secondary interactions. Considering these facts, it would be worth investigating the possibility of post-column pH-gradient compensation. The instrumental set-up for the approaches described in chapter-4 could be modified easily by including an in-flow pH sensor to ensure the effluent entering into C-CAD is at a pH level < 7.5.
- Response variation as a function of elution bandwidth variability is still a major barrier to achieving a uniform ELSD response. Therefore, further work is needed to confirm the precise role of the elution bandwidth in the response of ELSD. This can also help to improve the accuracy of the ELSD response prediction models.

Appendix

These articles have been removed for copyright or proprietary reasons.

M. M. Khandagale, J. P. Hutchinson, G. W. Dicinoski, P. R. Haddad, 2013, Effects of eluent temperature and elution bandwidth on detection response for aerosol-based detectors, J. Chromatogr. A 1308, 96-103.

M. M. Khandagale, E. F. Hilder, R. A. Shellie, P. R. Haddad, 2014, Assessment of the complementarity of temperature and flow-rate for response normalisation of aerosolbased detectors, J. Chromatogr. A 1356, 180-187.